

Dual-located Kinesin

A class XIV kinesin that can enter the nucleus

Zur Erlangung des akademischen Grades eines
Doktors der Naturwissenschaften
(Dr. rer. nat.)

der KIT-Fakultät für Chemie und Biowissenschaften
des Karlsruher Instituts für Technologie (KIT) -Universitätsbereich
genehmigte

Dissertation

von

Xu, Xiaolu

aus

Jiangsu, China

KIT-Dekan: Prof. Dr. Willem Klopper

Referent: Prof. Dr. Peter Nick

Korreferent: Prof. Dr. Reinhard Fischer

Tag der mündlichen Prüfung: 26. Juli, 2017

Die vorliegende Dissertation wurde am Botanischen Institut des Karlsruher Instituts für Technologie (KIT), Botanisches Institut, Lehrstuhl 1 für Molekulare Zellbiologie, im Zeitraum von September 2013 bis Juli 2017 angefertigt.

Hiermit erkläre ich, dass ich die vorliegende Dissertation, abgesehen von der Benutzung der angegebenen Hilfsmittel, selbständig verfasst habe.

Alle Stellen, die gemäß Wortlaut oder Inhalt aus anderen Arbeiten entnommen sind, wurden durch Angabe der Quelle als Entlehnungen kenntlich gemacht.

Diese Dissertation liegt in gleicher oder ähnlicher Form keiner anderen Prüfungsbehörde vor.

Karlsruhe, im Juni 2017

Xu, Xiaolu

Acknowledgments

I would like to greatly thank Prof. Dr. Peter Nick for providing me the position to study in Botanical Institute and for his wonderful guidance and encouragement during my study. I am really appreciated and inspired with his enthusiasm, sagacity, erudition, patience in his career as a scientist and supervisor. I am grateful that he has provided me a lot of constructive suggestions as well as the freedom, confidence and trust on this project.

Many thanks to Prof. Reinhard Fischer to agree to be my co-examiner and I really appreciate his time, devotion and expertise.

I thank Prof. Dr. Wim Walter and his colleagues for the great job in sliding assay.

Also I would like to thank Dr. Michael Riemann for his time, devotion and expertise during my study. Importantly, I really appreciate him for taking over the correction work. Many thanks for Dr. Jan Maisch for his help and especially his time on the translation work for my abstract.

I would like to especially thank Dr. Qiong Liu for her support and accompany. She is the one who helps me to start the life in Deutschland. We have established great friendship during the four years here and it will last forever. My heartfelt thanks extend to Sabine Purper, Nadja Wunsch, Ernst Heene, Max Seyfried and Sybille Woerner for their excellent job in maintaining the smooth running of our institute. Also there are many thanks to other colleagues and our Azubis for their companion and help.

Finally, I would like to thank my family. I thank my parents for their unconditional love in my life. I thank the great support from my sister and her lovely family. I thank Mengmeng Li for the love, companion and support. I will love you all forever. And I will miss my grandmother forever.

This work is financially supported by the China Scholarship Council (CSC). Great thanks to my country and I am really proud of you, China.

Table of Contents

Acknowledgments.....	I
Abstract.....	VII
Zusammenfassung.....	IX
1.1 Microtubule-one of the dynamic cellular players.....	2
1.1.1 Structure of microtubules	3
1.1.2 Functions of microtubules	5
1.2 Kinesins–MTs associated proteins	6
1.2.1 Molecular motors along cytoskeleton	7
1.2.2 Characteristics of kinesin motors.....	10
1.2.3 The superfamilies and functions of kinesins	12
1.2.4 The superfamily of Kinesin-14.....	16
1.3 The scope of this work.....	18
2. Materials and methods	21
2.1 <i>In silico</i> analysis	21
2.1.1 Phylogenetic analysis of Kinesins	21
2.1.2 Sequence analysis of OsDLK	21
2.1.3 Database search for cDNA clones and knock-out mutants.....	22
2.2 Cultivation materials	22
2.2.1 Cultivation media.....	22
2.2.2 Organisms.....	23
2.3 Primers.....	25
2.3.1 Primers for rice mutant screening.....	25
2.3.2 Primers for gene expression analysis of rice.....	26

2.3.3 Primers for gene expression analysis of tobacco cells	27
2.3.4 Primers for constructs	28
2.3.5 Primers for sequencing	29
2.4 Cultivation techniques	29
2.4.1 Cultivation of rice materials	29
2.4.2 Cultivation of BY-2 cell cultures	31
2.4.3 Cultivation of bacteria.....	31
2.5 Molecular analysis	31
2.5.1 Rice genotyping of rice mutant	31
2.5.2 cDNA synthesis and quantitative Real-Time PCR.....	34
2.5.3 Expression level of endogenous OsDLK in rice during germination ..	36
2.5.4 Cloning and manipulation of plasmids	37
2.6 Cell biological analytics	40
2.6.1 Stable and transient transformation	40
2.6.2 Microscopy and image analysis.....	41
2.6.3 Determination of packed cell volume	42
2.6.4 Determination of mitotic index	42
2.6.5 Cell cycle synchronization	43
2.6.6 Immunostaining of microtubules	43
2.6.7 Oryzalin dose-response curves	44
2.6.8 Leptomycin B treatment.....	44
2.6.9 Cold treatment	45
2.7 Protein expression and isolation in <i>E.coli</i>	45
2.7.1 Protein expression in <i>E.coli</i>	45

2.7.2 Western blotting	46
2.8 Motility assays <i>in vitro</i>	48
2.9 DPI-ELISA assay.....	49
3. Results	51
3.1 In <i>silico</i> analysis of OsDLK.....	51
3.1.1 OsDLK is a putative minus-end directed C-terminal motor of Kin-14	51
3.1.2 OsDLK is a highly conserved motor member of Kin-14	53
3.2 Homozygous rice mutants have lethal effects during seed germination	54
3.2.2 Rice heterozygous mutants show faint delay in seed germination	56
3.2.3 OsDLK potentially has a pivotal role during seedling development...	58
3.3 Localisation analysis of OsDLK in plant cells.....	58
3.3.1 Generated constructs for transformation	59
3.3.2 OsDLK is a dual localised kinesin	59
3.3.3 Visualisation of microtubules in fixed cells.....	65
3.3.4 Visualisation of OsDLK and further Kinesin-14 member OsKCH.....	68
3.4 Characterization of the biological role of OsDLK	69
3.4.1 Gene expression pattern in rice	69
3.4.2 Phenotype investigation of OsDLK overexpressor.....	71
3.5 Analysis of dynamic properties for OsDLK-GFP.....	77
3.5.1 The OsDLK-GFP overexpressor is more sensitive to oryzalin.....	77
3.5.2 The motor OsDLK-GFP exhibits dynamics <i>in vivo</i>	79
3.5.3 The motor OsDLK-GFP exhibits dynamics <i>in vitro</i>	80
3.6 Exposure for potential role of OsDLK in nucleus	80
3.6.1 OsDLK-GFP accumulates in cell nucleus in response to cold stress	81
3.6.2 Leptomycin B causes accumulation of OsDLK-GFP in the nucleus ..	85

3.6.3 OsDLK shows affinity to DNA binding motives	86
3.7 Summary of results	89
4. Discussion	91
4.1 OsDLK is a dynamic minus-end directed class XIV-kinesin	91
4.1.1 OsDLK is a C-terminal motor of Kinesin-14 members	91
4.1.2 OsDLK is a minus-end directed motor with high mobility	92
4.2 OsDLK has an important role in seedling development	93
4.2.1 Homozygous rice mutant is not viable	93
4.2.2 Rice mutant is delayed in the coleoptile elongation	95
4.3 OsDLK potentially interacts with other plant hormones	96
4.3.1 OsDLK is expressed tissue specifically	96
4.3.2 Gene expression of OsDLK in rice is regulated by red light	97
4.4 OsDLK affects the progression through the cell cycle	99
4.4.1 DLK stimulates cell proliferation	99
4.4.2 OsDLK overexpression affects cell expansion in tobacco	100
4.5 OsDLK is dynamically repartitioned during mitosis	101
4.6 OsDLK cycles between two locations during interphase	103
4.6.1 OsDLK has an unexpected dual localisations in interphase	103
4.6.2 OsDLK has two cycling subpopulations	105
5. Conclusion and Perspectives	107
6. Reference	109
7. Appendix	127
CURRICULUM VITAE	145

Abstract

The plant cytoskeleton is comprised of two different types of protein polymers: actin filaments and microtubules. They contribute to the cell innate directionality (cell axis, cell polarity) of plant cells that guide morphogenesis up to the organismic level. Motors are a kind of proteins which can bind to the cytoskeleton and use the energy from ATP hydrolysis to move and transport cargoes along the cytoskeleton with certain directionality. While myosins are actin-filaments based motors, kinesins and dyneins move along microtubules. Conventional kinesins have plus-end directionality and dyneins move towards the minus ends. However, one of the most striking peculiarities of plant directionality is the absence of microtubule minus end-directed cytoplasmic dynein motors in most Gymnosperms, and in all Angiosperms. In contrast, a specific class of minus end-directed kinesins, generally referred to as class-XIV kinesins, have been expanded the most in land plants. Some people believe that some of the functions of dyneins have been taken over by Kinesin-14 members.

In this study, the subcellular function of a class-XIV kinesin referred as OsDLK was addressed. Nevertheless, the heterozygous mutants of rice showed delay in coleoptile elongation in comparison with the wild type seedlings. The homozygous mutants were not able to gain during several generations. Later, *dlk* showed a relatively high transcripts level during the first 4 days of seeds germination, indicating an important role of OsDLK during early stage of rice seedling development.

In order to get insight of the subcellular role, OsDLK fused with fluorescent reporter was overexpressed in tobacco BY-2 cells (*Nicotiana tabacum*). We showed by in-vitro sliding that it has the ability to bind to microtubules and move towards its minus-end.

The overexpression of this GFP fusion protein stimulated proliferation and delayed the transition into cell expansion. By synchronising the cell cycle, we could show that the progression into metaphase was delayed in the overexpressor cells while the later phases were clearly accelerated.

Following its localisation during the cell cycle, fusion protein was observed to be repartitioned, colocalising with the wall associated arrays of microtubules (cortical microtubules, phragmoplast). Surprisingly, this protein was found to occur in two

populations in interphase - one subpopulation was associated with cortical microtubules as observed in other class-XIV kinesins, the other population was localised in the nucleus. The partitioning of the protein to the nucleus could be specifically stimulated by cold stress, or by inhibiting nuclear export by the inhibitor Leptomycin B (200 nM). This nuclear accumulation was reversible. Since this kinesin was able to shuttle between two locations in a specific manner, we named this particular kinesin OsDLK for Dual Localisation Kinesin.

Zusammenfassung

Das pflanzliche Zytoskelett besteht aus zwei verschiedenen Arten von Proteinpolymeren: Aktinfilamente und Mikrotubuli. Sie tragen zur zelleigenen Richtung (Zellachse, Zellpolarität) von Pflanzenzellen bei, welche die Morphogenese bis hin zur organismischen Ebene bestimmt. Motoren sind eine Art von Proteinen, die an das Zytoskelett binden und die Energie aus der ATP-Hydrolyse verwenden können, um z.B. Vesikel entlang des Zytoskeletts in eine gewisse Richtung zu bewegen und zu transportieren. Während Myosine Motoren sind, die entlang von Aktinfilamenten laufen, bewegen sich Kinesine und Dyneine entlang von Mikrotubuli. Konventionelle Kinesine bewegen sich in Richtung des Plus-Endes der Mikrotubuli, während Dyneine sich in Richtung des Minus-Endes bewegen. Eine der auffälligsten Besonderheiten der pflanzlichen Motorproteine ist jedoch das Fehlen von in Richtung Minus-Ende laufenden zytoplasmatischen Dyneinmotoren in den meisten Gymnospermen und in allen Angiospermen. Im Gegensatz dazu wurde eine spezifische Klasse von in Richtung Minus-Ende laufenden Kinesinen in Landpflanzen entdeckt, die im Allgemeinen als Klasse-XIV-Kinesine bezeichnet werden. So liegt es nahe, dass einige der Funktionen von Dyneinen von Kinesinen der Klasse- XIV übernommen wurden.

In dieser Doktorarbeit wurde die subzelluläre Funktion eines als OsDLK bezeichneten Klasse-XIV-Kinesins untersucht. Die heterozygoten Reismutanten zeigten eine Verzögerung in der Koleoptilenstreckung im Vergleich zu den Keimlingen des Wildtyps. Die homozygoten Mutanten konnten dieses verzögerte Wachstum auch während mehrerer Generationen nicht aufholen. Später zeigte *dlk* ein relativ hohes Transkriptionsniveau während der ersten 4 Tage nach der Keimung, was auf eine wichtige Rolle von OsDLK während des frühen Stadiums der Reiskeimung hindeutet.

Um einen Einblick in die subzelluläre Funktionen zu erhalten, wurde OsDLK, welches mit einem fluoreszierenden Reporter fusioniert wurde, in BY-2 Tabakzellen (*Nicotiana tabacum*) überexprimiert. Wir zeigten durch ein In-vitro-sliding Assay, dass es die Fähigkeit hat, an Mikrotubuli zu binden und sich in Richtung Minus-Ende zu bewegen.

Die Überexpression dieser GFP-Fusion stimulierte die Zellproliferation und verzögerte den Übergang in die Zellexpansion. Durch die Synchronisierung des Zellzyklus konnten

wir zeigen, dass der Übergang in die Metaphase in der Überexpressionslinie verzögert wurde, während die späteren Phasen deutlich beschleunigt wurden.

Die Lokalisierung von OsDLK während des Zellzyklus ergab, dass das Fusionsprotein neu verteilt wurde und mit den zellwandnahen Bereichen der Mikrotubuli (kortikale Mikrotubuli, Phragmoplast) kolokalisierte. Überraschenderweise stellte sich heraus, dass OsDLK in zwei Populationen in der Interphase auftritt: Eine Subpopulation war mit den kortikalen Mikrotubuli verbunden, was bereits bei anderen Klasse-XIV-Kinesinen beobachtet wurde, die andere Population wurde im Zellkern lokalisiert. Die Verteilung des Proteins auf den Zellkern konnte durch Kältestress oder durch Hemmung des Kernexports durch den Hemmstoff Leptomycin B (200 nM) spezifisch stimuliert werden. Diese Anhäufung von OsDLK im Kern war reversibel. Da dieses Kinesin in der Lage war, sich zwischen zwei Orten in einer bestimmten Weise hin- und herzubewegen, nannten wir dieses besondere Kinesin OsDLK, was für Dual Localisation Kinesin steht.

1. Introduction

Animals have the ability to move and their shape is fairly independent of environment. In contrast, plants are bound to their original position. Therefore plants have developed special adaptive mechanisms to environmental challenges. As a consequence, morphogenetic plasticity has become the major strategy for plants to escape from disadvantageous environmental changes (Nick, 2000). Mechanical stress is the main factor which can affect plant architecture to a large extent. For instance, a lot of aquatic plants have a large surface based on simple architecture maintained by buoyancy.

Plant shape and mechanisms of pattern formation have a very close relationship which is also defined by the individual cells. Plant cell shape depends on the interaction between cell wall and expanding protoplast. Rigid cell walls limit and counteract the force outwards provided by swelling vacuoles. Changes in an individual cell could also lead to changes in plant shape, improving the repartition and resistance to mechanical stress.

Axis and orientation play essential roles in a polar, patterned development. Spatial control of cell expansion and cell division contributes to morphogenesis in plant. The plant morphogenetic plasticity is mirrored by a cell axis in initial cell division and subsequent cell expansion, which are both related to microtubule arrays. In a certain sense, cell division is placed upstream because it determines the symmetry, axis and orientation of the newly formed cell wall and the framework of cell expansion. It is the cell division which lays down the spatial control of subsequent cell growth.

In addition, Vöchting, (1878) has found the key role of plant polarity for development in the regeneration of new organs on branch cuttings (Fig. 1). He found that in an inverted willow branch, the roots and shoots emerged according to the former orientation of the branch, demonstrating the innate polarity of the plant tissues was the major factor for regeneration rather than an environmental factor. This memory of the original axis was referred to as polarity and was traced down in individual cells. In other words, the polarity of tissues is due to the sum polarities of its cells. Cell polarity is intimately linked with the directional flow of signals, including plant hormones, especially auxin, and the organisation of cytoskeleton.

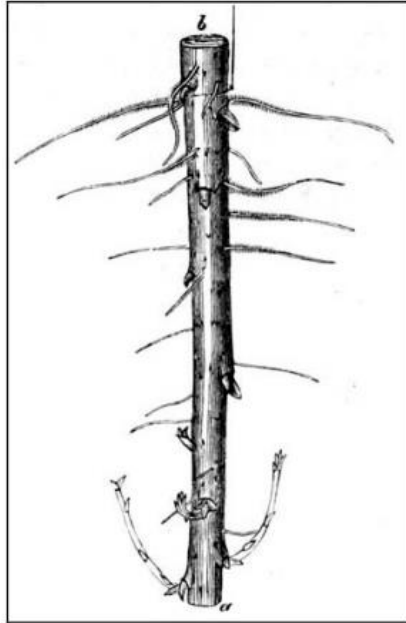


Figure 1 Evidence for a polarity of plant tissues. Cuttings taken along a willow branch all exhibit the same polar regeneration, even if the cuttings are kept inverted. Roots regenerate from the former base of a willow branch cutting (b), and bud growth occurs on its former apical side (a). Image source: Vöchting, 1878.

1.1 Microtubule-one of the dynamic cellular players

The cytoskeleton has the advantage to keep the structure, be highly dynamic and have the capacity to respond to a range of signals and further can control morphogenesis on cellular level, which in turn enhances the adaption of plant shape to various environment changes (Nick, 1999). In addition, cytoskeleton has also been found to convey the functions for driving intracellular transport. The cytoskeleton consists of three main components, which are actin filaments, microtubules and intermediate filaments (Fig. 2). Septins as a fourth component of the cytoskeleton was also identified (Mostowy & Cossart, 2012). However, both intermediate filaments and septins seem to be absent in plants.

Actin filaments and microtubules establish dynamic filamentous networks in plant cell. These are intimately involved in various cellular functions in development, including cell growth (division and expansion), cell morphogenesis, intracellular transport, and the maintenance of stability.

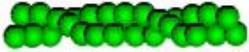



	Structure	Size	Subunit
Actin filaments		5-7 nm	actin
Intermediate filaments		8-12 nm	lamin, keratin, and others
Microtubules		25 nm	α -tubulin β -tubulin
Septins		5 nm	septin

Figure 2 Cytoskeletal components and their subunits. Image source: Schneider, (2015).

1.1.1 Structure of microtubules

Microtubules are composed of tubulin subunits of two 50 kDa proteins, α - and β -tubulin as the building blocks (Fig. 3a). They are rigid, hollow rods with a diameter of 25 nm (Fig. 3b). When GTP is bound, these two tubulins can polymerize end-to-end into protofilaments, forming parallel self-arranged hollow cylindrical filament. 13 tubulin dimers from different protofilaments can form one turn of the helix. With addition of tubulin subunits to the ends of protofilaments, the microtubules elongate. Due to polymerisation and depolymerisation of tubulin dimers, microtubules can undergo continuously rapid cycles of assembly and disassembly, regulated by GTP binding and hydrolysis by exchanging of a guanine nucleotide on the β -tubulin monomer (Fig. 3c). Polymerisation is typically initiated when GFP is loaded to the tubulin subunit. After incorporation of a subunit into microtubule, the GTP is hydrolyzed to GDP and release the inorganic phosphate.

Microtubules have dynamic structures. Treadmilling is one of the dynamic characteristics: On the one hand tubulin units are added to one side of the microtubules, on the other hand, subunits are constantly released at the other side, resulting in a section of filament seemingly "moving" across a stratum or the cytosol. Actually, assembly and disassembly can appear on both sides of the microtubules, which consequently results in polarity of microtubules with plus- and minus-end (reviewed by Mandelkow & Mandelkow, 1990). The plus end has quick growth and shrinkage

(Ambrose & Wasteneys, 2014) while the minus end is protected from depolymerisation (Goodwin & Vale, 2010). When the velocity of polymerisation is higher than GTP hydrolysis, a cap of GTP-bound subunits is generated at the plus-end. In addition, microtubules also have a characteristic so called dynamic instability. Tubulin polymerisation of elongating microtubules can be suddenly interrupted by depolymerisation. Phases of polymerisation and therefore elongation of microtubules are interrupted by sudden depolymerisation. These depolymerisation events start with “catastrophe” points and this can be “rescued” by a new polymerisation point. Due to the dynamic instability, microtubules have the ability to turnover rapidly within the cell in only several minutes, which is the half-life of typical microtubules (reviewed by Desai & Mitchison, 1997).

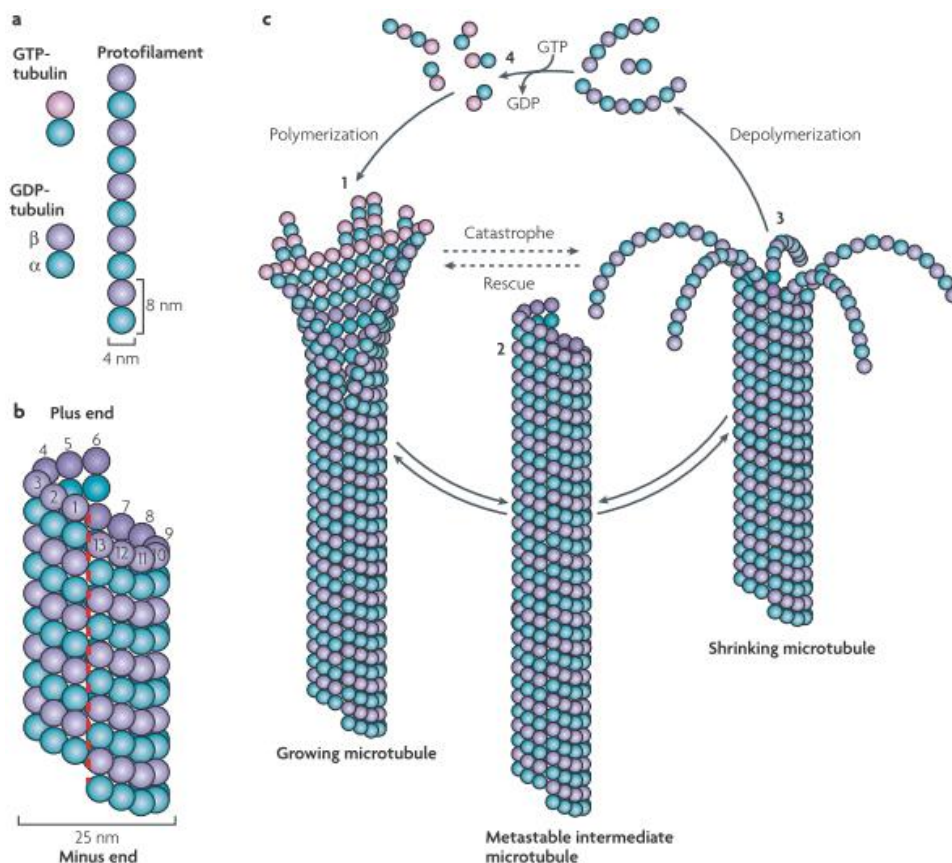


Figure 3 Microtubule structure and dynamic instability. (a) Microtubules are composed of stable α/β -tubulin heterodimers. (b) The cylindrical and helical microtubule wall typically comprises 13 parallel protofilaments generating the lattice seam (red dashed line) *in vivo*. (c) Assembly and disassembly of microtubules. GTP hydrolysis is not required for microtubule assembly, but is necessary for switching between catastrophe and rescue. 1, Polymerisation is typically initiated from a pool of GTP-loaded tubulin subunits. Growing microtubule ends fluctuate between slightly bent and straight protofilament sheets. GTP hydrolysis and release of inorganic phosphate occurs shortly after incorporation and is

promoted by burial and locking of the partially exposed nucleotide as a result of the head-to-tail assembly of dimers. 2, Closure of the terminal sheet structure generates a metastable, blunt-ended microtubule intermediate, which might pause, undergo further growth or switch to the depolymerisation phase. 3, A shrinking microtubule is characterized by fountain-like arrays of ring and spiral protofilament structures. This conformational change, which is presumably directed by tubulin-GDP, may destabilize lateral contacts between adjacent protofilaments. 4, The polymerisation–depolymerisation cycle is completed by exchanging GDP of the disassembly products with GTP. Image source: Akhmanova et al., 2008.

1.1.2 Functions of microtubules

Plant cytoskeletons play a pivotal role in fundamental processes such as cell division, expansion, differentiation and cell-to-cell communication during the development of multicellular organisms. Plant morphogenesis is strictly controlled by the orientation of cell division planes and the direction of cell expansion, both of which depend on microtubule arrays to a large extent. Higher plant microtubule arrays include cortical microtubules, radial microtubules, preprophase band, spindle, and phragmoplast. They convey numerous of functions such as spindle formation and chromosome separation during mitosis, and organelle- or vesicle trafficking, and signal transduction as well as the regulation of cell-wall texture during cell expansion (Nick, 2014). In addition, microtubules can also act as sensors in response to gravity, osmotic stress, cold or mechanical forces (Nick, 2008). They also are involved in pathogen defense in plants.

Plant microtubules (MTs) are pivotal for cell division (Fig. 4). Microtubule spindle apparatus, an array of MTs and their associated proteins play a key role in segregating genetic materials into daughter nuclei (Ambrose, 2005). At prometaphase and metaphase, microtubules extend from the spindle poles in an antiparallel manner, so that the slower-growing minus-ends are anchored at the spindle poles and the faster-growing plus-ends are attached and congressing chromosomes at the spindle equator (Euteneur & McIntosh, 1981; Hoyt & Geiser, 1996). The separation movement of chromosomes to the poles depends on the kinetochore microtubules. With the extension of non-kinetochore microtubules, two groups of chromosomes are distanced by elongated spindle. Besides, in plant cells, particularly presence of a microtubule-based preprophase band (PPB) before nuclear envelope breakdown functions in predicting the

cell division site and phragmoplast appearing in telophase guides vesicle deposition during cytokinesis for new cell plate formation.

MTs are also very important in plant cell expansion. Especially in elongating plant tissue, an ordered array of cortical microtubules (cMTs) defines the cell axis and determines the arrangement of cellulose microfibrils in the expanding cell wall by guiding cellulose-synthesizing complexes (Green, 1962; reviewed by Nick, 2008). In addition, the reorientation of these microtubule arrays could be stimulated by both endogenous and environmental factors. Hence, cell expansion and reorientation of MTs commonly appears in tip growth of pollen tubes or root hairs with directional cues.

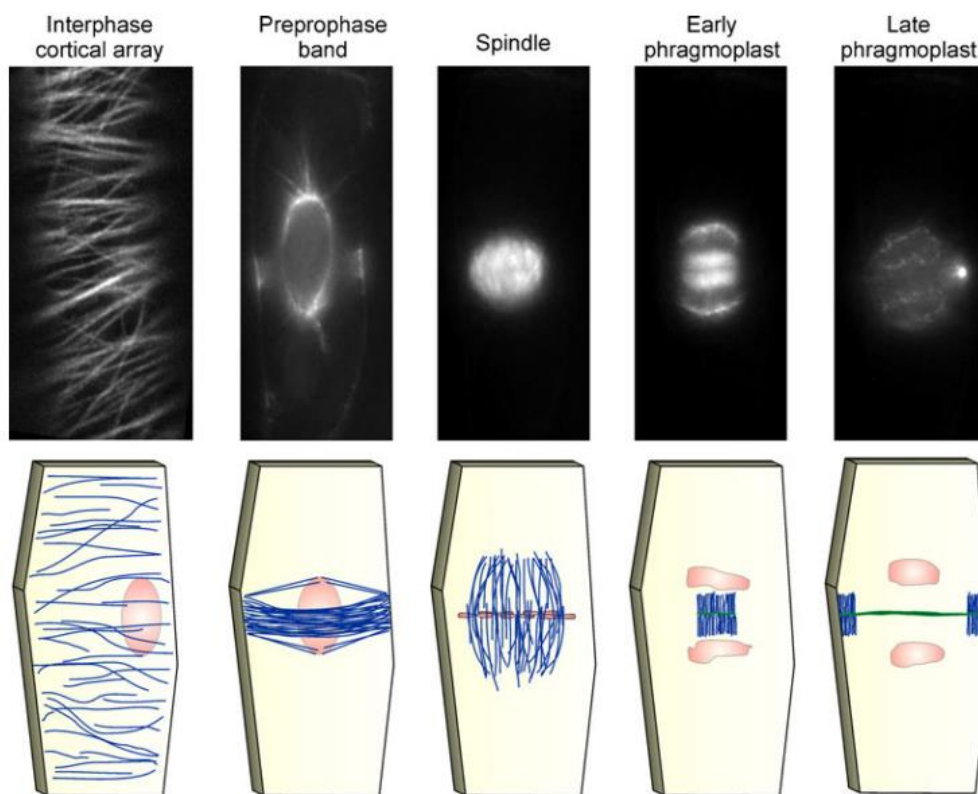


Figure 4 Plant microtubule arrays at various stages of the cell cycle. Images on the top show the major plant microtubule arrays visualized using GFP-labelled tubulin in tobacco BY2 cells. In the cartoons, the nucleus is shown in red, microtubules are shown in blue, and the cell plate is shown in green. Image source: Zhu & Dixit, 2012.

1.2 Kinesins–MTs associated proteins

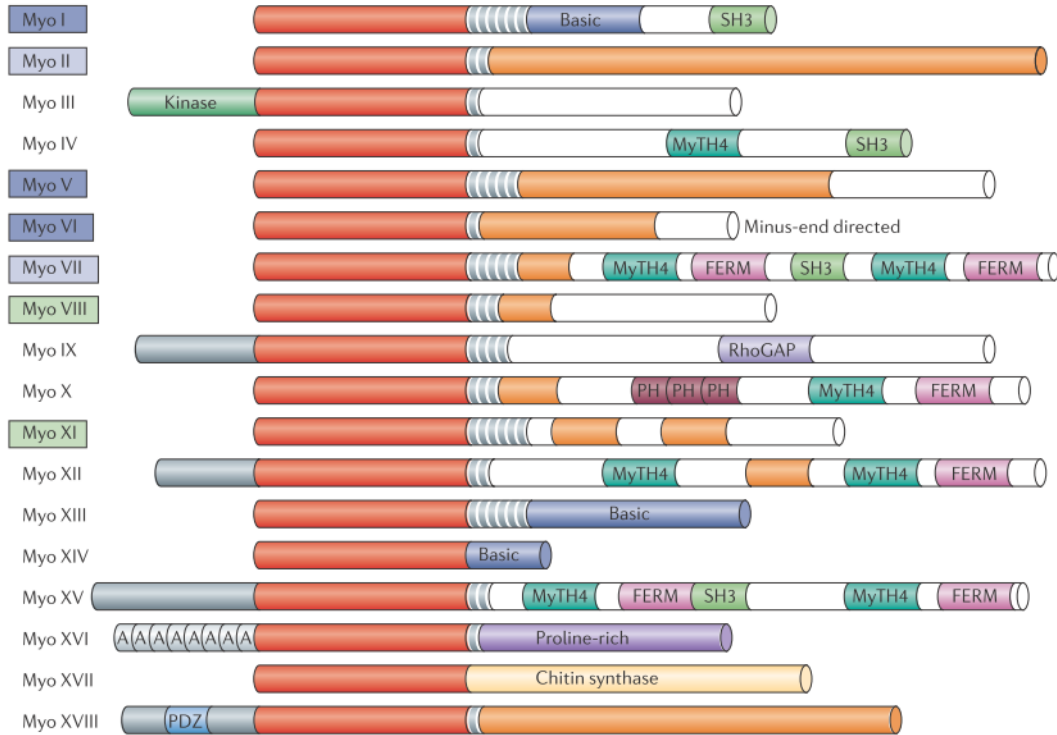
In animals and fungi, numerous proteins have been identified to be associated with the cytoskeleton, either in a bifunctional way or as complexes of monofunctional proteins.

Plant cells show a distinct directionality (cell axis, cell polarity) (Hyman & Mitchison, 1991), which is guiding morphogenesis up to the organismic level. Both, microtubules and actin filaments, are endowed with an innate directionality as well, which not only turns manifest as dynamic difference of the two poles of the polymer, but is translated, by molecular motors, into a directionality of dynamic processes.

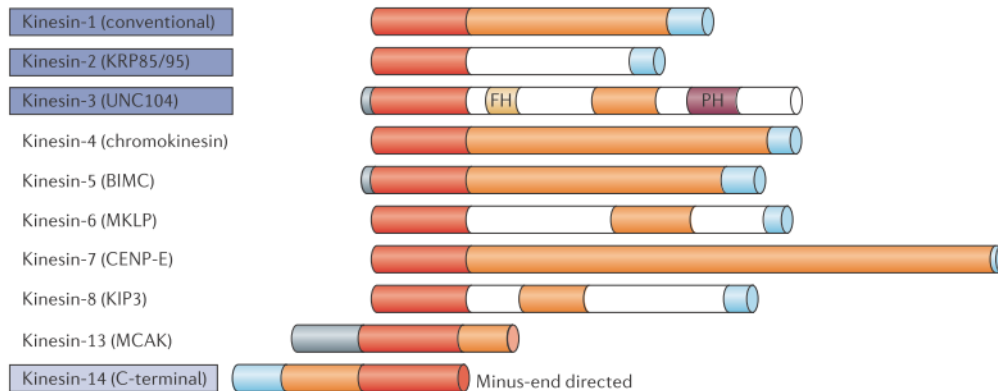
1.2.1 Molecular motors along cytoskeleton

In non-plant systems, three kinds of molecular motors including the microtubule-based motor (kinesins, dyneins) and actin-based motors (myosins) have been distinguished during last decades (Fig. 5) (reviewed by Soldati & Schliwa, 2006). Mammals have genes for over hundreds of motors, and any given cell might express more than 50 of them. Myosin superfamily comprises 24 classes (Foth et al., 2006) and dyneins can be divided into at least 15 subfamilies (Lawrence et al., 2004). Kinesins have been divided into 14 subfamilies and some orphans which will be talked in detail in the next paragraphs.

a Myosin motors



b Microtubule motors



c Dynein motors



Motor families involved in membrane trafficking	PH Pleckstrin-homology domain
Motor families with some members involved in membrane trafficking	AAA Triple A-domain (ATPase associated with various activities)
Myosin families of plants with members involved in membrane trafficking	Ankyrin repeats
Motor domain	PDZ PDZ domain
N-terminal domain (functions are largely unknown)	FH Forkhead-associated domain
IQ-motifs (light-chain-binding domains)	HC/IC Heavy chain-intermediate chain interaction domain
Tail region, non-homologous	M Microtubule interaction site
Coiled-coil domain (often interrupted)	Region encompassing the stalk
SH3 SRC-homology-3 domain	
MyTH4 Myosin tail-homology-4 domain	
FERM Protein 4.1, ezrin, radixin, moesin domain	

Figure 5 The structural diversity of molecular motors. (a) 18 of the myosin superfamilies are shown here because they have members that have, to a certain degree, been characterized. (b) A new kinesin nomenclature now lists 14 kinesin families, 10 of which are shown (old nomenclature in parenthesis). (c) 14 subfamilies of dyneins are involved in the movement of cilia and flagella, and one is involved in cytoplasmic transport (shown). So far, only one class each of the myosins and kinesins have family members that move towards the minus end of actin filaments or microtubules, respectively. Image source: Soldati & Schliwa, 2006.

Kinesins or kinesin superfamily proteins (KIFs) have been expanded the most in the class of molecular motors, especially in flowering plants (Lee & Liu, 2004). The first kinesin was identified from giant axon of the squid as an ATPase involved in vesicles transportation along microtubules (Vale et al., 1985). Since that time, there has been an explosion in the newly found kinesins and kinesin-related proteins in all eukaryotes, including the protists, fungi, invertebrates, animals, and plants. Recently, global databases of the fully sequenced genomes of plants have helped for the identification of a great number of kinesin candidate genes. According to the drafts of the genomes, there are more than 40 genes encoding kinesins in rice cultivar *indica* and *japonica* (Table 1, Richardson et al., 2006). However, the special functions of the different kinesins in plants is still little known, to investigate their functional analysis is a wide ongoing subject.

RGAP	RAP	Sub-family	Known as	RGAP	RAP	Sub-family	Known as
LOC_Os01g14090	Os01g0243100	14		LOC_Os04g57140	Os04g0666900	14	KCBP
LOC_Os01g15540	Os01g0260100	14		Not annotated	Not annotated	14	OsKCHI
LOC_Os01g33040	Os01g0513900	7	OsNACK1	LOC_Os05g02670	Os05g0117798	5	
LOC_Os01g42070	Os01g0605500	8		LOC_Os05g06280	Os05g0154700	13	Kinesin-13A
LOC_Os01g43580	Os01g0625200	13		LOC_Os05g33030	Os05g0397900	14	
LOC_Os01g54080	Os01g0744000	14		LOC_Os05g38480	Os05g0459400	10	
LOC_Os02g01180	Os02g0101800	6		LOC_Os05g44560	Os05g0521300	14	
LOC_Os02g13570	Os02g0229500	β		LOC_Os06g04560	Os06g0137100	UG	
LOC_Os02g13580	Os02g0229600	14		LOC_Os06g11380	Os06g0217600	14	
LOC_Os02g28850	Os02g0489800	12	Kinesin-12B	LOC_Os06g36080	Os06g0554700	14	
LOC_Os02g43050	Os02g0644400	7		LOC_Os07g01490	Os07g0105700	14	
LOC_Os02g43130	Os02g0645100	7		LOC_Os07g44400	Os07g0638000	12	
LOC_Os02g50910	Os02g0742800	4		LOC_Os08g02380	Os08g0117000	1	
LOC_Os02g53520	Os02g0775400	7	K16	LOC_Os08g43400	Os08g0547500	7	
LOC_Os02g56540	Os02g0810200	UG	PAKRP2	LOC_Os08g44420	Os08g0558400	5	
LOC_Os03g02290	Os03g0114000	14		LOC_Os09g02650	Os09g0114500	4	
LOC_Os03g05820	Os03g0152900	UG		LOC_Os09g25380	Os09g0421200	7	
LOC_Os03g17164	Not annotated	5		LOC_Os09g35890	Os09g0528000	7	
LOC_Os03g18980	Os03g0301800	14		LOC_Os10g36880	Os10g0512800	7	
LOC_Os03g39020	Os03g0587200	12		LOC_Os11g35090	Os11g0552600	7	
LOC_Os03g53920	Os03g0750200	12		LOC_Os11g37140	Os11g0581000	12	
LOC_Os03g56260	Os03g0773600	8		LOC_Os11g42800	Os11g0648100	14	
LOC_Os03g64415	Os03g0862200	14		LOC_Os11g44880	Os11g0672400	14	
LOC_Os04g28260	Os04g0350300	12	PAKRP1, Kinesin-12A	LOC_Os12g36100	Os12g0547500	14	
LOC_Os04g30720	Os04g0375900	10		LOC_Os12g39980	Os12g0590500	12	
LOC_Os04g45580	Os04g0538800	7		LOC_Os12g42160	Os12g0616000	14	
LOC_Os04g53760	Os04g0629700	14					

Table 1 List of kinesins in rice. IDs of these proteins were assigned by RGAP and RAP, respectively. Documented members are listed with their known names. Note that one of the Kinesin-14 members has

been annotated into two loci by RGAP and RAP, and OsKCH1 on chromosome IV was not annotated by both. Orphan kinesins were noted as UG for ungrouped. Image source: Guo et al., 2009.

1.2.2 Characteristics of kinesin motors

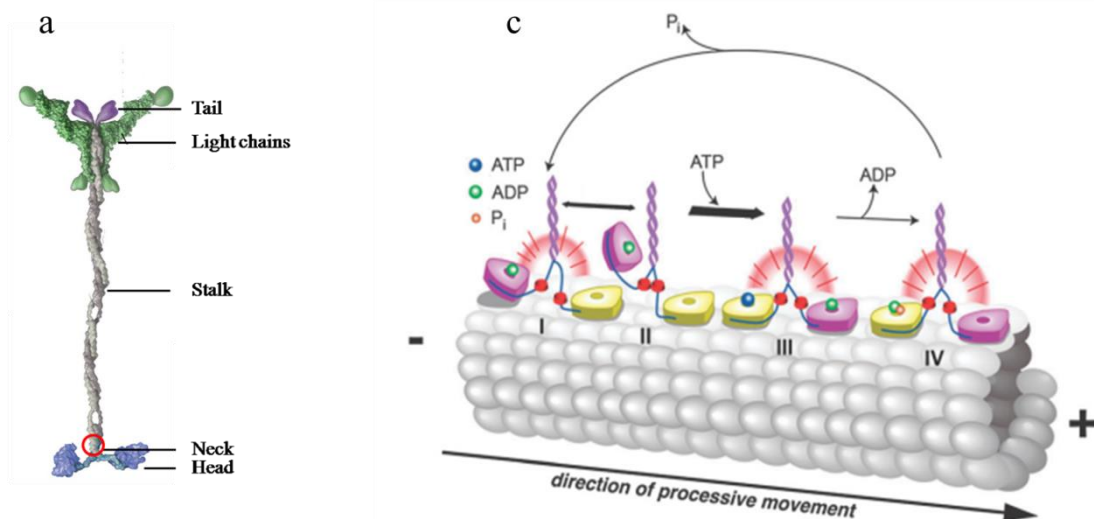
Although both structure and function are various in different kinesins, structural characteristics remain conserved to a large degree. Native kinesin often exhibiting tripartite structure consists of two light chains and two heavy chains. The heavy chain has three structural domains in common (Fig. 6a) (reviewed by Howard, 2001): a globular, 360-residue motor domain plus the neck generating directional forces located in the amino-terminal region, containing catalytic pockets for the ATP hydrolysis and the binding sites for microtubules, a central stalk region including one or several alpha-helical coiled-coil domains involved in oligomerization of kinesins to homo- or heterodimers or even tetramers, and a globular fan-shaped tail that binds to two light chains or recognizing diverse cargoes. With the energy released from ATP hydrolysis in the motor domain, kinesins can move along microtubules while the tail domain is responsible for recognition of various cargoes, such as proteins, lipids or nucleic acids or holoenzymes (reviewed in Miki et al., 2005; Hirokawa et al, 2009).

Members of kinesin superfamily transport intracellular cargoes along microtubules with characteristic polarity. Although in the motor catalytic cores, different kinesin proteins share $30\pm 50\%$ amino-acid identity, most kinesins move toward the unstable plus-ends of microtubules, others travel in the opposite direction, the more stable minus-ends. What is the directionality of plus- and minus-end kinesin movement based on? Actually, a “neck” domain in the motor region was found to be involved in directionality determination.

Endow & Waligora, (1998) showed that the complementary construct ncd-Nkin consisting of Ncd motor domain and a kinesin heavy chain stalk-neck region was a plus-end driven motor in vitro while in contrast NcdKHC1, the complementary construct consisting of the Ncd stalk-neck fused to a kinesin motor core, was a minus-end microtubule motor that reversed the directionality of kinesin (Fig. 6b). For the plus end-directed kinesins, the “neck” domain is formed by $\beta 9$ and $\beta 10$ strands and a helical coiled-coil region, containing 34 amino acids. The coiled-coil region has charged or

hydrophilic residues that destabilize and distinguish the neck from the more stable stalk. For minus-end-directed kinesins, a 14 amino acid peptide region is continuous with the stalk. The crystal structures between these two kinds of motors are different in the orientation of the heads relative to the stalks, reflecting the opposite directionalities (Kozielski et al., 1997, Sack & Mandelkow, 1999; reviewed by Endow, 1999).

Processivity, an intrinsic property for kinesins, is an interaction between feet, fuel and track (Delius & Leigh, 2011). The processive movement was first demonstrated for single molecules of conventional kinesin (Howard et al., 1989). The double-headed motor protein kinesin moves along microtubules in a way to hydrolyse one ATP molecule per 8-nm step (Schnitzer & Block, 1997; Hua et al., 1997; Coy et al., 1999). For a processive molecular walker, at least one foot should bind to the molecular track at all times to take successive steps before detaching (Asbury et al., 2003). A hand-over-hand (walking) model (Fig. 6c) for kinesin motility was strongly supported by Yildiz et al. (2004). However, several types of experiments have led to the conclusion that some kinesins are nonprocessive. They work cooperatively along the microtubules. Individual motors within the array bind weakly to the microtubule others bond tightly. The weakly bound motors maintain attachment of the cargo to the microtubule and permit diffusional sliding (Rogers et al., 2001; Endow & Barker, 2003).



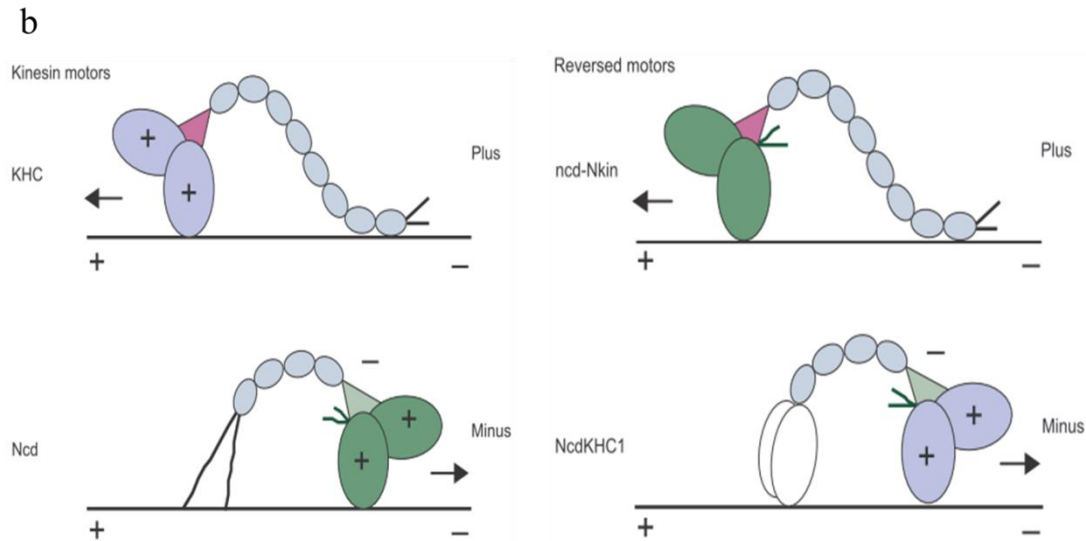


Figure 6 The structure and motility of kinesins. (a) Conventional kinesins. Modified from Vale, 2003. (b) Direction of the motors is indicated at the right. Kinesin motors. Conventional kinesin, a plus-end motor, and Ncd, a minus-end motor, both contain plus-end determinants in their motor cores. The neck of Ncd contains minus-end directionality determinants. Reversed motors. The ncd-Nkin reversed motor 31 consists of the Ncd motor domain (dark green) fused to a kinesin heavy chain stalk–neck region. The kinesin neck is shown in dark pink. The NcdKHC1 reversed motor 34 consists of glutathione-S-transferase (white) joined to the Ncd stalk–neck followed by the kinesin motor core (light blue). The Ncd neck is shown in light green. Image source: Endow, 1999. (c) Simplified 'hand-over-hand' model for kinesin-I motility. Image source: Toprak et al., 2009, adapted by von Delius & Leigh, 2011.

1.2.3 The superfamilies and functions of kinesins

Kinesins have been explored to have several kinds of functions in cell development (Table 2). In addition, kinesins are classified into 14 designated sub-families and some orphans according to the sequence homology in their motor domains (Lawrence et al., 2004). Remarkably, members of kinesins-14 including C-terminal motor members are reported to have minus-end directionality.

Most plant kinesins are evolutionarily divergent in the non-motor domains from their animal and fungal counterparts, except for members of Kinesin-5, Kinesin-6 and a few members of Kinesin-14 which have conserved non-motor sequences and mitotic functions (reviewed by Miki et al., 2005). Actually, researchers have tried to use a variety of approaches to analysis the completed genome sequences systematically to

identify the kinesins. The phylogenetic analysis of kinesins of a total of 529 kinesins from 19 species has revealed that there are some striking differences in the composition of kinesins between plants and other organisms (Fig. 7) (Richardson et al., 2006). Generally, angiosperms have the highest number of kinesins, especially for *Arabidopsis*, which has the largest repertoire of kinesins. Genome duplication may have contributed to the expansions of kinesins in this group.

Kinesin subfamily	Motor polarity	Functions
BimC	Plus	Cell division (required for SPB separation. Centrosome separation, bipolar spindle formation and maintenance)
Cel subfamily	ND	ND
Chromokinesin/KIF4 subfamily	Plus	Cell division (binds DNA, required positioning of chromosomes, spindle stabilization)
C-terminal motor subfamily	Minus	Cell division (required for spindle formation, spindle integrity, karyogamy) and trichome morphogenesis
KHC subfamily	Plus	Transport
KIP3 subfamily	ND	ND
KRP85/95 subfamily	Plus	Organelle transport, flagellar assembly/maintenance
MCAK/KIF2 subfamily	Plus	Cell division and transport
MKLP1 subfamily	Plus	Cell division (pole separation during anaphase B)
Unc 104 subfamily	Plus	Vesicle and organelle transport
Ungrouped kinesins	Plus	Cell division and flagellar beating

Table 2 Subfamilies of kinesins and their functions in plants (ND, not determined). Image source: Reddy, 2003.

The analysis of kinesin families should also provide some insights into evolution of kinesins in flowering plants (Fig. 7). For instance, although *Chlamydomonas reinhardtii*, a member of chlorophyte algae, which represents the sister group of the flowering plants, is unicellular, it has 23 kinesins (Richardson et al., 2006). Seven of the ten kinesin families in flowering plants are present in *Chlamydomonas* (Eichinger et al., 2005). Kinesin-1, -6 and -10 of flowering plants seem to have been lost in the *Chlamydomonas* lineage while two families (Kinesin-2 and Kinesin-9) which are present in *Chlamydomonas* are lost in the flowering-plant lineage. Totally, at least three families of kinesins (Kinesin-2, Kinesin-3, Kinesin-9 and/or Kinesin-11, it is unclear because of the unresolved flowering-plant clade), are conspicuously absent in all the sequenced flowering plants. And only four (Kinesin-5, -7, -12 and 14) are present in all photosynthetic eukaryotes (Richardson et al., 2006). In contrast, the Kinesin-7 and 14 families are greatly expanded in higher plants.

Huge disparity in the distribution of kinesins is still unclear. However, people have tried to understand of the reason behind. Members of either homo- or heterodimers from Kinesin-2 are present in ciliated and flagellated cells and are involved in transportation of flagellar organelles (Vale, 2003; Miki et al., 2005). *Chlamydomonas*, a flagellated unicellular photosynthetic eukaryote also has one Kinesin-2 member, which also function in flagellar organelles transport (Rosenbaum & Witman, 2002). The absence of flagella/cilia in the life cycle of flowering plants may have led to the loss of Kinesin-2 subfamily in this lineage. Instead, the pollen tube was developed. The members of the Kinesin-3 subfamily, which are involved in organelle transport, have expanded most in animal cells. Moreover, other kinesins in animal cells which may have a role in cargo-transport processes, are clearly decreased in flowering plants (Richardson et al., 2006), implicating that these function of kinesins are lost during evolution or performed by other motors, for instance, myosins (Reddy & Day, 2001). In addition, as mentioned above, dyneins as well as dynactin-complex proteins were identified only in members of lower members (Wickstead & Gull, 2007).

Conventional kinesins move towards the plus-end of the microtubule while dyneins have minus end-driven directionality in cytoplasm. Thus the lack of the flagellar Kinesin-2 motors and the absence of sequence homologues to cytoplasmic and flagellar dyneins suggest that these genes and their functions may have disappeared in angiosperms with the loss of the flagellar apparatus concomitantly. The rise of the minus-end directed class-XIV kinesins and the parallel fall of dyneins which is responsible for much of the minus end-directed membrane trafficking in plant cells (Vale, 2003), is probably linked with the loss of flagella-driven motility that was progressively confined to the motile sperm cells (in Bryophytes, Pteridophytes, and early Gymnosperms), and, eventually became dispensable by the development of a pollen tube. An interesting missing link is found in primitive gymnosperms, such as *Ginkgo* or *Cycas*, where the pollen tube bursts open only 50 μm before reaching the egg cell, releasing the flagellate spermatozoid (Fujii, 1899). In the red alga *Cyanidioschyzon merolae*, the absence of myosins and dyneins suggests that kinesins play key roles in this species (Matsuzaki et al., 2004; Richards et al., 2005).

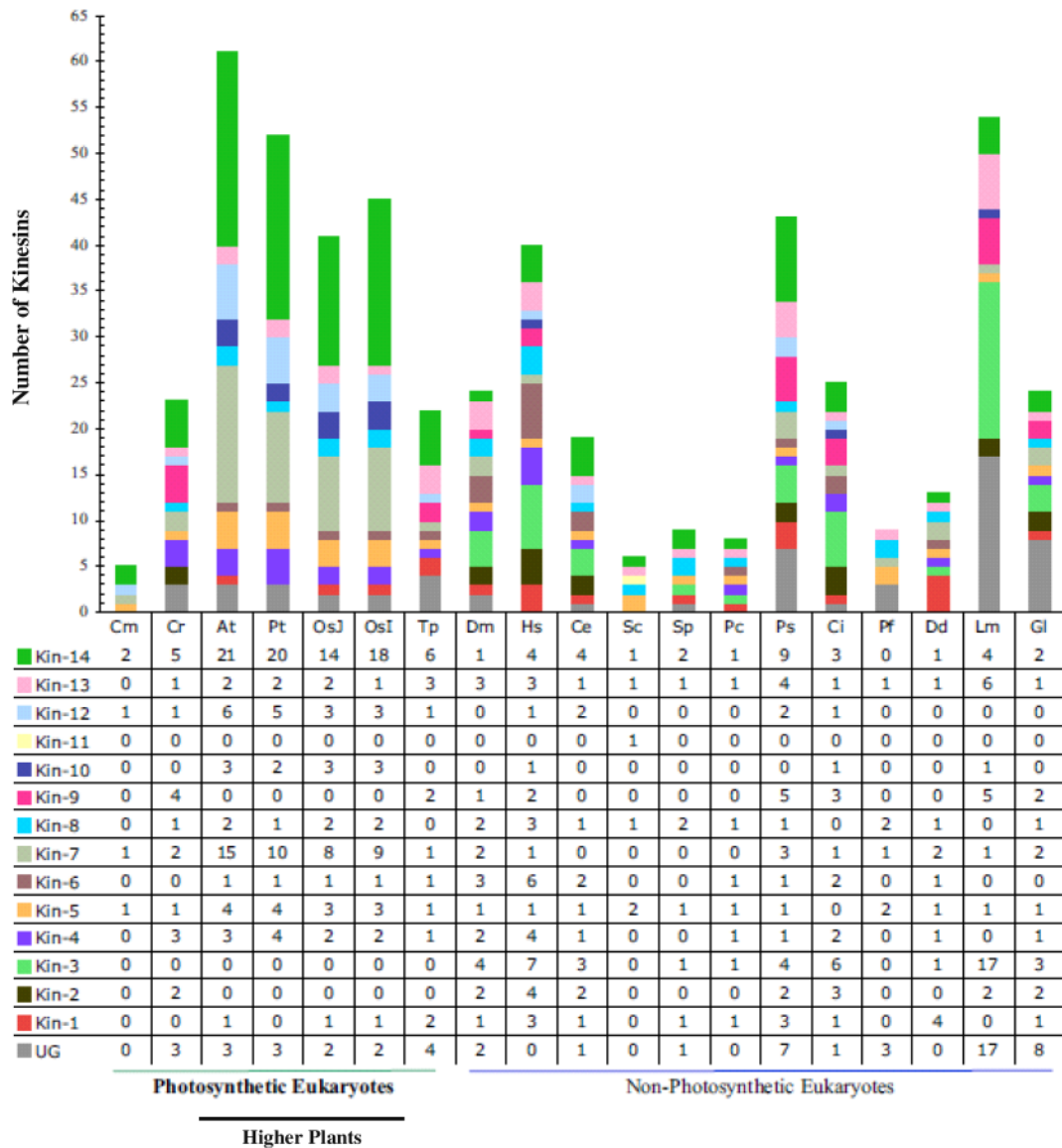


Figure 7 Number and distribution of kinesins. Tabular and graphical representation of the number of kinesins found in completely sequenced genomes used in our analysis. Different colours represent the distribution of kinesins into specific families. The data table below the chart details the specific number of kinesins in each family per species. For individual sequence IDs, please see Tables 2 through 7 and Additional files 1 through 12. Cm, *Cyanidoschyzon merolae*; Cr, *Chlamydomonas reinhardtii*; At, *Arabidopsis thaliana*; Pt, *Populus trichocarpa*; OsJ, *Oryza sativa* ssp. *Japonica*; OsI, *Oryza sativa* ssp. *Indica*; Tp, *Thalassiosira pseudonana*; Dm, *Drosophila melanogaster*; Hs, *Homo sapiens*; Ce, *Caenorhabditis elegans*; Sc, *Saccharomyces cerevisiae*; Sp, *Schizosaccharomyces pombe*; Pc, *Phaenerochaete chrysosporium*; Ps, *Phytophthora sojae*; Ci, *Ciona intestinalis*; Pf, *Plasmodium falciparum*; Dd, *Dictyostelium discoideum*; Lm, *Leishmania major*; Gl, *Giardia lamblia*. Image source: Richardson et al., 2006.

The loss of flagella was accompanied by a loss of centriole as major microtubule-organizing center (Lawrence et al., 2001). Instead, a novel microtubule structure, the

phragmoplast, emerged and adopted the spatial organisation of the new cell plate. In the recent comprehensive review, Buschmann & Zachgo, (2016), it is showed that the loss of centrosomes happened several times independently, while the alignment of the phragmoplast became supported by the emergence of a second, novel microtubule array, the preprophase band.

Since the functionality of the division spindle requires microtubule transport in both directions, the functions conveyed by dyneins in animal cells, must be taken over by minus-end directed kinesins in plants (Koonce, 1996; Sharp et al., 2000). In addition, several reports showed that the plants transport activities of macromolecules (e.g. RNA and proteins) and viruses from cell to cell through plasmodesmata also require kinesins (Reddy, 2001; Kim, 2005). These would be the explanations for the expansion of the Kinesin-14 in photosynthetic eukaryotes.

1.2.4 The superfamily of Kinesin-14

As mentioned above, all Kinesins-14 members possess the conserved neck which can determine minus-end motility (Mazumdar & Misteli, 2005). And this sub-family has been expanded the most during the evolution of flowering plants (about 35% of *Arabidopsis* kinesins fall in this group), which may reflect the fact that flowering plants do not have minus end-directed motor dynein.

Kinesin-14 is a diverse family existent in almost all major eukaryotic groups. The members of this family play important conserved cellular roles in evolution (Table 3). Kinesin-14 family members perform multiple functions in organelle transport during cell division and growth directly or indirectly in various tissues (Miki et al., 2005; Reddy, 2003). Members of the Kinesins-14 and 5 family function antagonistically in spindle assembly and function (Vale, 2003).

In the Kinesin-14 family, several subfamilies have been distinguished within this subfamily according to the localisation of their motor domain, located in the middle or at the N- or C-terminus. In *Arabidopsis*, functions of some Kinesin-14 family members have been investigated, including those that contain the motor domain at the C-terminus (KatA/ATK1 [At4g21270], ATK5 [At4g05190], KCBP [At5g65930]), N-terminus

(GRIMP/KCA1 [At5g10470]) and KCA2 [At5g65460]) or in the middle (KatD/KCH [At5g27000]) (Richardson et al., 2006). In fact, ATK1 (KatA) and ATK5 have been shown to bundle microtubules in the spindle midzone to generate inward forces to shorten the spindle length and focusing spindle poles by gathering parallel microtubules towards the poles (Liu et al. 1996; Ambrose et al. 2005). Both GRIMP/KCA1 and KCA2 interact with a cyclin-dependent kinase and localizes to MTs and phragmoplast, suggesting a role in cell division (Vanstraelen et al., 2004). GRIMP/KCA1 also interacts with a geminivirus replication protein (Kong et al., 2002).

Protein name	Sub family	Cellular localization	Ref.
AtKatA	14	mitosis MT arrays/spindle, phragmoplast, Chromosome segregation, spindle assembly	Mitsui et al., 1993; Liu et al., 1996
AtKatB	14	spindle, phragmoplast	Mitsui et al., 1994
AtKatC	14	spindle, phragmoplast	Tamura et al., 1999
AtKatD	14	microfilament- and microtubule-binding activity search and capture of antiparallel interpolar	Reddy et al., 1996
ATK5	14	microtubules	Ambrose & Richard, 2007 Reddy et al., 1996; Song et al., 1997; Day et al., 2000
AtKCBP	14	PPB, spindle, spindle poles, phragmoplast	Wang et al., 1996; Bowser & Reddy, 1997
NtKCBP	14	PPB, spindle, phragmoplast spindle, centrosomes, poles, spindle	Reddy, 1997
DmNcd	14	formation and integrity spindle, poles, Karyogamy (nuclear fusion	McDonald et al., 1990
ScKar3	14	after mating) opposite to Cin8/Kip1 Linkers between actin filaments and	Endow et al., 1994
OsKCH1	14	microtubules during nuclear positioning	Frey et al., 2009, 2010
NtKCH	14	Linkers between actin filaments	Klotz & Nick, 2012
AtKAC1/ KCA1	14	Actin-based chloroplast movement	Vanstraelen et al., 2004; Kong et al., 2002
AtKAC2/ KCA2	14	Actin-based chloroplast movement	Vanstraelen et al., 2004; Suetsugu et al., 2010
TvKCBP	14	Cell division	Vos et al., 2000
GhKCBP	14	Cell division Regulation of respiration during seed	Ni et al., 2005; Yang et al.,
AtKP1	14	germination at low temperature Dynamic microtubule–microfilament cross-	2011
GhKCH1	14	linking Dynamic microtubule–microfilament cross-	Preuss et al., 2004
GhKCH2	14	linking	Xu et al., 2009a

Table 3 Function and localisation of known kinesins-14 members. Modified from Li et al. (2012).

Many of the kinesin-14 members differ greatly in comparison to animal kinesin-14 with respect to structure and function. Some of them even contain additional plant-specific domains. Members of the KCH subgroup contain a motor core located in the center of the protein and an N-terminally positioned calponin-homology (CH) domain. They are involved in cross-talk between microtubules and actin microfilaments (Preuss et al., 2004; Xu et al., 2009; Frey et al., 2009, 2010). KCH members have been found in all investigated land plants while none partner has been found in animals, fungi and algae and one hypothesis suggests that the domain shuffling of a C-terminal motor may give rise to this group of internal motors (Richardson et al., 2006). A calmodulin-binding kinesin (KCBP/Zwichel) has been added to the group of Kinesin-14 (Reddy et al., 1996; Richardson et al., 2006). It contains a Ca^{2+} /calmodulin-binding peptide, and a myosin-tail homology domain (MyTH4) and a talin-like region (ERM). KCBP members contribute in MT organization/stability in cell division and trichome morphogenesis, regulated by calmodulin-binding in presence of calcium ions (Reddy et al., 1996; Oppenheimer et al., 1997; Vos et al., 2000; Reddy & Day, 2001), as the binding to microtubules is inhibited by calcium-calmodulin.

1.3 The scope of this work

Kinesin-14 member moves towards the minus end of microtubule which is in the opposite sense to classical kinesins. While in the dicot model *Arabidopsis*, the closely related class-XIV kinesins ATK1 and ATK5 both seem to localise to the phragmoplast, the monocot model rice harbours one homologue of these kinesins, leading to the question, whether this homologue (SwissProt accession number B8B6J5) might represent a minimal system to fulfil the functions conveyed by ATK1 and ATK5. However, very limited information has been obtained for other monocot species, such as rice.

In this study, a new kinesin was identified from the monocotyledon plant rice. We are going to characterise the molecular and cellular functions of this rice kinesin, named as OsDLK particularly. In order to see functional aspects in the context of the plant, you will work on regulation patterns in rice. We will also use the loss-of-function approach that *dlk* in rice genome was interrupted with Tos17 or T-DNA fragments. And the offsprings will be monitored with genotyping and the differences in morphology

between mutants and wild type plants should be investigated. However, since these mutants have shown to be lethal till sublethal, this approach has some limitations.

In order to see cellular aspects, especially the localisation, the heterologous system, tobacco BY-2 cell line will be used for the overexpression of OsDLK fused with fluorescent tag. A microscopic investigation should help in the localisation pattern of OsDLK and its association with microtubules during the cell cycle. The alterations of phenotype in BY-2 overexpression cells will also be detected. The progression of cell cycle will be monitored via synchronisation. Actually BY-2 suspension is the only plant system where the cell cycle can be synchronised. In companion, the nuclear migration will also be checked. The mobility of OsDLK will be investigated *in vivo* and *in vitro*. We will also detect the cycling between the two populations of cortical DLK and nuclear DLK with cold stress and the nuclear export inhibitor.

Finally, the protein of OsDLK was extracted from *E.coli* overexpression system to check the putative DNA-binding ability of OsDLK.

2. Materials and methods

2.1 *In silico* analysis

2.1.1 Phylogenetic analysis of Kinesins

To construct a phylogenetic tree, candidate kinesins from different kinesin subfamilies from different kingdoms, such as *Arabidopsis thaliana*, *Oryza sativa*, *Nicotiana tabacum*, *Gossypium hirsutum*, *Emericella nidulans*, *Drosophila melanogaster*, and *Saccharomyces cerevisiae* were aligned by the ClustalX algorithm (<http://www.clustal.org/download/2.0.11/>) and this alignment was then used to infer a phylogenetic tree by the neighbour-joining algorithm in MEGA5 (<http://www.megasoftware.net/>, Tamura et al., 2011).

Accession numbers in UniProtKB/Swiss-Prot (<http://www.uniprot.org/>) of protein sequence data used in the phylogenetic analysis can be accessed as follows: OsDLK (B8B6J5), DmNCD (P20480), EnKlpA (P28739), GhKCH1 (Q5MNMW6), NtTKRP125 (O23826), NtKCH (F8UN41), ScKar3 (P17119), OsACK1(Q9AWM8), OsKinesin13A (Q0DKM5), OsBC2 (Q6YUL8), OsKCH (Q0IMS9), AtARK2 (Q9LPC6), AtNACK1 (Q8S905), AtARK3 (Q9FZ06), AtKinesin12B (F4J464), AtNACK2 (Q8LNZ2), AtKCH (Q8W1Y3), ATK5 (F4JGP4), AtPAKRP2 (Q8VWI7), AtKatA (Q07970), AtKatB (P46864), AtMKRP2 (Q8W5R5), AtKCA1 (Q9LX99), AtKatD (O81635), AtKatC (P46875), AtKAC2 (Q9FKP4), AtKCBP (Q9FHN8).

2.1.2 Sequence analysis of OsDLK

The sequence motives and domains of OsDLK from *Oryza sativa* L. *japonica* were analysed by Prosite (<http://prosite.expasy.org/cgi-bin/prosite>) and SMART (<http://smart.embl-heidelberg.de/smart>). The neck region was predicted according to Amos & Hirose, (1997), and Endow, (1999). To determine potential coiled coil regions within the OsDLK sequence, the software COILs

(http://www.ch.embnet.org/software/COILS_form.html) was used according to the description in Lupas et al. (1991). The analysis was performed at window width of 14, 21, and 28 aa with both a weighted and an unweight matrix, respectively to minimize false positives. Only sequence stretches that did not differ by more than 20 percent in all analysis shown. A protein structure model was predicted using protein model portal (<http://www.proteinmodelportal.org>) and rebuilt by Software PyMOL with the minus-end-directed kinesin motor, 2NCD from *Drosophila melanogaster* as a template. Online NLS mapper (http://nls-mapper.iab.keio.ac.jp/cgi-bin/NLS_Mapper_form.cgi) was used to predict the nuclear localisation sequence in OsDLK. In addition, Leucine Zipper was identified via the website <http://2zip.molgen.mpg.de>.

2.1.3 Database search for cDNA clones and knock-out mutants

The genomic sequence of OsDLK (accession number Os07g01490) was screened for knock-out mutants in RiceGE (<http://signal.salk.edu/cgi-bin/RiceGE>). Finally Two T-DNA insertion lines (PFG_3A-07110.R, PFG_1B-09105.L) were found in rice cultivar *Dongjin* and one rice Tos17-insertion line (ND4501_0_508_1A) was found in rice cultivar *Nipponbare*.

2.2 Cultivation materials

2.2.1 Cultivation media

Several kinds of mediums have been used during the study (Table 4). Sometime, antibiotics were used for the selection according to the respective targets.

Medium	Ingredient	Amount	Remark
Murashige and Skoog (MS) medium	Murashige-Skoog salts (Duchefa, Haarlem, Netherlands)	4.3 g/L	BY-2 cell culture
	Sucrose	30 g/L	
	KH ₂ PO ₄	200 mg/L	
	Inositol	100 mg/L	
	Thiamine	1 mg/L	
	2,4-dichlorophenoxyacetic acid (2,4-D), pH 5.8	0.2 mg/L	
	* Agar-Agar, danish	0.8 [w/v]	
Paul's medium	Murashige-Skoog salts	4.3 g/L	BY-2 cell culture
	Sucrose	30 g/L	
Luria broth (LB) medium	Yeast extract	5 g/L	Bacteria culture
	Tryptone	10 g/L	
	NaCl	5 g/L	
	* Agar-Agar, Kobe I	1.5 % [w/v]	
Water agar	Phyto Agar (Duchefa Haarlem Netherlands)	0.6 % [w/v]	Rice culture

Table 4 Overview of the media compositions. *Added optionally, depending on the respective medium requirements.

2.2.2 Organisms

Rice materials

Name	Genotype	Application	Source
<i>Nipponbare</i> ND4501_0_508_1A	<i>Oryza sativa</i> L. <i>japonica</i> cv. <i>Nipponbare</i> , RTIM Tos17 insertion line	Phenotyping	NIAS, Tsukuba, Japan
<i>Dongjin</i> PFG_3A-07110.R	<i>Oryza sativa</i> L. <i>japonica</i> cv. <i>Dongjin</i> , T-DNA insertion line	Phenotyping	Postech, South Korea
<i>Dongjin</i> PFG_1B-09105.L	<i>Oryza sativa</i> L. <i>japonica</i> . c v. <i>Dongjin</i> T-DNA insertion line	Phenotyping	Psotech South Korea
<i>Nihonmasari</i>	<i>Oryza sativa</i> L. <i>japonica</i> cv. <i>Nihonmasari</i>	Transient expression	Botanical Garden KIT

Table 5 Overview of the rice materials. More information can be seen in supplementary 1 and 2.

Tobacco cell cultures

Name	Genotype	Application	Source
BY-2 WT	<i>Nicotiana tabacum</i> L. cv. Bright Yellow 2, wild-type	Phenotyping, transient expression	Nagata et al., 1992
BY-2 DLK	<i>Nicotiana tabacum</i> L. cv. Bright Yellow 2, CaMV-35s (EGFP, DLK), kan	Phenotyping	This work
BY-2 DLKM	<i>Nicotiana tabacum</i> L. cv. Bright Yellow 2, CaMV-35s (EGFP, DLKM), kan	Phenotyping	This work

Table 6 Overview of tobacco BY-2 cell cultures.

Bacteria

Name	Genotype	Application	Source
<i>A. tumefaciens</i> LBA 4404	pAL4404, pIG121	BY-2 transformation	Invitrogen, Karls- ruhe, Germany

<i>E. coli</i> DH5 α	F-, ϕ 80dlacZ Δ M15, Δ (lacZYA-argF)U169, recA1, endA1, gyrA96, thi-1, hsdR17, supE44, relA1	Cloning	Invitrogen, Karls- ruhe, Germany
<i>E. coli</i> BL21(DE3)RIL	F, ompT, gal, dcm, lon, hsdS _B (r _B ⁻ m _B ⁻), λ (DE3[lacI, lacUV5-T7 gene 1, ind1, sam7, nin5])	Protein expression	Provided by University of Tuebingen, Germany

Table 7 Overview of bacterial strains.

2.3 Primers

All primers were ordered at Sigma-Aldrich (Steinheim, Germany), or kindly provided by colleagues.

2.3.1 Primers for rice mutant screening

Name	Sequence	T _A °C	Application
pGA2715- RB-mod2	CATCGAAACGCAGCACG ATACGC	60	For T-DNA insertion line PFG_3A-07110.R, insert specific primer
pGA2717- NL1-RBmod	CGCGATCCAGACTGAAT GCCACAG	60	For T-DNA insertion line PFG_1B-09105.L, insert specific primer
LTRN6F	CTGTATAGTTGGCCCAT GTCCAG	60	For Tos17 insertion line, ND4501_0_508_1A, insert specific primer
Kinesin1cF1	GATTTTGTTCCTTGGGA CA	60	For ND4501_0_508_1A, upstream primer
Kinesin1cR1	GCTCGTACAATCAACAA AGCC	60	For ND4501_0_508_1A, downstream primer
Kinesin1cF2	ATGCGATATCTTCTAATG TAGGT	60	For PFG_1B-09105.L and ND4501_0_508_1A, upstream primer

Kinesin1cR2	TCAAGCATGAGAGGCTC T	60	For PFG_1B-09105.L, downstream primer
Kinesin1cF3	ATCTGCTAGCCACTAAT CGCAC	60	For PFG_3A-07110.R, upstream primer
Kinesin1cR3	TTATGCTTCTAACTTCAC TTCAGGC	60	For PFG_3A-07110.R, downstream primer

Table 8 Overview of primers for rice mutant screening. The primers were provided by Dr. M. Riemann (Karlsruhe, Germany), except pGA2715LBmod2.

2.3.2 Primers for gene expression analysis of rice

Name	Sequence	T _A °C	Application
*Ubiquitin 10 fw	GAGCCTCTGTTTCGTC AA GTA	60	Housekeeping gene, upstream primer
*Ubiquitin 10 rv	ACTCGATGGTCCATTAA ACC	60	Housekeeping gene, downstream primer
*GAPDH fw	CTGATGATATGGACCT GAGTCTACTTTT	60	Housekeeping gene, upstream primer
*GAPDH rv	CAACTGCACTGGACGG CTTA	60	Housekeeping gene, downstream primer
qDLK fw	AGATTTCCCAACTCATC CAA	60	qPCR detection of OsDLK, upstream primer
qDLK rv	ATCCTTTCTGGTCATGC AAT	60	qPCR detection of OsDLK, downstream primer
*JAZ11 fw	CAGCCTTGCCTACCAG ACATG	60	qPCR detection of JA-signal gene, upstream primer
*JAZ11 rv	GACGATCCTGTTCTTCC TCTTCTC	60	qPCR detection of JA-signal gene, downstream primer

Table 9 Overview of primers for gene expression during rice growth. *Primers were provided by Dr. M. Riemann (Karlsruhe, Germany).

2.3.3 Primers for gene expression analysis of tobacco cells

Name	Sequence	T _A °C	Application
*L25 fw	GTTGCCAAGGCTGTCAAGT CAGG	58	Housekeeping gene, upstream primer
*L25 rv	GCACTAATACGAGGGTACT TGGGG	58	Housekeeping gene, downstream primer
*EF1 α fw	TGAGATGCACCACGAAGCT CTTC	58	Housekeeping gene, upstream primer
*EF1 α rv	GCTGAAGCACCCATTGCTG GG	58	Housekeeping gene, downstream primer
CBF2 fw	CTCTACTAGCATCAGAAAG TGT	58	qPCR detection of CBF2, upstream primer
CBF2 rv	ACTTGCCTAACCAAGTCAT	58	qPCR detection of CBF2, downstream primer
ICE2 fw	GCTTTACATGCTGAGGTCT	58	qPCR detection of ICE2, upstream primer
ICE2 rv	GAGTTCGTTATGCAGGTCA TT	58	qPCR detection of ICE2, downstream primer
TOC1 fw	AAGAAATCCTCTGCTCTCA C	58	qPCR detection of TOC1, upstream primer
TOC1 rv	CGATTA ACTTCTCCGGTCC A	58	qPCR detection of TOC1, downstream primer
HY5 fw	TGTAGGTAAGGCCGAGAT	58	qPCR detection of HY5, upstream primer
HY5 rv	ATCACTCTCCATACCTTCA CA	58	qPCR detection of HY5, downstream primer
Gl fw	ACAGCTAGAGCAGTACAA C	58	qPCR detection of Gl, upstream primer
Gl rv	CGAACTGTGGCTGGTAAG	58	qPCR detection of Gl, downstream primer
LHY fw	TGGAGATGCTGGGAATCG	58	qPCR detection of LHY, upstream primer
LHY rv	GGCAACTTCTCTCTGGTG	58	qPCR detection of LHY,

			downstream primer
HOS1 fw	TGAGATTAGCGATTTGAGG C	58	qPCR detection of HOS1, upstream primer
HOS1 rv	ATCAAGGTCAGTTTACGCA	58	qPCR detection of HOS1, downstream primer
ELF3 fw	TCCTTCTCAACCACACAGT TTA	58	qPCR detection of ELF3, upstream primer
ELF3 rv	GTAGTTCAAACACTTGTAT CGC	58	qPCR detection of ELF3, downstream primer
Avr9/Cf9 fw	AAGAGGAATTCAGACAAG TG	58	qPCR detection of Avr9/Cf9, upstream primer
Avr9/Cf9 rv	AAAGTTCAAGCAAGCAGA AC	58	qPCR detection of Avr9/Cf9, downstream primer

Table 10 Overview of primers for cold response gene expression in chilling tobacco cells. *Primers were provided by Dr. Q. Liu (Karlsruhe, Germany).

2.3.4 Primers for constructs

Name	Sequence	T _A °C	Application
attB- DLK fw	GGGGACAAGTTTGTACAAAAA GCAGGCTTCATGTCCACGCGCGC CACTCGCC	63	Gateway ENTR cloning for OsDLK, upstream primer
attB- DLK rv	GGGGACCACTTTGTACAAGAAA GCTGGGTCTCCTTGCGCCAAGCT ACGCACT	63	Gateway ENTR cloning for OsDLK, downstream primer
attB- DLKM fw	GGGGACAAGTTTGTACAAAAA GCAGGCTTCATGGAGACGATGA CTGAGTATG	63	Gateway ENTR cloning for OsDLK, upstream primer
attB- DLKT rv	GGGGACCACTTTGTACAAGAAA GCTGGGTCAATTCTCTCCGTCCAA AATTTGTT	63	Gateway ENTR cloning for OsDLKT, downstream primer

Table 11 Overview of primers for *dlk* cloning.

2.3.5 Primers for sequencing

Name	Sequence	T _A °C	Application for genotyping
M13 fw	TGTAACGACGGC CAGT	55	Standard sequencing primer, (GATC, Konstanz, Germany)
M13 rv	CAGGAAACAGCTAT GACC	55	Standard sequencing primer, (GATC, Konstanz, Germany)
T7	TAATACGACTCACT ATAGGG	55	Standard sequencing primer, (GATC, Konstanz, Germany)
*pK7FWGR2	CTGCACGCCGTAGG TCAG	55	pK7FWG2.0 and pH7RWG2.0 sequencing primer
*pK7FWGP35s	CCAACCACGTCTTC AAAGCAAG	55	pK7FWG2.0 sequencing primer
*pK7RWGR2	GCGTTGGAGCCGTA CTGGAAC	55	pH7RWG2.0 sequencing primer
pET-DEST42- Rev	GTCAAACCCAAGTG CGTA	55	pET-DEST42 sequencing primer

Table 12 Overview of primers for sequencing. *Provided by Dr. Q. Liu (Karlsruhe, Germany).

2.4 Cultivation techniques

2.4.1 Cultivation of rice materials

2.4.1.1 Preparation of the seeds

Seeds in this study were propagated in the greenhouses of the Botanical Garden of the KIT (Karlsruhe Institute of Technology, Karlsruhe, Germany). Rice seeds were first incubated at 43 °C for 4 weeks to break dormancy. Seed husks were removed prior to cultivation. Seeds were further sterilized with 70% [v/v] absolute ethanol in a 50 mL Falcon tube (Eppendorf, Hamburg, Germany). After washing with deionized water, they

were incubated in fresh NaClO (5% w/v, Carl Roth, Karlsruhe, Germany) for 20 min with constant shaking at 90 rpm. Subsequently they were washed 4 times with deionized water under sterile conditions.

2.4.1.2 Cultivation of rice seeds

For seed propagation, 20 to 25 sterilized rice seeds were sown in Magenta boxes (Sigma-Aldrich, St. Louis, MO, USA) on 0.4% [w/v] water phytoagar (0.6% w/v, Duchefa, Haarlem, The Netherlands) under continuous daylight in sterile conditions. After 10 days, the young seedlings were planted in flower pots into soil supplemented with 4 g/L Osmocote fertilizer pearls (Scotts Cetaflor, Salzburg, Austria). Furthermore the plants were cultivated in growth chambers with the determined photoperiod (16 h day period at 28 °C and 8 h night period at 20 °C) with constant humidity at 70%.

Seedlings for coleoptile measurement, hormone treatment and particle bombardment were grown in Magenta boxes as mentioned above under sterile conditions. Seeds were sowed in the agar and raised for 3-4 days at 25 °C in darkness.

Seedlings for tissue specificity detection during germination or leaf measurement were grown in Magenta boxes as mentioned above for 10 days under continuous white light.

Seedling for only genotyping were grown on floating meshes in photo-biological darkness (using boxes wrapped in black cloth) and kept in dark chambers at 25 °C for 4 days, as described by Nick et al. (1994). Besides, plants cultivated were also monitored by genotyping.

Seedlings for red light treatment were grown in Magenta boxes as mentioned above. After 4 days seedlings were transferred into a phytochamber and irradiated with red light (λ_{\max} 650 nm) using custom made LED arrays (Qiao et al., 2010). Plants were treated with the fluency rates adjusted to 20 $\mu\text{mol}/\text{m}^2\text{s}$ for 3 min. Non-treated plants were used as negative control. Plant materials were harvested immediately after irradiation and transferred to liquid nitrogen.

2.4.2 Cultivation of BY-2 cell cultures

Tobacco BY-2 cells (*Nicotiana tabacum* L. cv. Bright Yellow 2) were maintained in liquid Murashige and Skoog (MS) medium. Cells were subcultured weekly by inoculating 1.5 mL of stationary cells into 30 mL of fresh medium in 100 mL Erlenmeyer flasks. Stably transformed OsDLK, OsDLKM and wild type BY-2 cell cultures were shaken in darkness at 25 °C and 150 rpm on an orbital shaker (IKA Labortechnik, Staufen, Germany). In case of the OsDLK and OsDLKM cell lines, the MS medium was supplemented with 100 mg L⁻¹ kanamycin.

2.4.3 Cultivation of bacteria

Cultures of *E. coli* were grown according to standard methods described by Sambrook & Russell, (2001). The wild type or transformed *E. coli* was grown on LB plates or liquid media containing the appropriate antibiotics at 37 °C overnight for different purposes. For transformation, the competent wild type bacteria were thawed from stock cultures, followed by heat shock with empty or recombinant plasmids. Then the transformed *E. coli* were grown on LB plates. For plasmid proliferation, single colony was isolated and incubated in liquid media under constant shaking at 180 rpm. Cultures of wild type or transformed *A. tumefaciens* were incubated similarly on LB plates or liquid media at 28 °C for 2 to 3 days. For storage purposes, the fresh bacterial suspensions were supplemented with 15% [v/v] sterile glycerol, frozen in liquid nitrogen and stored at -80 °C.

2.5 Molecular analysis

2.5.1 Rice genotyping of rice mutant

2.5.1.1 Isolation of rice genomic DNA

Coleoptile or leaf materials were immediately frozen in liquid nitrogen and stored at -

80 °C until isolation. For purification, the samples were ground up in a TissueLyser (Qiagen, Hilden, Germany). Genomic DNA was isolated from 100-200 mg pulverized materials with the CTAB (chloroform-isopropanol) protocol described by Sambrook & Russell, (2001). 900 µL preheated 2% CTAB buffer containing 150 mM Tris-HCl pH 8.0, 1.4 M NaCl, 30 mM EDTA, 2-Mercaptoethanol (8 µL/mL) (Roth, Germany) and polyvinylpyrrolidone (40 mg/mL) (Sigma, Germany) were added into the samples. Then the samples were incubated at 60 °C in a water bath for 1 hour with gently vortex every 20 min. The samples were incubated for another 30 min with supplement of 10 µL Proteinase K (10 mg/mL) (Sigma). After that, 750 µL chloroform: isoamylalcohol (Roth) (24:1) was added before centrifugation. To precipitate DNA, 160 µL NaCl (5 M, Roth) and 55 µL NaAc (3 M, Roth), and 500 µL isopropanol (Roth) were added inside the samples followed by incubation at -20 °C for 30 min. Finally the samples were centrifuged again and the pellets were dissolved in 50 µL TE buffer (1 mM Tris-HCl, 1 mM EDTA, pH 8.0) with 2 µL Rnase (1 mg/mL) (Qiagen) and before incubation at 37 °C for 60 min. Genomic DNA was generally stored at 4 °C for short time or -20 °C for long time.

2.5.1.2 Determination of genomic DNA concentration

Concentrations of genomic DNA were determined photometrically according to the manufacturer instructions by Nano-Drop 2000 (Thermo Scientific, Wilmington, USA) at a wavelength of 260 nm.

2.5.1.3 Agarose gel electrophoresis

Quality of genomic DNA was also monitored with gel electrophoresis. 1% [w/v] agarose gel (Roth) was dissolved in TAE buffer (50x stock: 2 M Tris-HCl, 0.57% [v/v] acetic acid, 50 mM EDTA; pH 7.5) with 0.5x SYBR Safe (Invitrogen, Karlsruhe, Germany) for detection. DNA samples were mixed with 5x loading dye (50% [v/v] glycerine, 0.05% [w/v] bromphenol blue, 0.05% [w/v] xylencyanol) before loading. Samples were separated on the gel for 30 min together with DNA ladder (NEB, Frankfurt, Germany) at 75-100 V for 30 min. Bands were visualized on a Safe Imager blue light transilluminator (Invitrogen) and photographed with a Rainbow Camera system (Hama, Monheim, Germany).

2.5.1.4 Polymerase chain reactions detection

Generally, Tos-17 or T-DNA inserted rice mutants were screened using a PCR-based method with two polymerase chain reactions (PCR), independently, which was described by Winkler & Feldmann, (1998). In the first reaction, the primers were designed according to the sequence around both sides of the putative insertion site. In the second round, the pair of primers was based on the specific site of the insertion and the genome sequence surrounding one side of the putative insertion. The sequences of primers for different mutants were listed in Table 8. The PCR products were separated on 1% [w/v] agarose gels. The isolated chromosomal DNA of plants was used as template in the PCR. Standard compositions of PCRs were performed as Table 13. PCRs were run in a Primus 96 Advanced or Cyclone 25 thermocycler (PeQlab, Erlangen, Germany). The program was generally shown in Table 14.

Component	Amount μL
Template gDNA, ~200 ng/ μL	1
10x ThermoPol buffer (NEB)	1.5
5 mM each dNTP Mix (NEB)	0.5
10 μM primer forward	0.5
10 μM primer reverse	0.5
5 U/ μL Taq Polymerase (NEB)	0.1
* 100 % [v/v] DMSO	4
* 5 M betaine	1.6
dd H ₂ O	To 15

Table 13 Standard set-up for analytical PCRs (15 μL). * added into the system optionally.

Step	Temperature	Time
Heating up	95 °C	5 min
Denaturation	95 °C	30 s
Annealing	60 °C	30 s
Elongation	72 °C	*30-60s
Extension	72 °C	*2-5 min

Table 14 Cycling parameters for PCRs. *Elongation time was different for respective PCR requirements. 42 cycles were repeated from denaturation to elongation step.

2.5.2 cDNA synthesis and quantitative Real-Time PCR

2.5.2.1 RNA isolation and quantification

The RNA was purified from 100 mg of pulverized samples using an innuPREP plant RNA kit (Analytik Jena, Germany), including on-column digestion of genomic DNA with RNase-free DNase I (Qiagen) according to the manufacturer instructions. The isolated RNA was checked for the purity and integrity with both Nano-Drop 2000 and % [w/v] agarose gels as described above. The samples were stored at -20 °C until cDNA synthesis.

2.5.2.2 cDNA synthesis

cDNA was synthesized from 1 µg of total RNA extracts using the M-MuLV cDNA Synthesis Kit (NEB), with Oligo(dTs) (Thermo Fisher, Germany) according to the instructions of the manufacturer. The RNase inhibitor (NEB) was used to protect the RNA from degradation.

2.5.2.3 Semiquantitative RT-PCR analysis

Semiquantitative RT-PCR, was set up with standard system as described in Table 13 and 14, with Taq polymerase (NEB). The cycle number was chosen to be 28-32, such that the amplifications of templates for all primers (Table 9) were in an exponential range where the products were clearly distinguished on 2% [w/v] agarose gels.

2.5.2.4 Quantitative real-time PCR analysis

iQ SYBR Green Supermix (Bio-Rad, München, Germany) was used for the signal formation in Quantitative real-time PCR analysis. The components of the reaction system are shown in Table 15. The master mix was split up in so-called triplet-mixes and then mixed with the respective cDNA. RT-PCR reaction was performed using a Bio-Rad CFX detection System (Bio-Rad) according to the manufacturer instructions with the following cyclers conditions: 3 min, 95 °C, 39× (95 °C for 15 s, annealing at 60 °C for 40 s). The primers designed for q-PCR are shown in Table 9.

Component	Amount μL
Template cDNA (1:10)	1
5x GoTaq Puffer buffer (NEB, Frankfurt, Germany)	4
5 mM each dNTP Mix (NEB, Frankfurt, Germany)	0.4
10 μM primer forward	0.4
10 μM primer reverse	0.4
0.5 U/ μl GoTaq Polymerase (NEB, Frankfurt, Germany)	0.1
SybrGreen	0.95

MgCl ₂ (50mM)	1
dd H ₂ O	11.75
Final volume	20

Table 15 qPCR mix per reaction.

2.5.3 Expression level of endogenous OsDLK in rice during germination

To investigate the endogenous OsDLK expression level during rice seedling development, seedlings of rice cultivar *Nipponbare* were in darkness for 6 days. Each day 3-4 intact plants were harvested for the isolation of total RNA. Each time point was repeated at least three times. To investigate the endogenous OsDLK expression level in different tissues of the plant, seedlings of rice cultivar *Nipponbare* were grown under continuous white for 10 days. The different tissues of plants included first leaf (FL), second leaf blade (SLB), second leaf sheath (SLS), third leaf (TL), seminal root (SR) and crown root (CR), and were separated carefully. Tissues for at least 12 seedlings were collected cumulatively over a minimum of three independent experimental series. For the short-time red light treatment, coleoptiles and leaves from rice cultivar *Nipponbare* were carefully isolated under green-safe light immediately after the irradiation. Samples were gained from at least 12 seedlings cumulatively over a minimum of three independent experimental series, individually for the coleoptile and leaf study. The RNA isolation, cDNA synthesis, semiqPCR and qPCR methods are shown above in this chapter. Primer qDLKfm/rv (shown in Table 9) was used for the expression level detection of OsDLK. Primers JAZ11 fw/rv were used for expression level detection of the JA-signalling gene.

2.5.4 Cloning and manipulation of plasmids

2.5.4.1 Isolation and cloning of OsDLK

Rice (*Oryza sativa* L. *japonica*) cultivar *Nipponbare* seedlings were grown in darkness at 25 °C. After 4 days coleoptiles were excised. Total RNA was extracted with the innuPREP Plant RNA kit and cDNA was synthesized subsequently. The full-length coding sequence of OsDLK (residue 1-2295 bp) was amplified from the cDNA template with a pair of primers containing attB-sites (Table 11). Primers attB-DLKfw and attB-DLKrv were used to get the full-length of OsDLK. To get OsDLKM (residue 1110-2295 bp), containing the whole motor and partial tail, the primers attB-DLKM fw and attB-DLKrv were used. For the whole tail part of OsDLKT (residue 1-1209 bp), primers attB-DLK fw and attB-DLKTrv were used.

Component	Amount μL
Template (cDNA), ~200 ng/ μL	1
5x HF Phusion buffer (NEB)	10
5 mM each dNTP Mix (NEB)	1
10 μM primer forward	2
10 μM primer reverse	2
2 U/ μL Phusion Polymerase (NEB)	0.4
100% [v/v] DMSO	4
5 M betaine	1.6
dd H ₂ O	To 50

Table 16 Standard set-up for preparative PCRs (50 μ L).

Step	Temperature	Time
Heating up	95 °C	5 min
Denaturation	95 °C	30 s
Annealing	63 °C	30 s
Elongating	72 °C	*2-3 min
Extension	72 °C	*5-10 min

Table 17 Cycling parameters for preparative PCRs. *Elongating time was different for respective PCR requirements. 42 cycles were repeated from denaturation to elongation step.

The components of the PCR system are shown in Table 16 and the reaction conditions are shown in Table 17. Subsequently, the desired DNA fragments or PCR products were separated and cut out of the agarose gels under blue light illumination and purified using a NucleoSpin Extract II Kit (Macherey-Nagel, Düren, Germany).

2.5.4.2 Generation of fluorescent protein fusion constructs

The fluorescent protein fusion constructs for the protein expression in tobacco BY-2 cells were established using the GATEWAY[®]-Cloning technology (Invitrogen Corporation, Paisley, UK). The amplified PCR products of OsDLK, OsDLKM and OsDLKT were first recombined into the entry plasmid pDONR/Zeo (Invitrogen) (Table 18) via standard BP reactions as follows: 50 fmol of both PCR product and entry plasmid were mixed and incubated with 2 μ L BP Clonase Enzyme Mix for 18-20 h at 25 °C. 2 μ L Proteinase K was added in the mixture and incubated for 10 min at 37 °C to arrest recombination. Then the reaction mixture was transformed in chemically competent DH5 α cells and incubated at 37 °C with continuous shaking at 180 rpm overnight. Plasmids were extracted with Roth[®]-Prep Plasmid MINI kit (Roth, Germany) and the positive plasmids were determined via PCR with the primers M13 fw/rv (Table 12). Correct and complete insertion was verified by DNA sequencing (GATC Biotech, Cologne, Germany). All the plasmids were assessed for sample purity and nucleic acid

concentrations by photometric measurement. The LR reactions (volume of 10 μL : 2 μL of LR Clonase Enzyme Mix, 50 fmol of recombined entry plasmids, and 2 μL Proteinase K, incubated the same as BP cloning) were conducted to clone the OsDLK, OsDLKM and OsDLKT into the binary plasmid pK7FWG2, pH7WGF2 and pET-DEST42 (Table 18). Then the mixtures were transformed into competent DH5 α cells for plasmid propagation. Finally the recombined protein fusion construct were sequenced (GATC Biotech, Cologne, Germany) again with the primers shown in Table 12. In constructs pK7FWG2, pH7WGF2, respective proteins were expressed under control of the constitutive CaMV-35S promoter. And the green fluorescent protein (GFP) or red fluorescent protein (RFP) was located C-terminally.

Name	Annotations	Application	Source
pDONR/ZEO	Zeo ^R , pEM7, M13, T7, att1_Kan ^R ccdB_att2, SP6, T7	ENTR vector for Gate-way cloning	Invitrogen, Karlsruhe, Germany
pK7WGF2.0	RB-p35S EGFP, att1_ccdB_att2, Kan ^R -LB, Sm/Sp ^R	Binary destination vector for Gateway cloning	Karimi et al., 2002
pH7WGF2.0	RB-p35S ERFP, att1_ccdB_att2, Hyg ^R -LB, Sm/Sp ^R	Binary destination vector for Gateway cloning	Karimi et al., 2002
pET-DEST42	RB-T7, lacO_att1_ ccdB_V5-6xHis_att2, Amp	Binary destination vector for Gateway cloning	Provided by University of Tuebingen, Germany

Table 18 Overview of fusion constructs.

2.5.4.3 Generation of his-tag fusion constructs

For protein-DNA interactions screening, the protein was expressed in *E.coli*. The his-tag fusion constructs for the protein expression in bacteria were also built via gateway cloning as mentioned before. The proteins OsDLK and OsDLKT were cloned into the binary plasmid pET-DEST42. The proteins were expressed under the control of the strong bacteriophage T7lac promoter, with a His-tag placed at the C-terminally of the insertion.

For kinesin mobility test, the OsDLK bacterial expression construct was amplified with pDONR/Zeo-OsDLK as template using the primers 5'-CACAGCAGCGGCCTGGTGCCGACTCGCCCCGGGATGCTCCACCAGAAG and 5'-CTTTCGGGCTTTGTTAGCAGCCGGATCTCATCCTTGCGCCAAGCTACGCACT TGGG and inserted into the pET28a bacterial expression vector (Novagen) via overlap extension cloning (Bryksin & Matsumura, 2013).

2.6 Cell biological analytics

2.6.1 Stable and transient transformation

2.6.1.1 *Agrobacterium*-mediated transformation

Stable overexpression of OsDLK-GFP and OsDLKM-GFP in BY-2 was achieved via *Agrobacterium*-mediated transformation based on the protocol by Buschmann et al. (2011) with minor modifications described in Klotz & Nick, (2012). *Agrobacterium tumefaciens* strain LBA4404 (Invitrogen) was transformed with pK7FWG2-OsDLK or pK7FWG2-OsDLKM, respectively and then cocultivated with wild-type BY2 cells in form of suspension droplets plated on solid Paul's medium for three days, followed by transferring onto selective solid MS medium with 100 mg·L⁻¹ cefotaxime sodium and 100 mg·L⁻¹ kanamycin. Kanamycin-resistant calli were pooled and transferred into liquid MS medium after 3-4 weeks of incubation at 25 °C in darkness. Cell suspension cultures were then established and maintained in liquid MS with 100 mg L⁻¹ kanamycin as appropriate antibiotic. For transient transformation, OsDLK-RFP or OsDLKM-RFP was transformed into LBA4404, subsequently grown on solid Paul's medium for 3 days, and then examined microscopically without preceding selection. Microtubules were visualised with the construct pCambiaTuB6, in which GFP was fused to *Arabidopsis* β-Tubulin 6 (Nakamura et al., 2004). Besides, OsDLK-RFP was also co-transformed together with OsKCH1-fl GFP to investigate the co-localisation between these two Kinesin-14 proteins.

2.6.1.2 Biolistic, transient transformation of rice seedlings

In order to investigate the subcellular localisation of kinesin OsDLK in rice, transient transformation was carried out via particle bombardment. The second leaf blades of rice cultivar *Nihonmasari* were used for this experiment. For preparation, 120 mg of gold particles were suspended in 50% [v/v] sterile glycerol with vortexer. 12.5 μ L of the vortexed gold suspension were transferred to a 1.5 mL eppi tube and were coated with 1 μ g of the construct DLK-GFP, under continuous vortexing and successive addition of DNA, 12.5 μ L of 2.5 M sterile CaCl₂, 5 μ L of 0.1 M sterile spermidine. The DNA-coated gold particles were vortexed thoroughly for additional 3 min and were spun down briefly. The gold particles were washed with 125 μ L absolute ethanol. Finally, they were resuspended in 40 μ L absolute ethanol. The DNA-coated gold particles were loaded onto a macrocarrier (BIO-RAD) in three times with 15 min interruption. Particle bombardment was performed immediately after total evaporation of the ethanol.

For biolistic transformation, plants material were arranged on the middle of PetriSlides (Millipore, Schwalbach, Germany) with 0.4% phytoagar and fixed with a wire grid. For each plasmid solution, three petri dishes were prepared. The petri dishes were then placed in the particle gun and were bombarded three times at a pressure of 2.5 bar in the vacuum chamber at -0.8 bar. Following bombardment, the transformed rice blades were incubated in the dark at 25 °C for 24 h and examined by microscopy.

2.6.2 Microscopy and image analysis

Two types of microscopes were used to investigate subcellular localisation and phenotypic consequences of overexpression: Cellular details of individual cells were examined under an AxioObserver Z1 microscope (Zeiss, Jena, Germany) equipped with a spinning-disc device (YOKOGAWA CSU-X1 5000) and a cooled digital CCD camera (AxioCam MRm; Zeiss), using a Plan-Apochromat 63x/1.44 DIC oil objective. GFP fluorescence was observed through the 488 nm emission line of an Ar-Kr laser (Zeiss). RFP and TRITC fluorescence signals were observed through the 561 emission line of the same laser. For subcellular localisation, time-lapse series were recorded every 5 s over a period of at least 60 min. Acquired images were operated via the Zen 2012 (Blue

edition) software platform. For kymograph measurements, time-lapse series of 3-day-old transgenic BY-2 cells were recorded by capturing z-stacks 5 min. Kymographs were constructed using the kymograph plugin of ImageJ (NIH, Bethesda, USA), according to the instructions at <http://www.embl.de/eamnet/html/kymograph.html>.

For statistical phenotyping of cell populations, cells were examined under an AxioImager Z.1 microscope (Zeiss) equipped with an ApoTome microscope slider for optical sectioning and a cooled digital CCD camera (AxioCam MRm; Zeiss). For cell size and density, samples were scanned under the differential interference contrast (DIC) using a 20x objective (Plan-Apochromat 20x/0.75) with the MosaiX module of the imaging software (Zeiss). Images were processed and analysed using the AxioVision (Rel. 4.8.2) software. Each data point represents mean and standard error from at least three independent experimental series with at least 500 individual cells for each time. DNA labelling by Hoechst 33258 was recorded using the filter set 49 DAPI (excitation at 365 nm, beamsplitter at 395 nm, and emission at 445 nm). Images were measured using the periphery tool of ImageJ. The 4-day old coleoptiles of rice raised in darkness were measured using the periphery tool of ImageJ (NIH).

2.6.3 Determination of packed cell volume

To quantify culture growth, packed cell volume (PCV) was measured as described in Jovanovic et al. (2010), at days 4 (after the proliferation phase) and 6 (at the end of expansion phase) after subcultivation. The cell suspension was poured into a 15-mL falcon tube and kept vertically at 4 °C for 48 hours, till most cells had settled to the bottom. The PCV could then be read directly from the scale of the 15-mL falcon tube. Each data point represents mean value and standard error from at least three independent experimental series.

2.6.4 Determination of mitotic index

Tobacco BY-2 cell cycle progress was monitored by mitotic indices (MI), defined as the relative frequency of dividing cells. BY-2 cells were first fixed by Carnoy fixative [3:1 (v/v) 96% (v/v) ethanol: glacial acetic acid, complemented with 0.25% Triton X-42

100]. The nuclei were stained with 2'-(4-hydroxyphenyl)-5-(4-methyl-1-piperazinyl)-2,5-bis(1H benzimidazole)-trihydrochloride (Hoechst 33258; Sigma) at a final concentration of $1 \mu\text{g mL}^{-1}$, and samples were immediately investigated under the microscope. Each data point represents mean and standard error from at least three independent experimental series, corresponding to at least 3000 cells per time point.

2.6.5 Cell cycle synchronization

Cells were synchronized according to a protocol modified from Samuels et al. (1998) by using hydroxyurea instead of aphidicolin (Kuthanov á et al., 2008). After cultivation for 7 days, stationary cells of BY-2 were subcultured in 120 mL liquid MS medium complemented with 4 mM hydroxyurea (HU; Sigma). After 24 hours, HU was washed out by a Nalgene filter holder (Thermo Scientific,) in combination with a Nylon mesh with pores of diameter of 70 μm (Mehlsieb, Franz Eckert, Waldkirch, Germany). This time point was recorded as “HU release point” and an aliquot of cells was sampled for the determination of the mitotic index. After washing three times with washing medium (sterile 3% sucrose in water), the cells were resuspended in 50 mL of fresh MS medium, returned into flask and shaken for a further 3 h. Propyzamide (Sigma) was added to a final concentration of 6 μM into the culture and the suspension shaken for another 6 h. Subsequently, propyzamide was removed with the Nalgene device. This time point was defined as “Propyzamide release point” and an aliquot was collected to determine the MI. After washing, cells were resuspended again in 50 mL of fresh MS medium and cultured on a shaker, while MI was monitored every 30 min over 4 hours. Reported values represent means and standard errors for a population of more than 3000 cells collected from three independent experimental series.

2.6.6 Immunostaining of microtubules

Microtubules were visualized by indirect immunofluorescence as described in Nick et al. (2000). Suspended cells were fixed for 10 min at 20 °C in 3.7% (w/v) paraformaldehyde in microtubule stabilizing buffer (MSB, 50 mM 1,4-piperazine diethane sulfonic acid (PIPES), 2 mM ethylene glycol-bis (β -aminomethyl ether)-

N,N,N',N'-tetraacetic acid (EGTA), 2 mM MgSO₄, pH 6.9). Afterwards, 0.1% Triton was added to the fixative and cells were fixed for another 50 min. Subsequently, the cell wall was digested using 1% (w/v) Macerozyme (Duchefa, Haarlem, The Netherlands) and 0.2% (w/v) Pectolyase (Duchefa) in MSB for 7 min at 20 °C. After washing three times for 10 min each with MSB, 0.5% (w/v) bovine serum albumin (BSA, Carl Roth) diluted in phosphate-buffered saline (PBS, 150 mM NaCl, 2.7 mM KCl, 1.2 mM KH₂PO₄, and 6.5 mM Na₂HPO₄, pH7.2) were used to block unspecific binding sites. The cells were kept for 30 min at 20 °C. Samples were subsequently directly incubated with mouse monoclonal antibodies against α -tubulin (DM1A, Sigma) diluted 1:1000 in PBS at 4 °C overnight. After removing unbound primary antibody by washing the cells three times with PBS solution, the sample was later incubated with a polyclonal secondary TRITC-conjugated anti-mouse IgG antibody (1:200 in PBS; Sigma), for 45 min at 37 °C. In some cases, the DNA was also stained with Hoechst 33258 as described above.

2.6.7 Oryzalin dose-response curves

Oryzalin (Sigma) in different concentration was added at the beginning of subcultivation to BY-2 cells stably overexpressing OsDLK-GFP, and non-transformed wild type BY-2 cells, respectively. Cell number and PCV were checked after three days of cultivation under standard conditions. The BY-2 cells were treated in the same way with equivalent concentrations of the solvent dimethylsulfoxide (DMSO) as a control. The mean values from three independent experimental series were plotted relative to the control value in the absence of oryzalin.

2.6.8 Leptomycin B treatment

To measure the accumulation of OsDLK in nuclei, OsDLK-GFP BY-2 cells in their exponential phase of growth (3 days after inoculation) were treated with 200 nM Leptomycin B (Sigma), an inhibitor of nuclear export. The cells were incubated for further 48 h under standard conditions, and z-stacks of the GFP signal were recorded (AxioImager Z.1). For the quantification, geometrical projections (maximum intensity

algorithm) were quantified using ImageJ. Intensity profiles along a very broad probing line (in the thickness of roughly the nucleus) were collected across the entire cross section of the cell and then a second time along the same plane, but just covering the nucleus. The two integral over these two profiles were used to calculate the percentage of signal located inside the nucleus. Control treatments were performed by treating the cells with the corresponding volume of solvent [70% methanol] and growing the cells under standard cultivation conditions. Reported values represent means and standard errors for at least 60 cells collected from three independent experimental series.

2.6.9 Cold treatment

Suspensions of 3-day-old BY-2 cells stably overexpressing OsDLK-GFP in Erlenmeyer flasks were placed in a bath of ice water to maintain a temperature of 0 °C and shaken on an orbital shaker at 100 rpm in darkness for 24-72 h. The rice leaf blades transformed with OsDLK-GFP was also placed in a bath of ice water to maintain a temperature of 0 °C in darkness for 24 h. BY-2 cells overexpressing OsDLK-RFP and TuB6-GFP were also treated in cold stress for investigating the association between OsDLK and MT in chilling cells. Samples of cells were collected at specified time points during the cold treatment for cytological observation and immunostaining.

2.7 Protein expression and isolation in *E.coli*

2.7.1 Protein expression in *E.coli*

2.7.1.1 Protein expression and isolation for DNA binding screening

The expression plasmids pET-DEST42-OsDLK and pET-DEST42-OsDLKT were transferred into the *E. coli* strain BL21-Codon Plus (DE3)-RIL. They were incubated in 5 mL culture flasks containing LB medium supplemented with ampicillin overnight. Before the induction, the precultures were transferred to 300 mL LB media with the

start OD around 0.1. They were grown to an OD 600 of ca. 0.6-0.8 at 37 °C and shaken at the speed of 180 rpm. The crude extract was gained on ice. After cooling down for 15 min at 4 °C, 200 nM isopropyl- β -D-thiogalactopyranoside (IPTG) was added into the cultures, and subsequently incubated for 4 h at 37 °C. Cells were harvested by centrifugation at 4500 g at 4 °C for 20 min (Hermle Universal centrifuge, Wehingen, Germany). The pellets were washed with DPI-ELISA buffer (4 mM HEPES pH 7.5, 100mM KCl, 8% Glycerol) plus 1 mM PMSF (stock 100 mM) and proteinase inhibitor cocktail (Roche, Germany). The proteins inside the cells were released with by sonication (UP100H, Hielscher, Germany) with the frequency of 6 cycles of 15 s with 15 s interruption, 80% power; 1 cycle. After centrifugation at 4500 g at 4 °C for 20 min, the supernatant was kept as the crude extract, which would be the material for the DPI-ELISA assay. Empty vector pET-DEST42 was also induced to get the negative control.

2.7.1.2 Protein expression and isolation for DNA for kinesin mobility test

C-terminally hexa-histidine-tagged OsDLK (aa1-764) was expressed in *E. coli* BL21(DE3)-pRARE (Millipore) grown in LB medium and induced with 0.2 mM IPTG for 3 h at 37 °C. Harvested cells were resuspended in buffer A (274 mM NaCl, 5.4 mM KCl, 16.2 mM Na₂HPO₄, 3.52 mM KH₂PO₄, 2 mM MgCl₂, 1 mM ATP, 1 mM dithiothreitol (DTT), and EDTA-free protease inhibitors (Roche), pH 7.4) and lysed using a high pressure homogenizer. The crude lysate was centrifuged at 17,400 g at 4 °C and loaded onto a 5 mL HiTrap NiNTA column (GE, Healthcare). The column was washed with 50 mL buffer A containing 30 mM imidazole. Proteins were eluted in buffer A containing 500 mM imidazole, pH 8.0. Proteins were snap-frozen in liquid nitrogen and stored at -80 °C.

2.7.2 Western blotting

2.7.2.1 Electrophoresis with SDS-Polyacrylamide gel

The components for discontinuous SDS-polyacrylamide gels used for protein separation are shown in Table 19 (Laemmli, 1970).

Component	Separation Gel	Stacking Gel
Acrylamide (30 % [v/v] acrylamid 0.8 % [v/v] bisacrylamid)	8.2 mL	1.3 mL
Separation buffer (1.5 M Tris-HCl, pH 8.8)	6.2 mL	
Stacking buffer (0.5 M Tris-HCl, pH 6.8)		2.3 mL
H ₂ O	10.3 mL	6.2 mL
10 % [w/v] APS	215.9 μ L	105 μ L
40% TEMED	108 μ L	52.8 μ L

Table 19 Composition of 10% SDS-polyacrylamide gels.

The crude extract samples and Color Prestained Protein standard (NEB) were mixed with 3x sample buffer (30% [v/v] glycerine, 300 mM DTT, 6% [w/v] SDS, 48% [v/v] stacking gel buffer, 0.01% [w/v] bromophenol blue). They were incubated at 95 °C for 5 min. The proteins were loaded and were separated equally on two SDS-polyacrylamide gels, in a miniPAGE chamber (Atto, Tokyo, Japan) containing running buffer (25 mM Tris, 192 mM glycine, 0.15% [w/v] SDS) at 25 mA supplied by an electrophoresis powersupply PHERO-stab 300 (Biotec-Fischer, Germany) per gel for 90 min.

One of the gels was stained in Coomassie staining solution (0.04% [v/v] Coomassie Brilliant Blue R250, 40% [v/v] methanol, 10% [v/v] acidic acid) for 2 hours and destained in 30% [v/v] ethanol supplemented with 10% [v/v] acetic acid for another 2 hours. Then gels were scanned using a HP ScanJet 3400C (Hewlett-Packard, Palo Alto, USA) for the documentation, and they were dried for long term storage. The other gel was used for western blotting to check the expression with His-tag antibody.

2.7.2.1 Western blotting

For preparation, the polyvinylidene fluoride (PVDF) membrane (Pall Gelman Laboratory, Dreieich, Germany) was activated by incubation in methanol (Roth) for 1 min. The blotting paper (Whatman, Dassel, Germany) was soaked for 5 min in transfer buffer (14.4 g/L glycine, 12.07 g/L Tris-HCl, 20% [v/v] MeOH). Proteins were transferred onto the membrane with Trans-Blot® Semi-Dry Transfer Cell (Bio-Rad) at

a constant current of voltage 20 V for 60 minutes per gel. After blotting, the membrane was blocked for 60 min, with 3% [w/v] milk buffer which was containing 20 mM Tris-HCl (pH7.6), 150 mM NaCl. The transferred protein on membrane was rinsed for 10 min twice in TBST buffer (TBS buffer, Tween-20) and one time in TBS buffer. The blot was then incubated overnight at 4 °C with the primary antibody (Anti-penta His, 1:2000 diluted in TBS buffer) which is a mouse monoclonal antibody targeting penta his-tagged protein. After washing, the membrane was incubated with the secondary antibody (Anti-mouse IgG, alkaline phosphatase-conjugated, 1:50000 diluted in TBS buffer) for 60 min. The secondary antibody was washed away by rinsing for 10 min in TBST for 4 times. The signal was developed with an alkaline phosphatase-based development method. The membrane was incubated in staining buffer (100 mM Tris-HCl, 100 mM NaCl, pH 9.7) freshly supplemented with 1/10 magnesium stock (500 mM) for 15 min in prior to the development. The membrane was developed in 5 mL developer solution consisting of 66 µL nitrobluetetrazolium (NBT; 75 mg/mL in 75% [v/v] dimethylformamide, Thermo scientific) and 33 µL 5-bromo-4-chloro-3-indoxylphosphate-p-tuloidin (BCIP; 50 mg/mL in 75% [v/v] dimethylformamide, Thermo scientific) which were diluted freshly with 5 mL staining buffer with 1/10 magnesium stock solution for 1 min. The reaction was stopped by rinsing in H₂O. The blots were dried and scanned for documentation.

2.8 Motility assays *in vitro*

Microtubules were polymerized as described by Fink et al. (2009) using DyLight594-labeled or a mixture of Cy5-labeled and digoxigenin-labelled (1:5) tubulin. For the microtubule sliding motility assay, microtubules co-labelled with digoxigenin and Cy5 were immobilized to the glass surface via digoxigenin antibodies (Roche, Germany). After blocking with 1% Pluronic F127 OsDLK motors were added to the microtubules in absence of ATP. Subsequently, microtubules labelled with DyLight594 in imaging solution were allowed to bind to the motors and transport was monitored in presence of 2 mM ATP. Fluorescently labelled microtubules were visualized using epi-illumination on an inverted fluorescence microscope (Ti-E, Nikon) equipped with an EMCCD camera (iXon Ultra, Andor). Positions of microtubules were obtained using FIESTA tracking software as described before (Ruhnow et al., 2011). The mean velocity was

determined by fitting the velocity histograms to Gaussian functions using MatLab (Mathworks).

2.9 DPI-ELISA assay

The crude extraction from *E.coli* (Strain: BL21(DE3)RIL) cell culture including protein pDEST42-DLKT and pDEST42-DLK were send to University of Tuebingen for DNA-protein-interaction (DPI)-ELISA screen for identification of hexanucleotide DNA-binding motifs with an optimized double-stranded DNA (dsDNA) probe library (Fig. 8). The workflow of the DPI-ELISA was modified from Brand et al. (2010). 10 μ L prepared immobilised ds-bio DNA probes were incubated with 20 μ L TBST buffer at 37 $^{\circ}$ C for 1 hour so that they could bind to the streptavidin-coated plates. After washing with TBST for 3 times, residual binding spots of the micro well plate were blocked with 5% non-fat dry milk (Roth, Germany). 125 μ g crude protein extract was added for the binding of immobilised ds-bio DNA. After washing, 30 μ L α -His-HRP antibody (Qiagen) diluted 1:1000 in PBS-T was added for incubation at 22 $^{\circ}$ C for 1 hour. Photometric detection (peroxidase reaction) was carried out via ELISA-reader in less than 1 hour. The relative unit data was calculated by normalization of the mean of two independent samples and standard deviation to the negative control. The cis-elements were predicted via Plant Care (<http://bioinformatics.psb.ugent.be/webtools/plantcare/html/>).

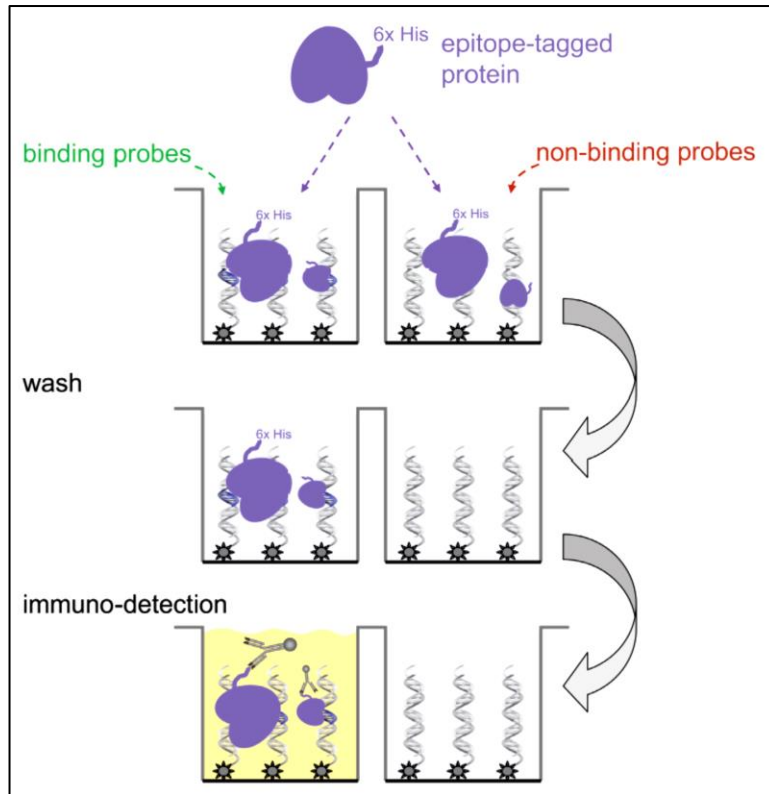


Figure 8 Schematic explanation of the DPI-ELISA library screening system. Image source: Brand et al., 2013.

3. Results

3.1 In *silico* analysis of OsDLK

3.1.1 OsDLK is a putative minus-end directed C-terminal motor of Kin-14

A putatively full-length cDNA for rice DLK was isolated by RT-PCR using total mRNA from coleoptiles of rice (*Oryza sativa* L. *japonica* cv. 'Dongjin') as template. The obtained sequence coding for the OsDLK protein consists of 764 amino acid residues and is identical to the sequence published for the rice reference genome of the *japonica* cultivar 'Nipponbare' (UniProtKB/Swiss-Prot accession no. B8B6J5). The calculated molecular mass is 85.6 kDa. The putative kinesin is predicted by the Prosite and SMART tools to harbour a highly conserved kinesin motor domain (amino acids 404-764) at the C-terminal region, including an ATP-binding consensus (amino acids 498-506), and a putative microtubule binding site (amino acids 700-706) (Yang et al., 1989) (Fig. 9a).

A 14-amino-acid neck-linker region directly upstream of the catalytic core comprises the consensus neck motif found among kinesins that move towards the minus end of microtubules (Endow, 1999), such as DmNCD from fruit fly and ATK5 from *Arabidopsis* (Ambrose et al., 2005). Specifically, this region contains two critical amino acids known to be crucial for kinesin minus-end directed movement (Fig. 9a; Suppl. Fig. S2). Thus, OsDLK displays all sequence motives indicative of a microtubule minus end-directed motor.

A N-terminal domain spanning amino acids 109-422 (Fig. 9b) is predicted to form α -helical structures with characteristic periodic heptapeptide repeats, as often associated with protein dimerization or oligomerization (Lupas et al., 1991). To assess the impact of this N-terminal domain, in some experiments, the core motor construct, OsDLKM

(amino acids 371-764), containing the whole motor domain and partial tail domain of OsDLK, but lacking this N-terminal domain was employed.

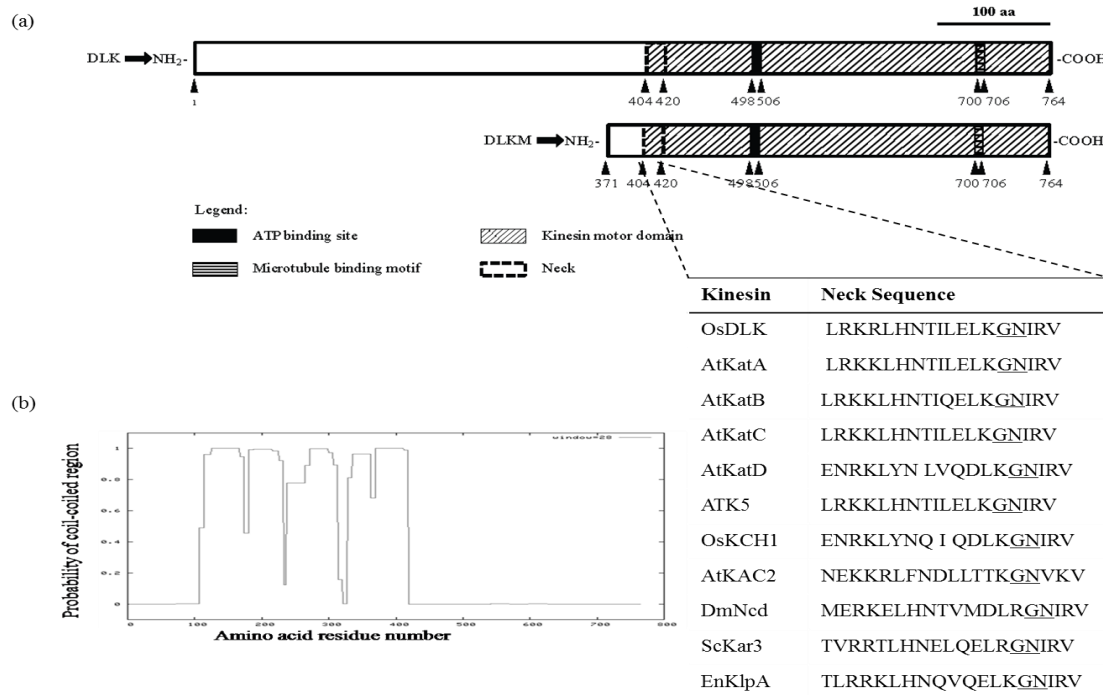


Figure 9 Sequence analysis of OsDLK from *Oryza sativa* L. *ssp. japonica*. (a) Predicted domains in the full-length protein (upper row) and set-up of the truncated DLKM construct. A putative kinesin motor domain is found in the C-terminal region and includes a conserved neck region, and ATP- and microtubule-binding sites. The table in the right side shows the identified neck sequences found among kinesins that move towards the minus-end of microtubules. The two amino acids known mostly by to connect with kinesin minus-end directed movement are underlined. (b) Secondary structures predicted for OsDLK. A probability value > 0.5 is indicative for coiled-coil region.

The predicted structure model of the OsDLK motor part was shown in Fig 10. The ATP binding sites and MT binding sites were highlighted in the model. The head and stalk were tightly linked by the neck domain.

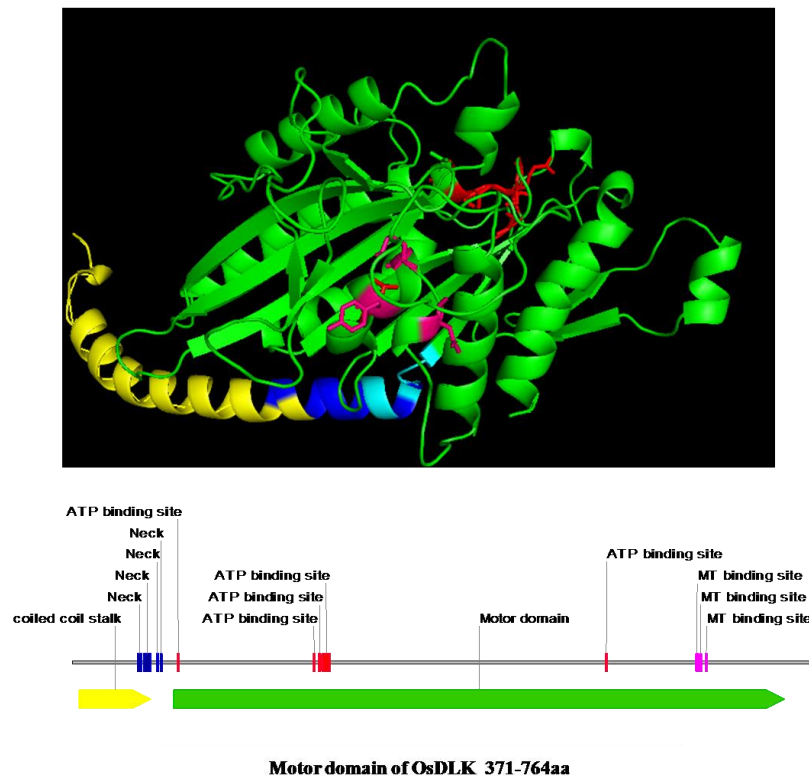


Figure 10 The predicted three-dimensional structure of motor part of kinesin OsDLK.

3.1.2 OsDLK is a highly conserved motor member of Kin-14

A protein BLAST search of OsDLK was performed in EXPASY (<http://web.expasy.org>), and the candidate kinesins were used to construct a phylogenetic tree with software MEGA5. OsDLK shows clear homology with other kinesin-14 sequences known from other organisms (Supp. Fig. S2). For instance, the N-terminus of the *Arabidopsis* kinesins ATK1 and ATK5 (with mutual amino-acid identities of 75.5%), exhibits 38.2% and 40.6% amino-acid similarity to OsDLK, respectively. In the motor domains, both ATK1 and ATK5 (Ambrose et al., 2005; Marcus et al., 2002) showed around 75% amino acid identity to OsDLK. Both ATK1 and ATK5 are C-terminus localized kinesins with a coiled-coil stalk in the middle of the protein. Interestingly, three putative NLS were predicted. While one motif of 11 amino acids length (amino acids 401-411) overlaps with the neck-linker domain, there are two additional putative bi-partite sites with long linkers at positions 64-93 and 207-237 aa.

A phylogenetic tree of the full-length sequences (Fig. 11) placed OsDLK (marked by an asterisk) clearly into the class-14 kinesins, more specifically, OsDLK clusters into the

Kinesin-14 subgroup with a C-terminal motor domain, with a close relationship to ATK5 and ATK1.

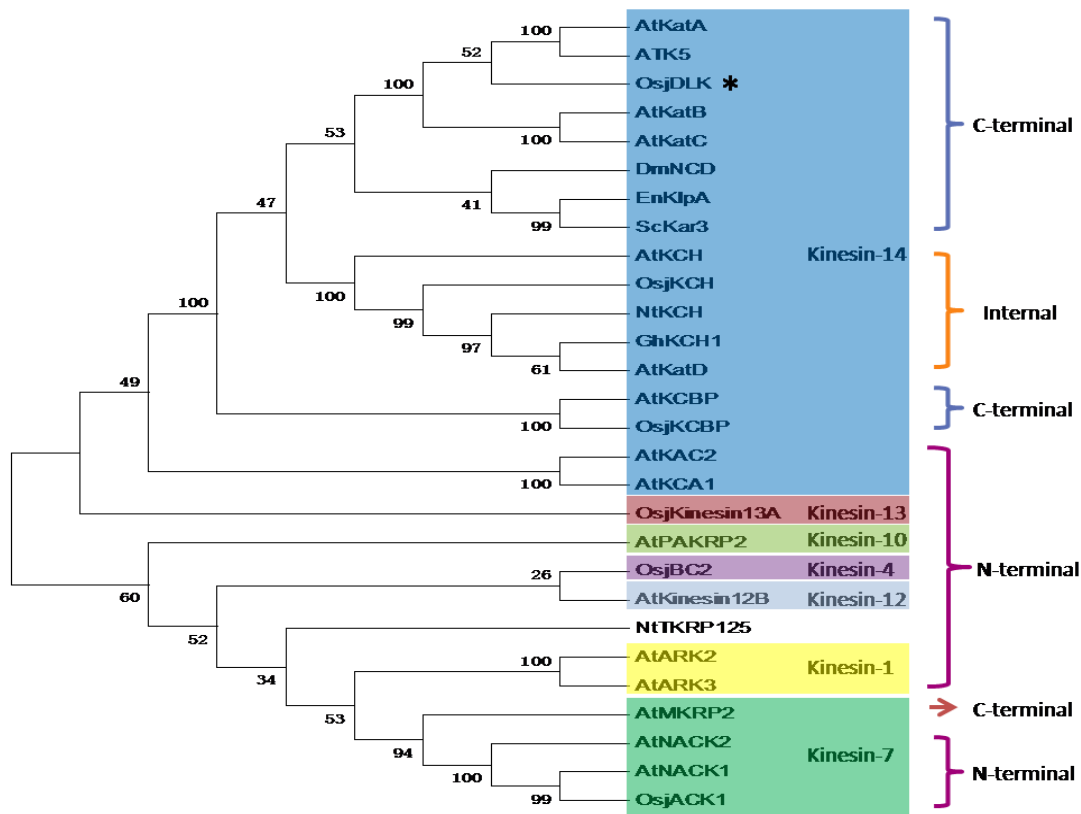


Figure 11 Phylogenetic relationship of OsDLK (marked by an asterisk) with other members of the Kinesin-14 family and selected members from other several kinesin subgroups from different animals and plants.

3.2 Homozygous rice mutants have lethal effects during seed germination

To investigate the potential function of OsDLK in rice, we were trying to screen the homozygous mutant of rice seedlings in which the gene *dlk* was interrupted by T-DNA fragment or the rice retrotransposon Tos-17. Thus we rose several generations (to more than T2 generation) heterozygous populations of the T-DNA and Tos-17 lines, and monitored them by genotyping via PCR. In no case we were able to identify a homozygous mutant plant in which only the PCR product indicative of the insertion could be amplified, but not the PCR product amplified by primers flanking the insertion

site (Fig. 12a,b). The ratios of the genotype didn't show the Mendelian law of inheritance (Fig. 12c). However this may due to the insufficient samples. For both T-DNA and Tos-17 insertion lines, most of the seeds could germinate into young seedlings. However, some of them stopped their development at the early the stage (Fig. 12d). The analysis of such seedlings revealed that homozygous *dlk* mutants were not viable.

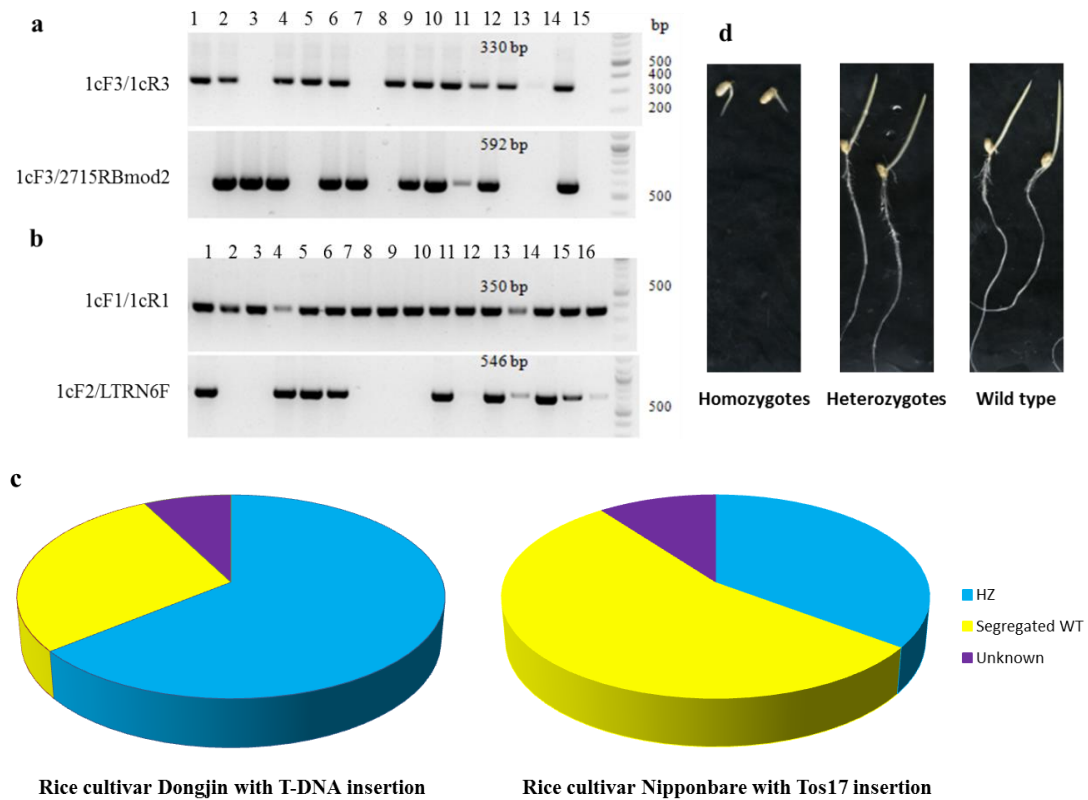
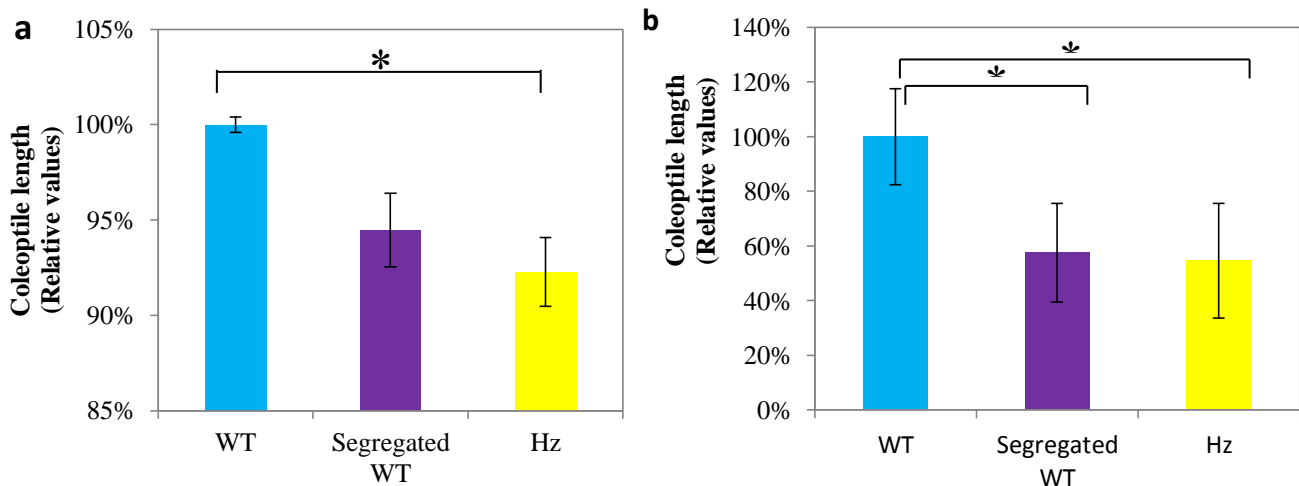


Figure 12 Representative results for rice insertion lines genotyping. (a) Representative PCR genotyping results from 15 samples of genomic DNA extracted from T-DNA insertion line PFG_3A-07110.R as templates. Two rounds of PCR were carried out with two pairs of primer which were genome-specific (1cF3/1cR3) and insertion-specific (1cF3/2715mod2), respectively. (b) Representative genotyping results for 16 samples of genomic DNA from Tos-17 insertion line ND4501_0_508_1 using genome specific (1cF1/1cR1) and insertion-specific primer combinations (1cF2/LRTN6F), respectively. (c) Genotyping ratios of Tos17 and T-DNA insertion rice lines in cultivar *Nipponbare* and *Dongjin*, respectively. (d) Representative figures for 4 day old seedlings of wild type, heterozygous and homozygous mutant.

3.2.2 Rice heterozygous mutants show faint delay in seed germination

Both of the heterozygotes from Tos17 insertion lines (cultivar *Nipponbare* as background) and T-DNA insertion lines (cultivar *Dongjin* as background) showed a significantly delay in coleoptiles elongation compared with the hereditary WT seedlings (Fig. 13a, b). However, when comparing with the segregated WT coleoptiles, they only exhibited very week delay (Fig. 13a, b). The difference between hereditary WT and the segregated WT coleoptiles may due to the different generations.

However, when look more into the segregation analysis, the coleoptile lengths of Tos-17 insertion heterozygotes distributed more in 3.0-3.5 cm while less in 3.5-4.0 cm in comparison to the segregated WT and the hereditary WT (Fig. 13c). In the T-DNA insertion, the coleoptiles had the most length of 0.5-1.0 cm, which was also showed clearly delay comparing with the segregated WT (1.0-1.5 cm) and the hereditary WT (2.5-3.0 cm) (Fig. 13d).



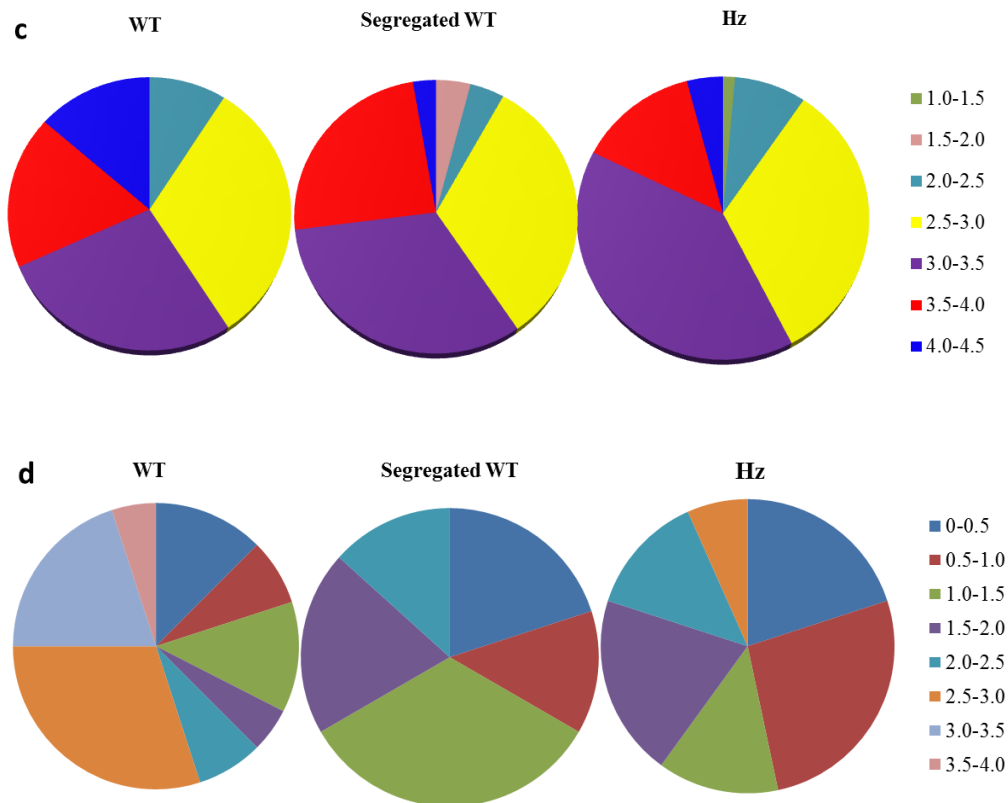


Figure 13 Heterozygous mutants of rice show a week delayed elongation in coleoptiles. (a) Coleoptile length of Tos17 and (b) T-DNA inserted rice seedlings grown up in darkness for 6 days. Error bars represent the standard deviation of biological triplicates. Hz: Heterozygous mutants. Asterisks (*) indicate differences between the WT and significant at $P < 0.05$ as evaluated by a t test for unpaired data. (c) The segregation analysis for the 6-day-old coleoptiles of Tos17 inserted rice lines and T-DNA inserted rice lines. Unit: cm.

These results indicated a very obvious delay of coleoptile growth in the heterozygous rice mutant of OsDLK. However, the hereditary background of OsDLK inside the rice Hz mutant could not be removed clearly. We could not get rid of the OsDLK effect actually.

3.2.3 OsDLK potentially has a pivotal role during seedling

development

We raised seedlings of wild type rice cultivar *Nipponbare* in darkness for 6 days to monitor the expression level of OsDLK seedling development. The results in Fig. 14a indicate that OsDLK had a relatively higher expression level in rice during the first 4 days of cultivation. On the first day we observed a high transcript level of a gene encoding for OsJAZ11, which is inducible by the plant hormone jasmonate acid (JA), an important regulator of seedling growth (Fig. 14b). As transcript level of OsDLK is high at very early stages in development of the wild type rice seedlings. In companion, the homozygous *dlk* rice mutants are arrested in development at the same stage. Hence, OsDLK was hypothesized to participate crucially in rice germination. The importance of this gene for seedling development is further substantiated.

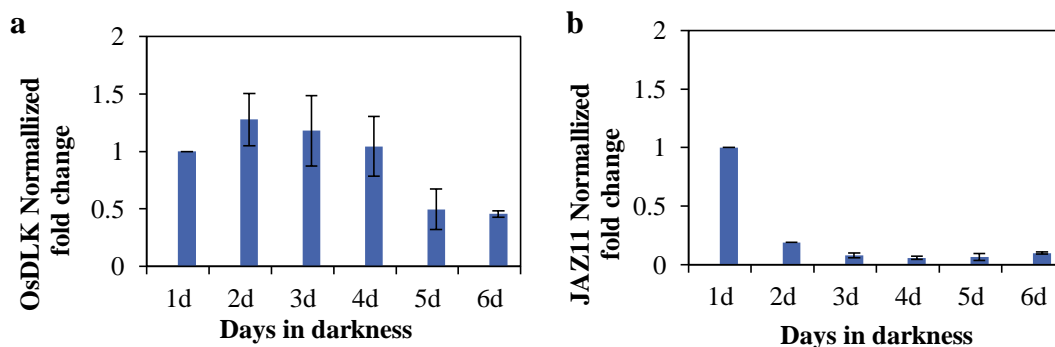


Figure 14 OsDLK expression is activated early in rice embryogenesis. (a) The transcripts level of OsDLK and (b) a representative Jasmonate acid, JAZ11 in rice during seed germination and seedling development. Datas in qPCR analysis were normalized using two standard genes, OsGAPDH and OsUBQ10. The fold change induction was calculated relative to a corresponding data of 1d as control. The datas represent the average of at least three independent experiments.

3.3 Localisation analysis of OsDLK in plant cells

Since the *dlk* rice mutant was not viable, it was not possible to investigate the biological function of OsDLK in rice development. Hence, we decided to apply a gain of function strategy by overexpressing the *dlk* gene from the rice cultivar *Nipponbare* fused to a

fluorescent, transiently in the rice cultivar *Nihonmasari*, and stably in *Nicotiana tabacum* L. cv. Bright Yellow 2 cells. We found that OsDLK is localized on both, cell cortex and nuclei in interphase cells, decorating cortical microtubules. And it also dynamically repartitioned spindle apparatus during mitosis.

3.3.1 Generated constructs for transformation

In order to gain insight into the unknown functions of OsDLK during the dynamic reorganisation of microtubules during the cell cycle, two constructs (OsDLK-GFP, and OsDLK-RFP) were generated for transient and stable expression in tobacco BY-2 cells under the control of a 35S promoter: a full-length OsDLK cDNA (2295 bp) was fused upstream of the green fluorescent protein (GFP) or red fluorescent protein (RFP). Besides, in some experiments, the truncated version OsDLKM (1110-2295 bp, harbouring the entire motor domain, but lacking most of the N-terminal half of the protein) was fused to the same position. The sequences corresponding to different length variants of *dllk* were amplified from the cDNA clone using the respective primers listed in Table 11. The DNA fragments with attB sites were transferred firstly entry clone vector pDNOR-zeo and later destination vector pK7FWG2.0 and pH7RWG2.0 (Table 18). The recombinant vectors are shown in Suppl. Fig. S6.

3.3.2 OsDLK is a dual localised kinesin

3.3.2.1 OsDLK is dynamically repartitioned during the cell cycle

To get insight into the putative function of OsDLK during cell cycle, localisation studies were performed. The recombinant construct OsDLK-GFP coding for the target protein OsDLK in fusion with GFP was transformed into tobacco BY-2 cells via *Agrobacterium* to establish stable cell lines overexpressing the target protein OsDLK. When the subcellular localisation of OsDLK-GFP was followed through the cell cycle the fluorescent signal underwent a dynamic reorganisation in a manner characteristic for microtubules, manifested by structures that showed all features including spindle and phragmoplast (Fig. 15).

In early prophase cells, identified by the lack of nucleolus and condensing chromosomes, OsDLK-GFP signal appeared in thread-like structures overlapping mostly with chromosomes (Fig. 15a-d). In the late prophase, the signal in the cell cortex disappeared completely, and the intranuclear signal was replaced by a mesh-like structure wrapping the nucleus (Fig. 15e-h). During early metaphase, OsDLK-GFP was found to be condensed more tightly around the chromosome band in the center of the cell (Fig. 15i-l). During metaphase, OsDLK-GFP was found as (relatively scarce) beads on a string distally from the metaphase plate, along with agglomerations in the metaphase plate, mostly proximally of the chromosomes (Fig. 15m-p). During anaphase (Fig. 15q-t), the signal distal to the metaphase plate had increased into clear and continuous fibers, whereas the signal in the metaphase equator had almost vanished. When anaphase was completed, OsDLK-GFP returned to the equatorial region (Fig. 15u-x) to give rise to the phragmoplast. Phragmoplast is the microtubule array which deposits cell plate material as it expands outward, and therefore, similar to the cortical microtubules that form later, shares its association with the cell wall.

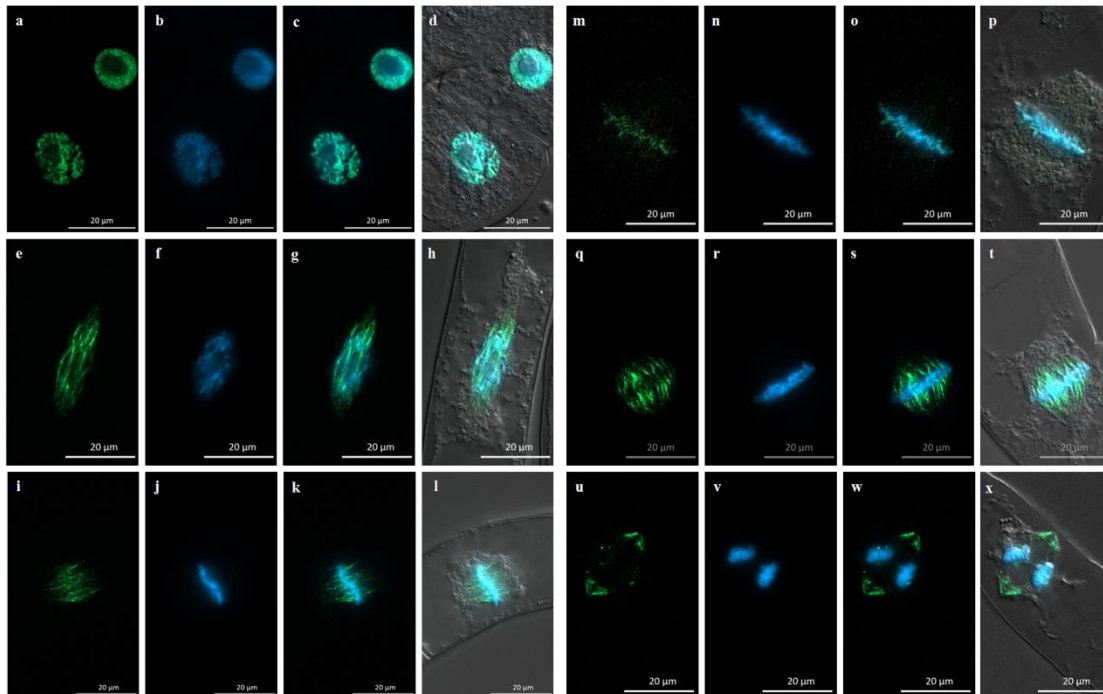


Figure 15 Subcellular localisation of OsDLK-GFP upon heterologous expression in tobacco (*Nicotiana tabacum*) BY-2 cells. (a-x) Cells in subsequent stages of mitosis upon dual visualisation of full-length OsDLK (GFP signal) and DNA (Hoechst 33258). (a-h) prophase. (i-p) metaphase. (q-t) Transition metaphase to anaphase. (u-x) Transition anaphase to telophase. The GFP signal indicative of OsDLK is shown in a, e, i, m, q and u; the Hoechst 33258 signal indicative of DNA is shown in b, f, j, n, r and v;

both GFP and Hoechst signal channels are merged in c, g, k, o, s and w; d, h, l, p, t and x show the merge of all the channels. Scale bars: 20 μm .

To get more insight into these complex migrations of OsDLK-GFP during the later phase of mitosis, detailed time-lapse series were recorded (Fig. 16). These series show how OsDLK-GFP at the final stage of metaphase is organised in rod-like structures at the proximal edge of the metaphase plate that are aligned polewards. Then, within 3 min, the signal moves towards the spindle poles and contracts in two helmet-like clusters just beneath a terminal, smaller cluster. Then, the whole structure shortens rapidly, such that 5 min later the two helmets have reached the equator again lining from two sides a dark zone that probably corresponds to the newly emerging cell plate. During this contraction process, the first strongly aggregated bundles in the helmet detach into finer fibers that probably represent the microtubules of the phragmoplast. During expansion of the phragmoplast, OsDLK-GFP remains closely linked with phragmoplast microtubules over the next 15 min till the expanding phragmoplast reaches the lateral walls. Afterwards, the signal starts to appear at the nuclear envelopes of the newly formed daughter nuclei, and first concentrates at the trailing edge of the nuclei (that move apart from the cell plate). Later, when the daughter nuclei have reached their position in the symmetry planes of the newly formed cells, this gradient is progressively levelled out.

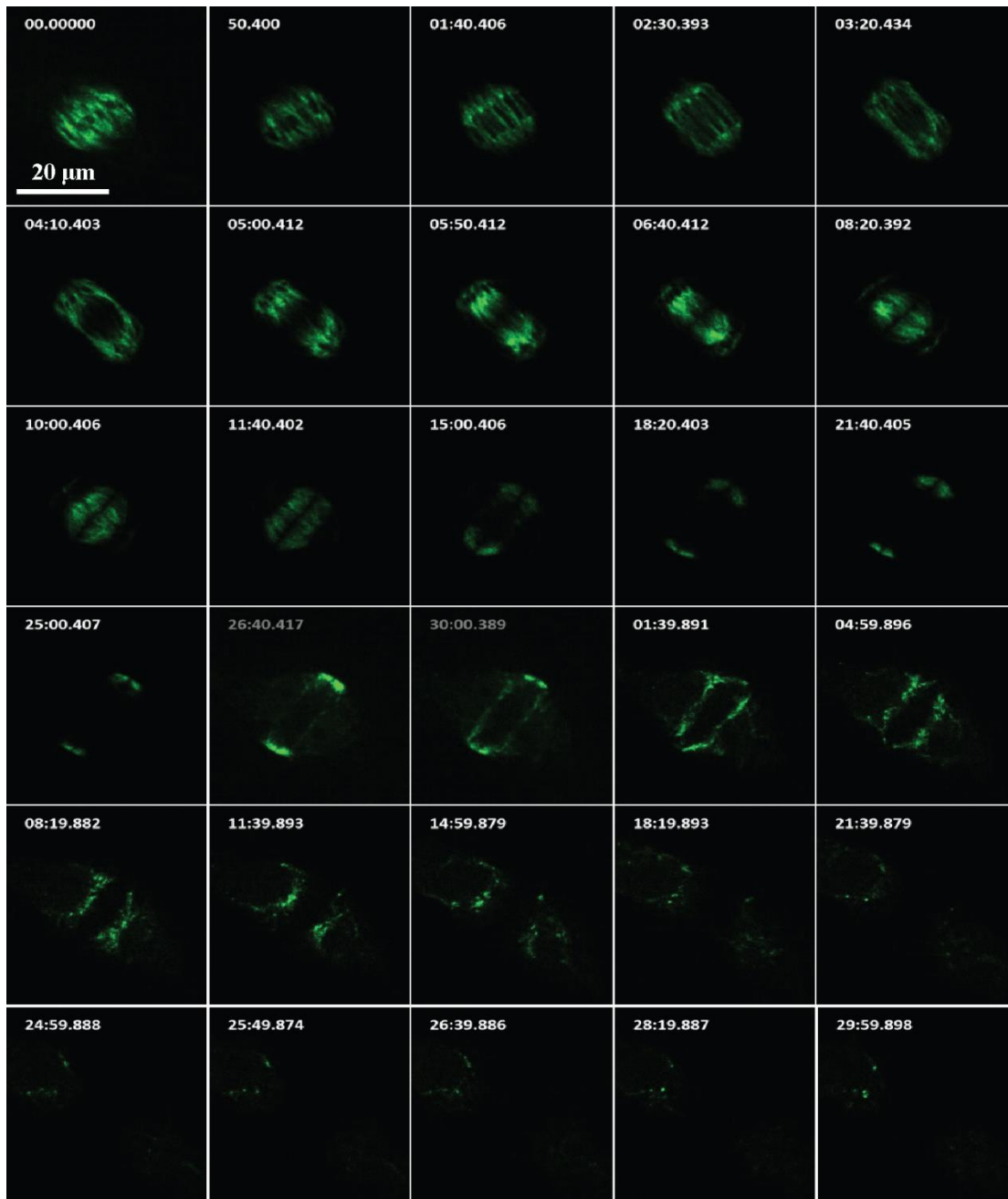


Figure 16 Time-lapse series of DLK-GFP localisation during the later phases mitosis and during cytokinesis, time unit: s.

The localisation of the truncated protein OsDLKM-GFP containing the whole motor part and partial of the coil-coiled stalk of the kinesin was visualized during the cell cycle in stable BY-2 cell line (Fig. 17). The signal concentrated around the nucleus and emanated towards the periphery in a radial network in prophase cells. Afterwards GFP signal decorated the spindle in metaphase and anaphase. Then OsDLKM wrapped the newly formed nuclei in the last phase of cell mitosis. In cytokinesis, the signal of

OsDLKM-GFP appeared only on filaments that span longitudinally from the nuclei towards the cell poles.

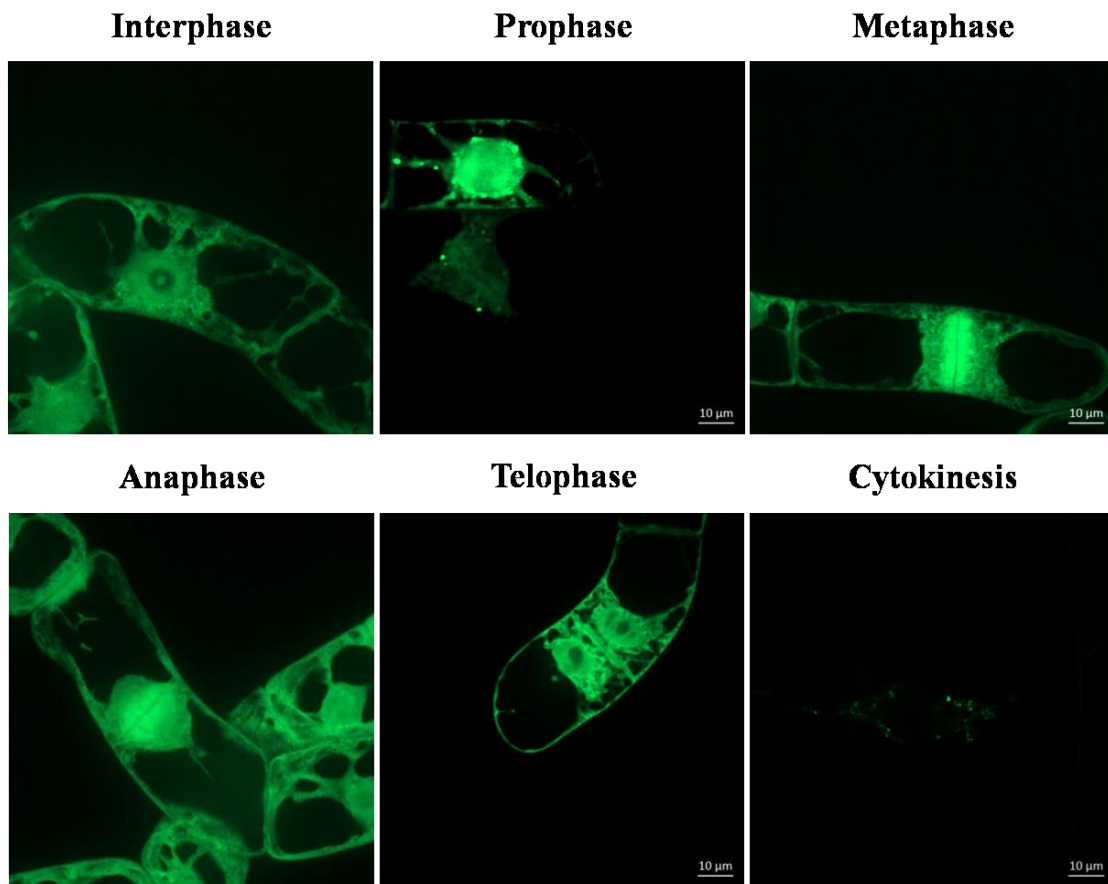


Figure 17 Subcellular localisation tracking of OsDLKM-GFP upon heterologous expression tobacco BY-2 cells during interphase and mitosis. Scale bars: 10 µm.

3.3.2.2 OsDLK is dual located during interphase

Interphase cells stably expressing the OsDLKM-GFP did not decorate cortical microtubules. Instead, the fluorescent signals were found around in a diffuse manner in cytoplasmic strands and as punctate signal around the nucleus (Fig. 18d-f).

However, surprisingly, the full-length kinesin OsDLK-GFP was localised in two populations in interphase of BY-2 cell in a stable cell line: On the one hand, OsDLK-GFP was continuously decorating lateral cortical microtubules (Fig. 18a-c), which was in contrast to the truncated OsDLKM-GFP. Simultaneously, intensive fluorescent signals were found inside the nucleus. This observation suggested a potential role of the N-terminal tail part of OsDLK missing in this truncated construct for the localisation on

cortical microtubules, although the putative motor domain was present. Adversely, the N-terminal part had scant determinational effect of kinesin for decorating the mitosis.

For double confirmation, OsDLK-GFP construct was also transformed transiently into coleoptiles of rice. The result was consistent with that in BY-2 cells that OsDLK had dual localisations during interphase (Fig. 18g-h).

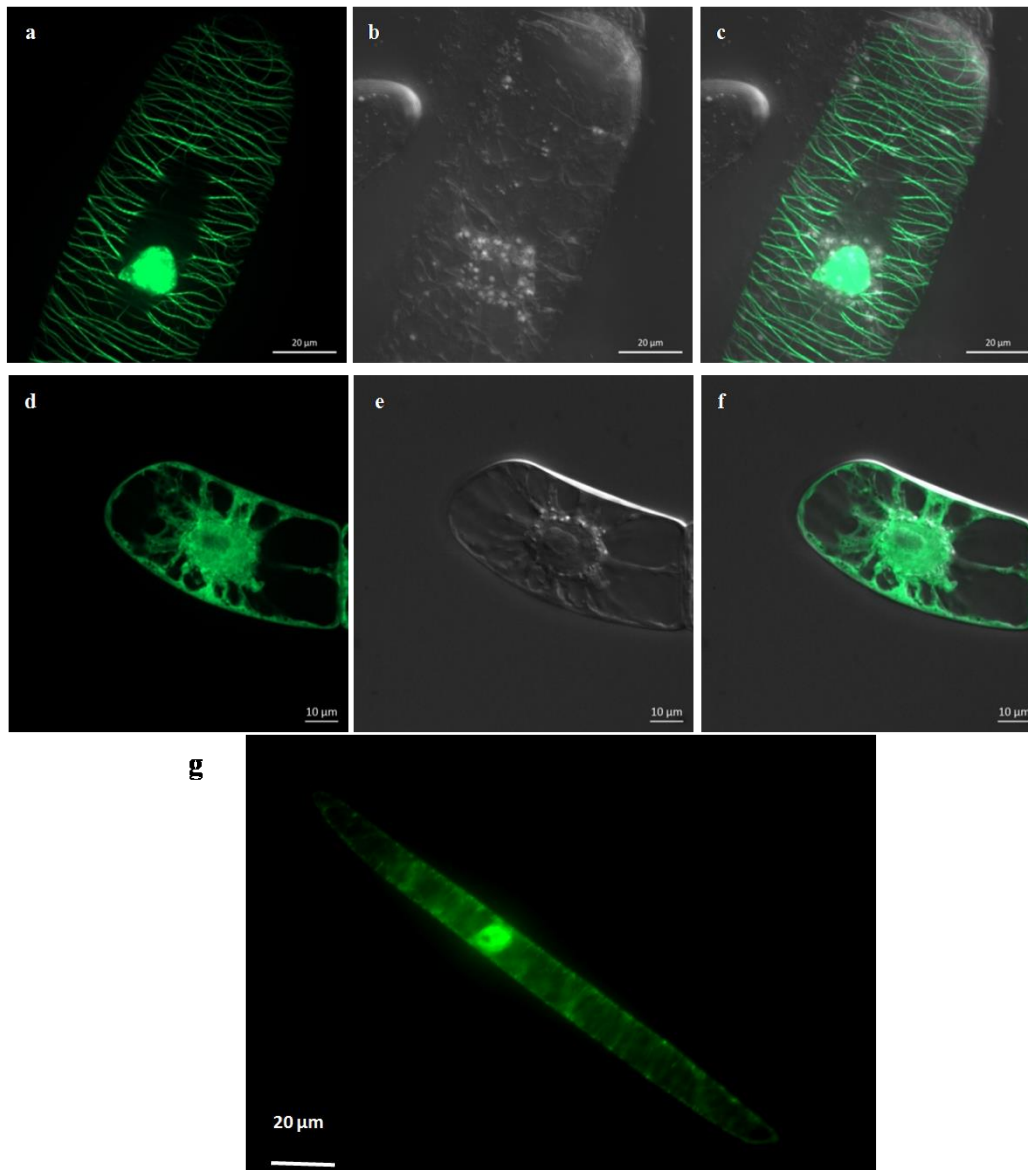
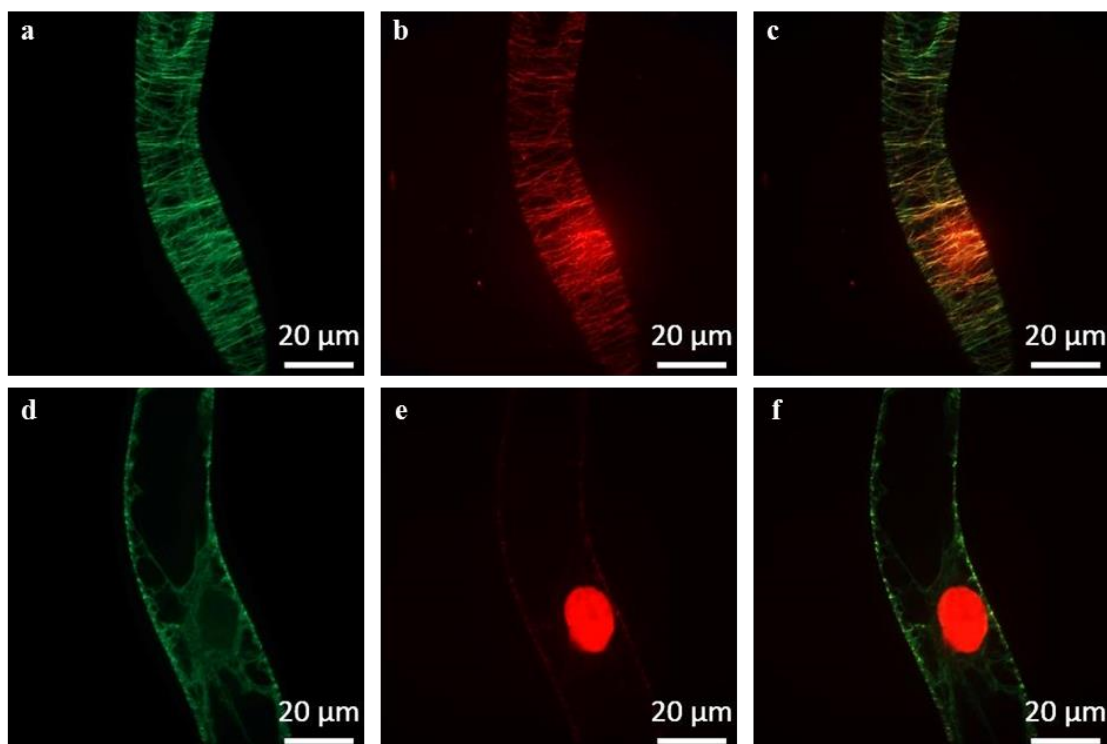


Figure 18 Subcellular localisation of OsDLK-GFP in interphase in heterologous expression tobacco and rice cells. (a-c) Dual localisation of full-length DLK-GFP during interphase in BY-2 cells. (d-f) Subcellular localisation of the truncated DLKM during interphase. (g) Dual localisation of full-length OsDLK in rice cells. GFP signal (a, d, g), differential interference contrast (DIC) (b, e) and merged images (c, f). Scale bars: 10, or 20µm.

3.3.3 Visualisation of microtubules in fixed cells

To test, whether OsDLK was associated with microtubules, we used two approaches - transient co-transformation of OsDLK (as fusion with RFP) and the microtubule marker TuB6 (as fusion with GFP), as well as immunolabelling of microtubules in cells expressing OsDLK-GFP in a stable manner using TRITC-conjugated secondary antibodies. By the co-transformation, we found that OsDLK-RFP decorated the GFP-labelled cortical microtubules (Fig. 19a-c), whereas the nucleus of the same cells harboured the RFP signal indicative of OsDLK, but no microtubule signal (Fig. 19d-f). This uncoupling of the two signals in the nucleus could also be confirmed using TRITC-based immunostaining of microtubules. After staining microtubules in the stable cell line overexpressing OsDLK, the colocalisation between OsDLK and MT was clearly observed (Fig. 19g-j, o-q). Conversely, immunolabelling of the phragmoplast (Fig. 19k-n) showed a tight colocalisation of OsDLK-GFP and microtubules, whereas the interior of the newly formed daughter nuclei was not labelled.



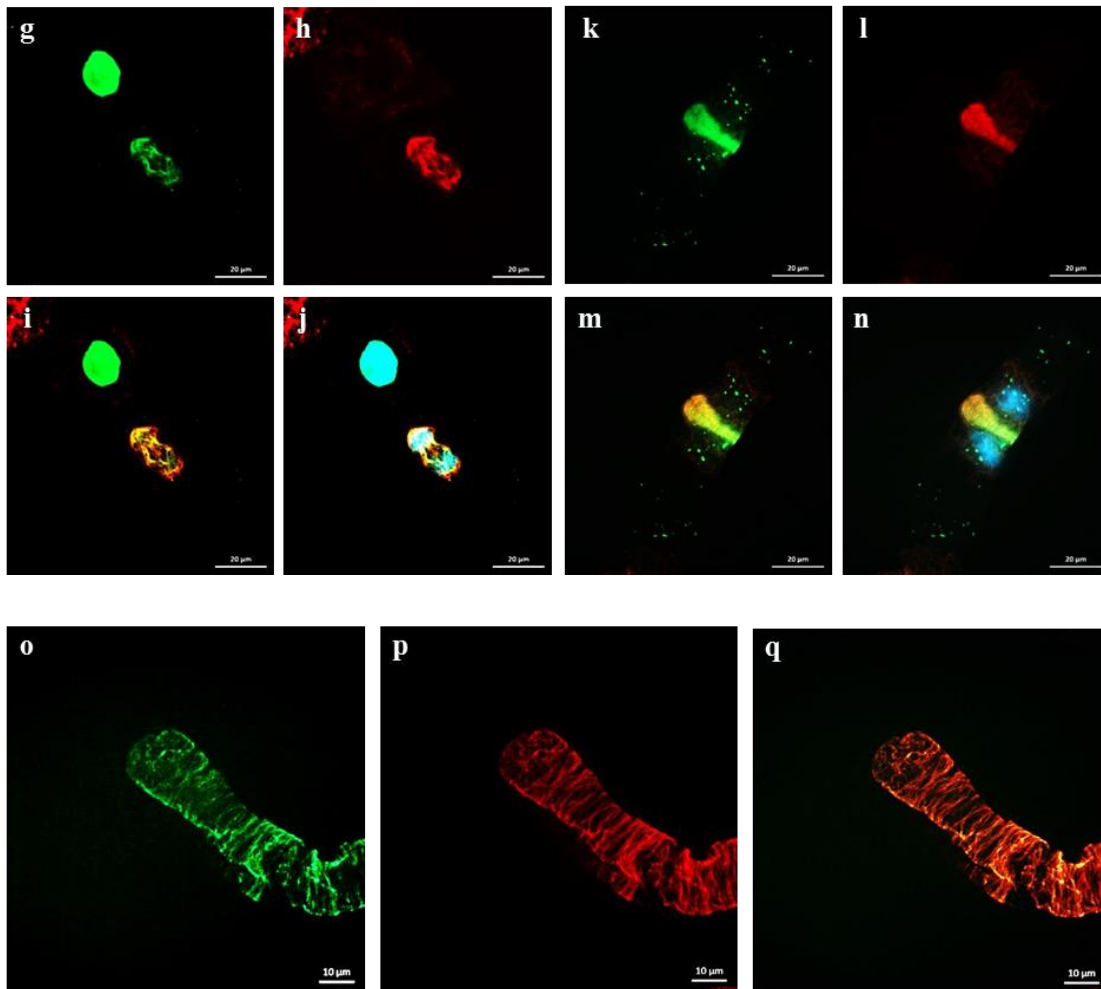


Figure 19 Co-localisation of OsDLK fusions with fluorescent proteins and microtubules upon heterologous expression in tobacco BY-2 cells. (a-o) Transient co-transformation of OsDLK-RFP and marker TuB6-GFP into wild type BY-2 cells. (a-f) Cortical and central confocal section of a cell transiently transform with OsDLK-RFP and GFP-pCambiaTuB6 showing the colocalisation of OsDLK (b) with cMTs (a) in periphery, and the intranuclear localisation of OsDLK-RFP (e) while pCambiaTub6 (d) localized in radial MTs tethering the nucleus. Merged signals are shown in c and f. (g-q) Immuno-staining of MT in OsDLK-GFP overexpresspr. (g-i) Triple staining of OsDLK-GFP, microtubules visualised by immunofluorescence with rhodamine, and DNA visualised by Hoechst 33258 of representative cells in late anaphase (g-j) and telophase (k-n). (o-q) Double staining of OsDLK and MT in interphase cells. The OsDLK-GFP signal is shown in g, k and o, the microtubule signal in h, l and p, the merge of these signals in i, m and q, the merge of all three signals in j and n. Scale bars: 10, or 20 μm.

Thus, OsDLK-GFP colocalised with the wall-associated arrays of microtubules (cortical microtubules, phragmoplast). However, during interphase, it can occur in a second form that resides inside the nucleus and seems to be dissociated from microtubules. Since GFP and RFP are smaller than the exclusion size of nuclear pores, the intranuclear fluorescence would be consistent with a scenario, where the intranuclear label is caused

by cleavage of GFP from DLK, The fact that the intranuclear signal depends on the cell cycle (present in interphase, absent in telophase) argues against such a cleavage scenario. Moreover, cleaved label should equally label the cytoplasmic strands in a diffuse manner, which is not seen.

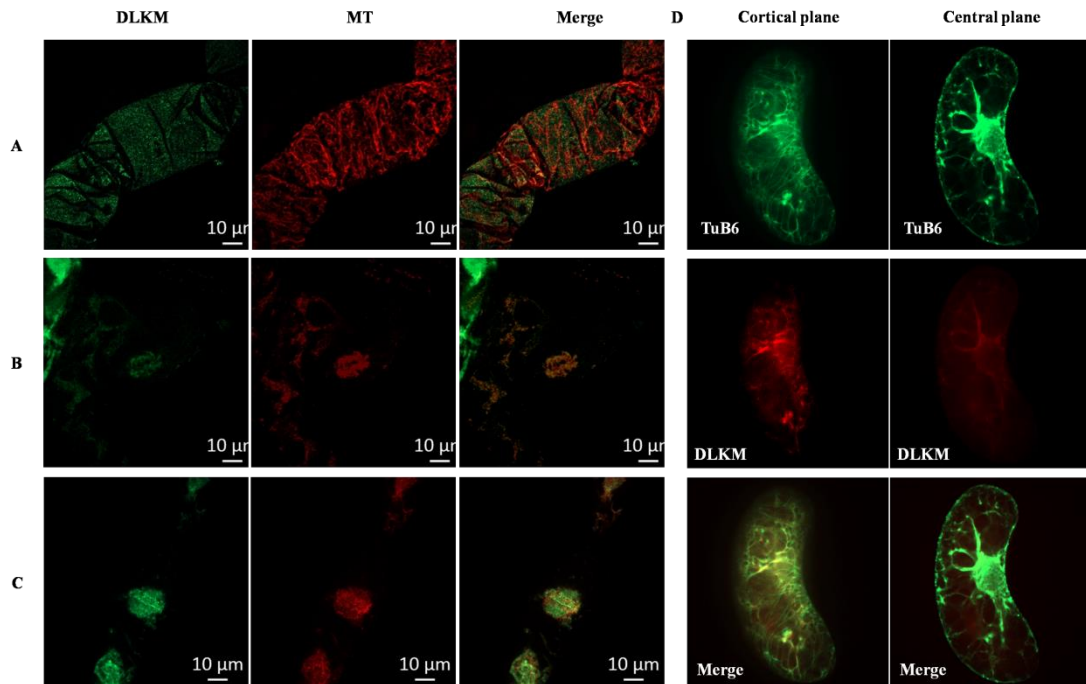


Figure 20 Co-localisation of OsDLKM fusions with green fluorescent proteins and microtubules in tobacco BY-2 cells. Microtubules (MT) in cells in interphase (A), metaphase (B) and anaphase (C) overexpressing truncated OsDLKM protein was immunostained with primary anti-alpha Tubulin antibody and TRITC-conjugated secondary antibody. (D) Transient co-transformation of DLKM-RFP and TuB6-GFP in undividing cells. Scale bars: 10 μ m.

When immunolabelling of microtubules in the overexpressor OsDLKM-GFP using TRITC-conjugated secondary antibodies, the truncated protein OsDLKM was found to diffuse in the interphase BY-2 cells, with rare co-localisation with microtubule (Fig. 20A). Nevertheless, OsDLKM was well overlapped with spindle MT in dividing cells (Fig. 20B, C). In the co-transformation, signal of OsDLKM-RFP was diffused in the whole cells in interphase and the colocalisation with MT was indistinct, as shown in Fig. 20D. The result was consistent with immunolabelling and further with localisation study shown in Fig. 18, 19.

3.3.4 Visualisation of OsDLK and further Kinesin-14

member OsKCH

For more information of OsDLK interacting with other kinesin member in subfamily 14, we tried to transform OsDLK-RFP into 4-day-old wild type tobacco BY-2 cells, together with GFP-OsKCH, a calponin-homology kinesin involved in the interaction and cross-talk between microtubules and actin microfilaments (Frey et al., 2010). The representative result is shown in Fig. 21. Localisation of OsDLK exhibited strong signals in both cortex and nucleus in interphase while OsKCH appeared on the cortex and around but not inside the nucleus (Fig. 21A). In the premitotic cell, OsKCH1 was clearly aligned punctually along filaments with mesh-like structures on both sides of the nucleus and spanned over and surrounded the nucleus which was consistently strong as reported before, while OsDLK was aligning as filaments on both side of the nucleus, tethering the nucleus with strong signal inside (Fig. 21B). Taken together, the Kin-14 proteins OsDLK and OsKCH were not co-localizing.

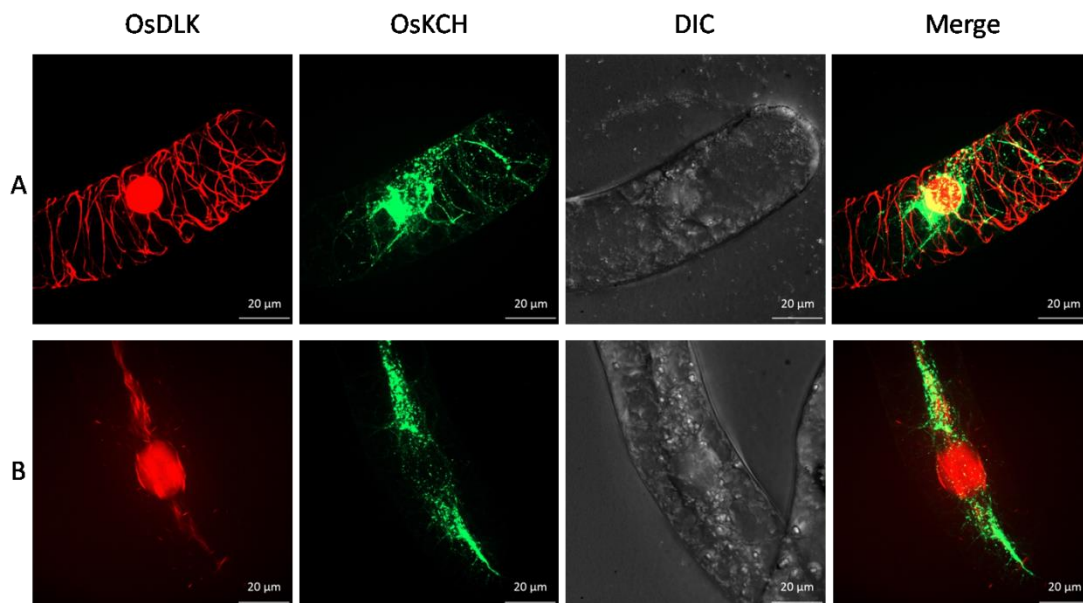


Figure 21 Co-localisation of Kin-14 proteins fusion with fluorescent proteins in upon heterologous expression in tobacco BY-2 cells. (A) Representative interphase cell and (B) dividing cell double transformed with OsDLK and OsKCH, with RFP and GFP respectively. Scale bars: 20 µm.

3.4 Characterization of the biological role of OsDLK

As shown in sections before, OsDLK is highly repartitioning during cell cycle and associated with microtubule arrays such as spindle and phragmoplast. And OsDLK has two populations in interphase cells: on the one hand, OsDLK localises on the cortex of the overexpression tobacco cells; on the other hand, it occurs in the nucleus. However, the biological role remains elusive. In this chapter, we addressed the role of OsDLK by investigation of gene expression patterns in rice and development specificities in transgenic tobacco BY-2 cells.

3.4.1 Gene expression pattern in rice

3.4.1.1 Investigation of OsDLK tissue specificity in rice

In order to investigate the potential physiological role of OsDLK, we quantified the gene expression by real-time PCR in different tissues of *Nipponbare*, which were raised under continuous white light for 10 days.

The gene expression pattern of OsDLK in different tissues is shown in Fig. 22. The results showed that the abundance of transcripts was high in the third leaf, especially in the sheath of the second leaf.

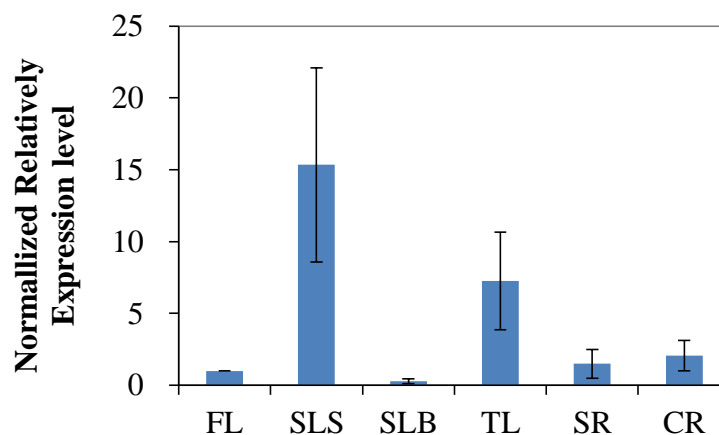


Figure 22 Gene expression pattern of OsDLK in rice. Expression of OsDLK in rice seedlings of the wild type *Oryza sativa* ssp. *japonica* cv. *Nipponbare* measured by real-time PCR. FL: First leaf; SLS: Second

leaf sheath; SLB: Second leaf blade; TL: Third leaf; SR: Seminal root; CR: Crown root. The data represent the average of at least three independent experiments.

3.4.1.2 Gene expression of *OsDLK* is regulated by red light

To test whether there is some interaction of *dlk* and Jasmonate-signalling pathway, the coleoptiles and leaves from rice (wild type *Nipponbare*) young seedlings were exposed transiently to red light. After specific time points, samples were collected for the analysis by real-time PCR. Along with the transcriptional regulation of endogenous *OsDLK* also representative JA-signalling gene, *OsJAZ11*, was examined.

The results showed (Fig. 23) that *OsJAZ11* was induced by red light and its expression level peaked 1 h after the onset of irradiation in comparison with dark control (nearly 20-fold induction), both in coleoptiles and leaves (Fig. 23b,d). When coleoptiles were treated, the transcript of *dlk* was reduced slightly and stimulated soon afterwards, peaking after 12 h (Fig. 23a). However, it became weaker 24 h after irradiation by red light.

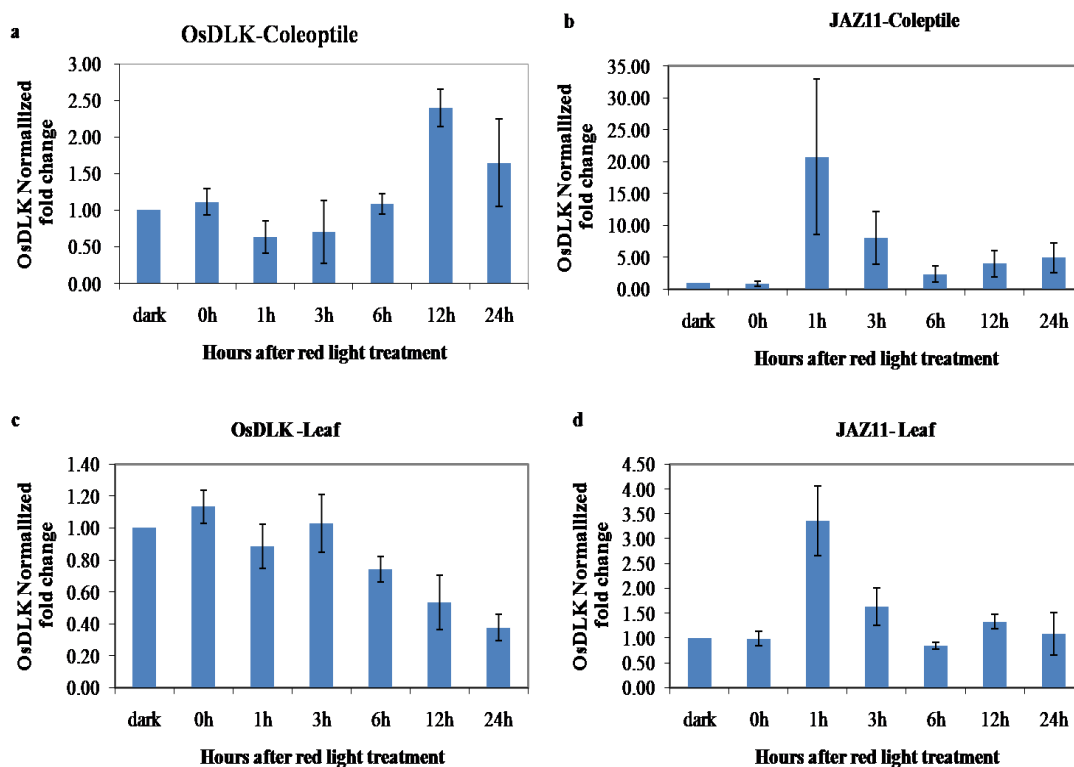


Figure 23 Transcript levels of the rice *OsDLK* and JA-signalling gene *OsJAZ11* in light irradiation. qPCR analysis was carried out with UBQ10 and GAPDH as housekeeping genes. The samples maintained in

darkness were used for normalization. (a) Transcripts levels of endogenous *OsDLK* and (b) *OsJAZ11* in coleoptiles of wild type rice cultivar *Nipponbare* treated with red light for 3 min. (c, d) The transcript level in leaves treated with red light for 3 min. Each point represents the average of 20-30 seedlings collected from at least three independent sets of experiments.

3.4.2 Phenotype investigation of *OsDLK* overexpressor

3.4.2.1 *OsDLK* overexpressor stimulates cell proliferation

In order to test the cellular function of *OsDLK* in cell proliferation, the mitotic index of the stable cell line overexpressing *OsDLK*-GFP was followed for 6 days in comparison with the non-transformed BY-2 cell line. The results showed that the mitotic index of the transgenic cell line was significantly higher during the 4 days after subcultivation, especially on the second and third day (Fig. 24a). To find out, whether this increase in the frequency of mitotic cells was caused by a higher mitotic activity or by a elongation of the cell cycle, the doubling time of the two cell lines was determined from the time course of cell number (Fig. 24b). The doubling time of the *OsDLK*-GFP overexpressor was found to be 23.9 h, the doubling time of the wild type was found to be 24.5 h. Thus, the increase in mitotic index was not caused by a shorter cell cycle, and therefore must come from a higher frequency of cells entering mitosis.

However, at the end of the proliferation phase (after 4 days of cultivation), the packed cell volume of the *OsDLK*-GFP overexpressor was significantly decreased compared to the WT cell line (Fig. 24c). Interestingly, this decrease was compensated during the following two days, such that the packed cell volume exhibited no difference after 6 days of cultivation (Fig. 24d).

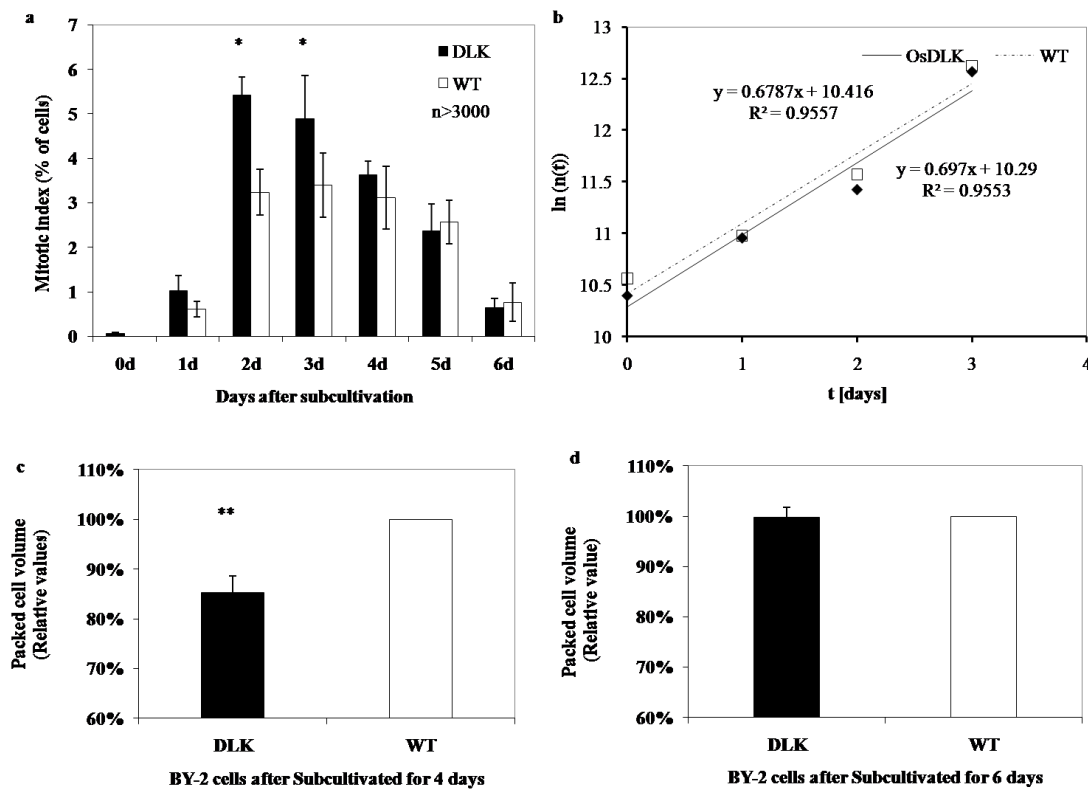


Figure 24 Measuring of mitotic index (MI) of overexpressed BY-2 cells in comparison to WT. (a) Stimulation of MI in OsDLK-GFP BY2 compared to non-transformed BY-2 WT. More than a total of 3000 cells per time point and sample were collected cumulatively from three independent experimental series. Asterisk (*) indicate significant differences between the cell lines at $P < 0.05$ as evaluated by a t test for unpaired data. Error bars represent the standard error of triplicate measurements. (b) Estimated cell cycle lengths for OsDLK-GFP and non-transformed BY-2 WT. (c, d) Packed cell volume in the OsDLK-GFP overexpressor compared to the non-transformed BY-2 WT 4 days (c), and after 6 days (d). **significant difference between the cell lines at $P < 0.01$ as evaluated by a t test for unpaired data. Error bars represent the standard deviation of triplicate measurements.

3.4.2.2 OsDLK overexpressor delays cell elongation

In order to determine whether this compensation of PCV was due to cell expansion or cell proliferation, cell length and width were determined. At day 3, the OsDLK-GFP cells were significantly shorter but broader compared to the WT cells (Fig. 25a). However, at day 7 cell length between the two lines was equal, while the cell width of overexpressor cells was slightly, but significantly decreased (Fig. 25a). Thus, overexpression of OsDLK-GFP stimulated mitotic activity during the proliferation phase of the culture while delaying cell elongation. This was then compensated by a

more pronounced elongation during the expansion phase of the culture. Representative WT and overexpressor cells cultivated for 3 and 7 days were shown in Fig. 25b.

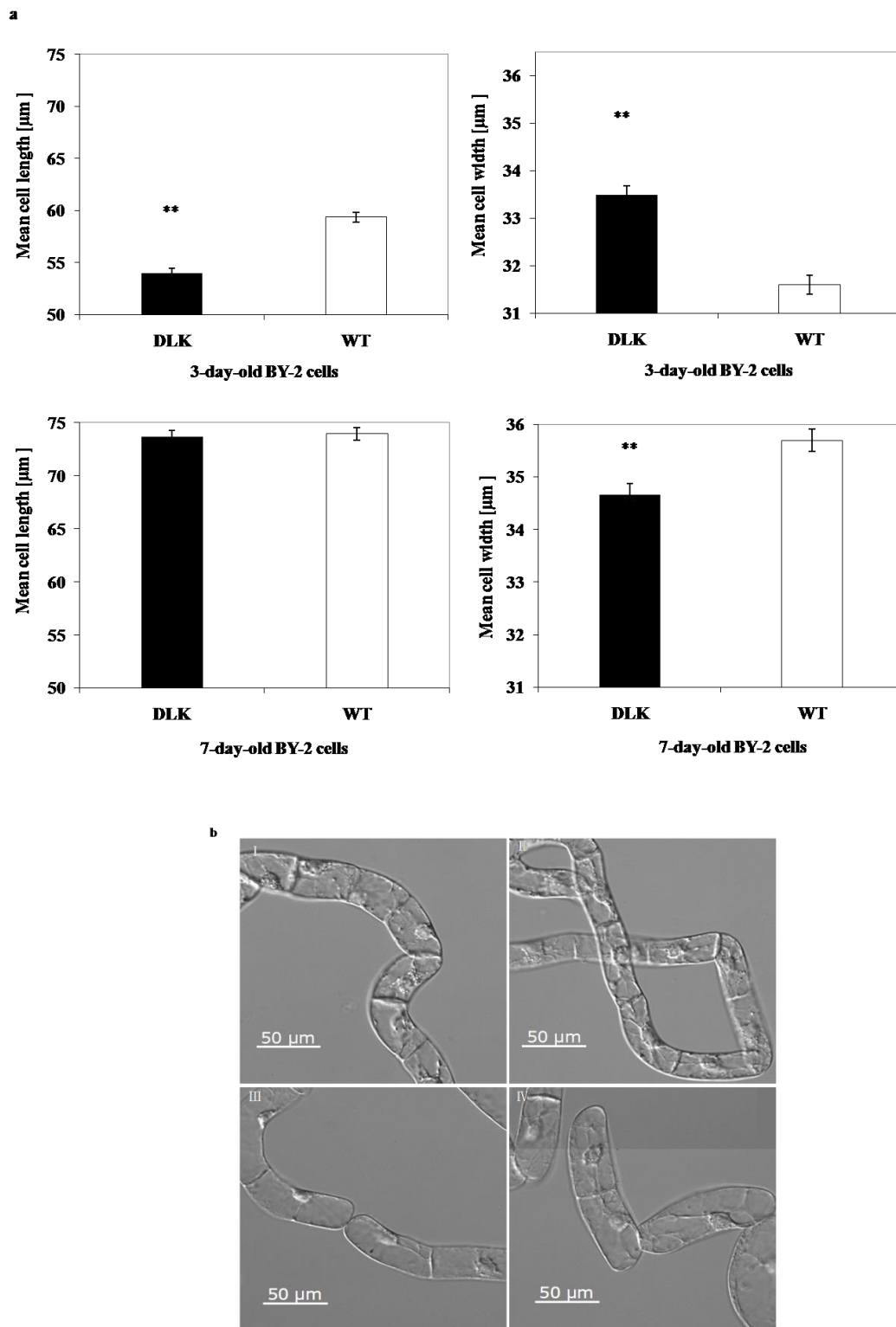


Figure 25 Measuring of cell length and width of overexpressed BY-2 cells in comparison to WT. (a) Promoted cell elongation during the expansion phase of late cultivation cycle in the OsDLK-GFP overexpressor versus the non-transformed WT. Cell length and cell width at day 3, and at day 7. Error

bars represent the standard deviation of triplicate measurements. Asterisks (**) indicate $P < 0.01$ as evaluated by a t test for unpaired data. (b) Representative cell files of the OsDLK-GFP overexpressor (I, III) compared to the non-transformed wild type (II, IV) at day 3 (I, II) and at day 7 (III, IV); (I) OsDLK-GFP at day 3; (II) WT at day 3; (III) OsDLK-GFP at day 7; (IV) WT at day 7.

3.4.2.3 OsDLK overexpressor delays the transition into metaphase

Although the OsDLK-GFP overexpressor exhibited a higher mitotic index (Fig. 24a), the length of the cell cycle did not differ from the values observed in the non-transgenic BY-2 (Fig. 24b) indicating that the lines differ with respect to the duration of mitosis. We therefore decided to monitor the temporal progression through mitosis in synchronized BY-2 cells.

For this purpose, cells were treated first with the ribonucleotide reductase inhibitor hydroxyurea (which arrests the cells in S-phase) and then with the reversible anti-microtubule inhibitor propyzamide (which arrests the cells in prophase). Following the treatment with hydroxyurea, the mitotic index was 0% indicative of full suppression of cell cycle progression into the M-phase. Upon release from propyzamide, mitotic indices reached 70% in the non-transformed WT, indicative of a high degree of synchronisation (Fig. 26a). In the OsDLK-GFP overexpressor line, synchronisation was less efficient with mitotic indices of 60% (Fig. 26a).

When the frequency of the individual mitotic phase were followed over time (Fig. 26b), significant shifts in the relative timing of individual phases became evident (Fig. 26c, d). Whereas the metaphase peak in the OsDLK-GFP line was seen 90 min after removal of propyzamide, which was half an hour later than in the WT (Fig. 26c), the telophase peak of OsDLK-GFP cells occurred 30 min earlier than in the WT (Fig. 26d). These time courses report that, in the OsDLK-GFP overexpressor, the mitotic phases preceding metaphase were prolonged, whereas the mitotic phases following metaphase were accelerated.

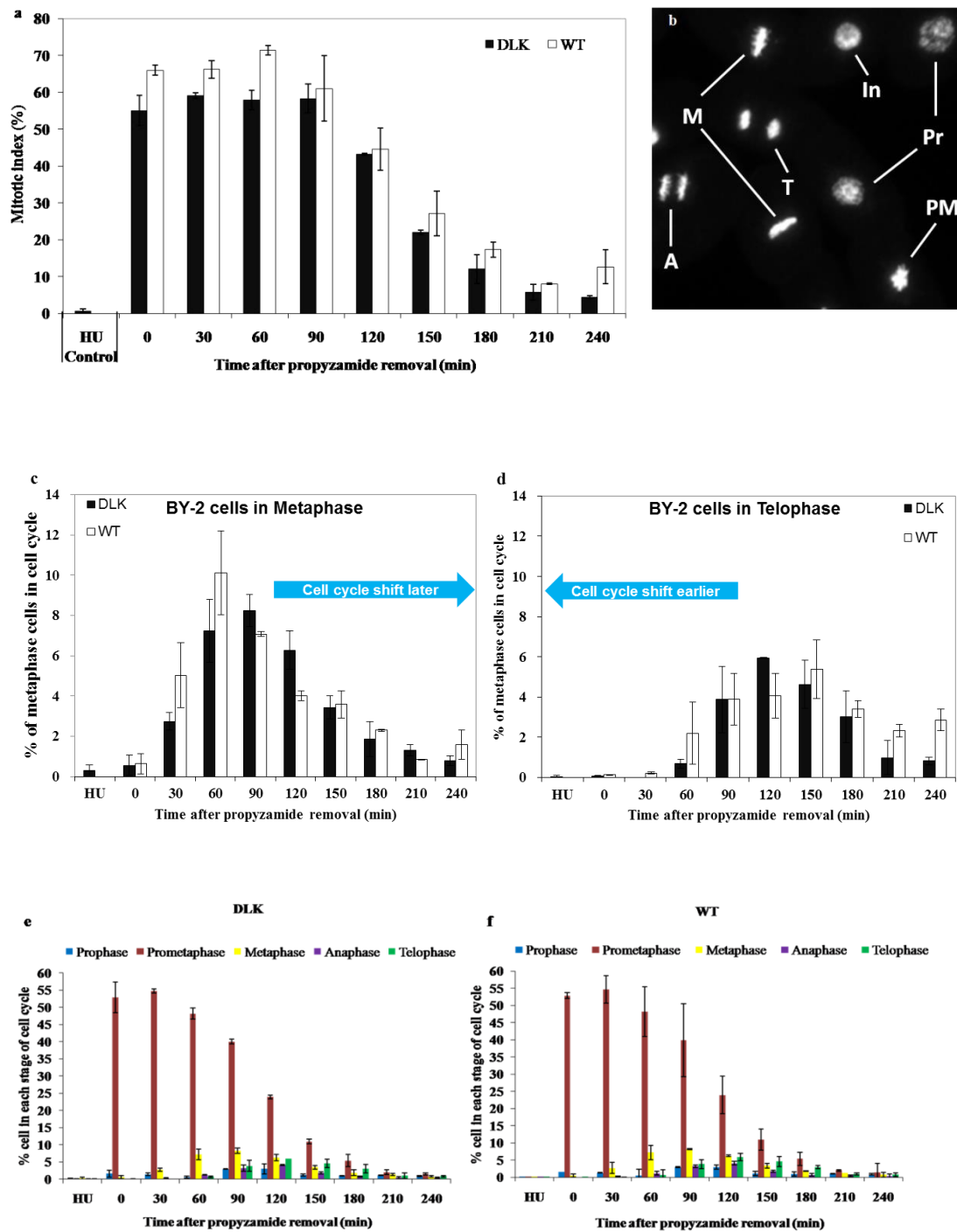


Figure 26 The temporal mitosis progression was monitored in synchronized BY-2 cells. (a) Time course of mitotic index (MI) in OsDLK-GFP cells (black bars) and non-transformed wildtype cells (white bars) after synchronisation with hydroxyurea (HU) for 24 h and with propyzamide for 3 h. Time points represent the interval after release from propyzamide treatment. (b) Representative image of cells stained for DNA after release from propyzamide. In, Interphase cells; Pr, Prophase cell; PM, Prometaphase cells; M, Metaphase cells; A, anaphase cells; T, Telophase cells. (c) Frequency of metaphase of cells over the time after release from propyzamide. (d) Frequency of telophase cells over the time after release from

propyzamide. (e) Time course for the frequency of individual mitotic stages following release from propyzamide in OsDLK-GFP and (f) non transformed WT BY-2. Error bars represent the standard error of from biological triplicates comprising a population of 3000 cells per data point. Error bars represent the standard deviation of biological triplicates comprising a population of 3000 cells per data point.

These results are corroborated by time courses of nuclear positioning recorded over the cultivation cycle (Fig. 27). Here, the initial premitotic migration of the nucleus from the lateral wall to the cell center was slowed down in the OsDLK overexpressor as compared to the non-transformed WT, consistent with a time-limiting step during early mitosis that is delayed by the overexpression of OsDLK-GFP.

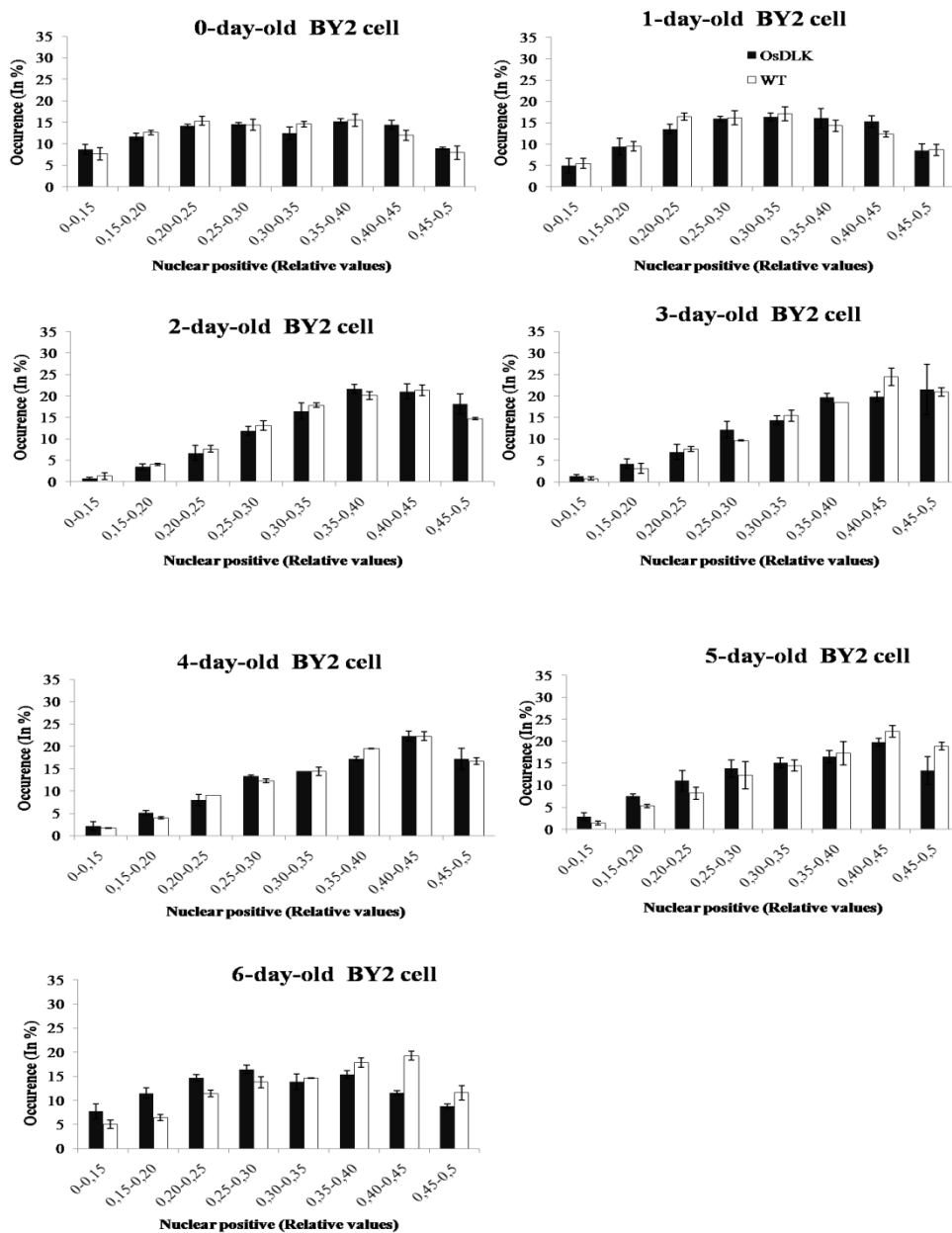


Figure 27 Time course of nuclear positioning. Frequency distributions of nuclear position were recorded in OsDLK-GFP BY-2 (black bars) and the non-transformed WT (grey bars) at daily intervals over the entire cultivation cycle. A value of 0.5 represents a position in the cell center, a value of 0 represents a position at the lateral walls. Error bars represent the standard error from biological triplicates comprising a population of 1500 cells per data point.

3.5 Analysis of dynamic properties for OsDLK-GFP

The ability to walk unidirectionally along microtubules is one of the intrinsic characteristic of many kinesins. Our previous study has shown that OsDLK associated tightly with microtubules. The overexpressor was treated with tubulin assembly inhibitor oryzalin to check the effect of OsDLK on MT dynamics. The mobility of this motor was detected *in vivo* and *in vitro*, respectively. The observations from oryzalin treatment assay and mobility detection showed that OsDLK harbours dynamic properties, suggesting a putative role of OsDLK that it is not only a structural but also a dynamic coordinator of cytoskeleton.

3.5.1 The OsDLK-GFP overexpressor is more sensitive to oryzalin

To get insight into potential changes of microtubule lifetimes in consequence of OsDLK-GFP overexpression, we recorded the response of cell density and packed cell volume over different concentrations of the plant specific microtubule polymerization inhibitor oryzalin. Since oryzalin is known to sequester tubulin dimers from assembly into the microtubule, stable microtubules should be less affected as compared to dynamic microtubules. For both cell lines packed cell volume decreased progressively with an increasing concentration of oryzalin (Fig. 28a), but the curve for the OsDLK-GFP overexpressor line was shifted to lower concentrations. For instance, at 50 μM of oryzalin, the packed cell volume in the non-transformed wild type was at 90% of the control level, whereas the value had dropped to around 60% in the OsDLK-GFP line. Since packed cell volume depends on cell number and on cell volume, we also determine cell densities at 0, 25, 50, and 200 μM of oryzalin (Fig. 28b). Here again, the

OsDLK-GFP overexpressor was seen to be more sensitive, indicative that the difference between the lines in the packed cell volume is linked to cell proliferation. When we tested the cellular effect of the treatment by microscopy (Fig. 28c), it turned out that oryzalin eliminated cortical microtubules leaving only punctate remnants in the cortical cytoplasm (Fig. 28cI, II). Instead, the signal was almost exclusively seen in the nucleus, where it was organised in filamentous structures. Individual confocal sections placed in the central karyoplasm showed these filaments to be located clearly inside of the nuclear envelope (Fig. 28cIII, IV).

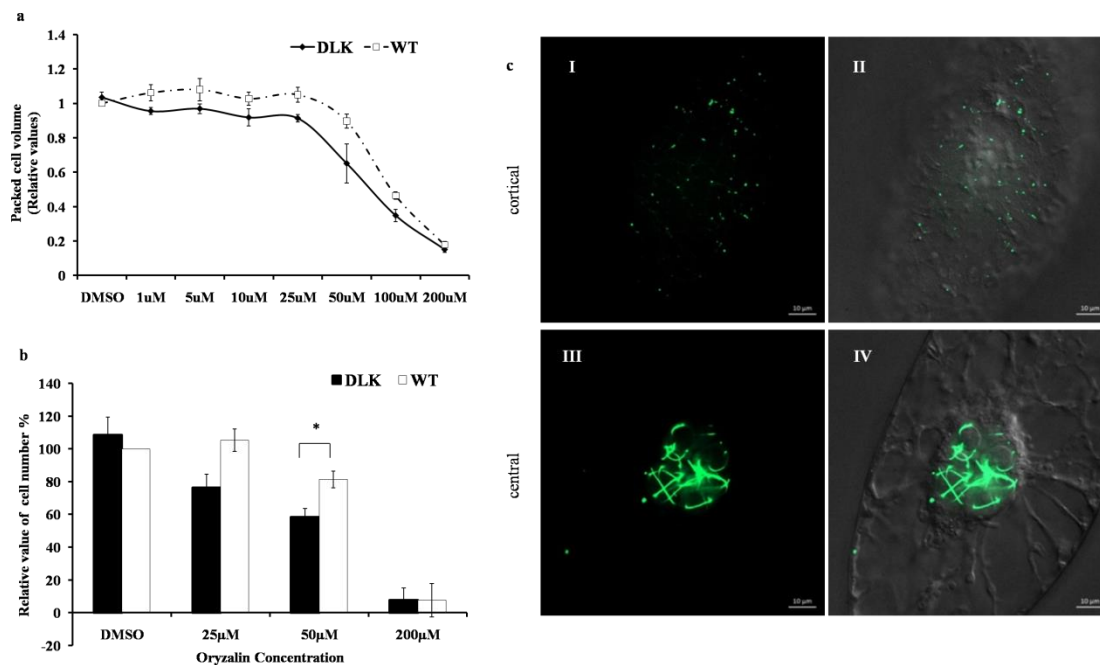


Figure 28 Dose-response of cell density (a) and packed cell volume (b) over oryzalin in the OsDLK-GFP overexpressor could increase the dynamics of MT in ox. Values are given in % of the value for the non-treated WT. Cells treated with equivalent concentrations of the solvent dimethyl sulfoxide (DMSO) were used as control. Treatment was initiated at the subcultivation and lasted for 3 d. Error bars represent the standard deviation of biological triplicates. Asterisks (*) indicate differences between the cell lines significant at $P < 0.05$ as evaluated by a t test for unpaired data. (c) Representative cells of the OsDLK-GFP overexpressor treated with 200 μM of oryzalin over 3 days. GFP signals of confocal sections collected in the cortical (cI), and central (cIII) regions, (cII, cIV) merged images of the GFP images shown in (cI, cIII) with the respective differential interference contrast (DIC) image to show the topology. Scale bars: 10 μm .

3.5.2 The motor OsDLK-GFP exhibits dynamics *in vivo*

To determine whether OsDLK is really dynamic, a kymograph analysis was carried out *in vivo* where the fluorescent protein fusions of OsDLK to follow the movement of the motor directly inside the BY-2 cells. Time-lapse studies were conducted with a microscope equipped with a spinning-disc device.

The kymograph data revealed that OsDLK-GFP moved with an average speed of $16.28 \pm 1.05 \mu\text{m min}^{-1}$ on cMTs during interphase (Fig. 29a-c). This indicated that OsDLK-GFP harbours a high mobility that exceed far than most other kinesin-14 members (Fig. 29d), while there exist members of other kinesin families (such as KHCs) that are much faster.

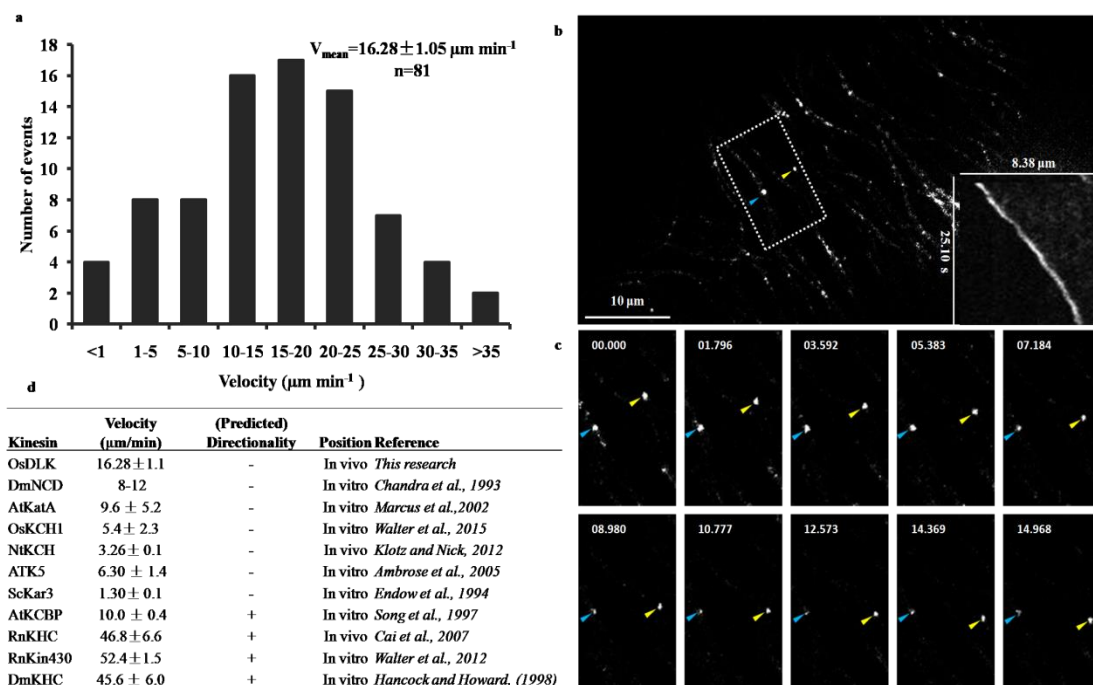


Figure 29 Time-lapse studies on the dynamic behaviour of different OsDLK subpopulations in stably transformed OsDLK-GFP BY-2 cells. (a) Velocity distribution of OsDLK-GFP moving on cortical microtubules (cMTs) with an average velocity $16.28 \pm 1.05 \mu\text{m min}^{-1}$ ($x \pm \text{SE}$; $n=81$). (b) Representative kymograph experiment showing kinesin movement in an interphase BY-2 cell. The kymograph shown in the bottom right corner represents the OsDLK-GFP signal marked by a yellow arrowhead. The left bar indicates the time, and the top bar indicates the distance. (c) Time-lapse series showing in detail the dynamic behaviour of the OsDLK-GFP highlighted with blue and yellow arrowhead. Time unit: s, Scale bars: $10 \mu\text{m}$. (d) Velocity of OsDLK-GFP *in vivo* compared to velocities of other class-XIV kinesins from

plant and animal species and the conventional KHC from *Drosophila melanogaster* and *Rattus norvegicus*.

3.5.3 The motor OsDLK-GFP exhibits dynamics *in vitro*

In order to get further information of the interaction between OsDLK and microtubules, we performed microtubule sliding motility assays where motors could interact simultaneously with surface-immobilized and free microtubules in the presence of ATP (Fig. 30a). We found that OsDLK actively microtubules along each other in a unidirectional manner (Fig. 30b) with a distinct velocity $v = 87 \pm 18 \text{ nm s}^{-1}$ (mean \pm SD, $N = 155$, Fig. 30c), which is much higher than other kinesins members as shown in Fig. 29d.

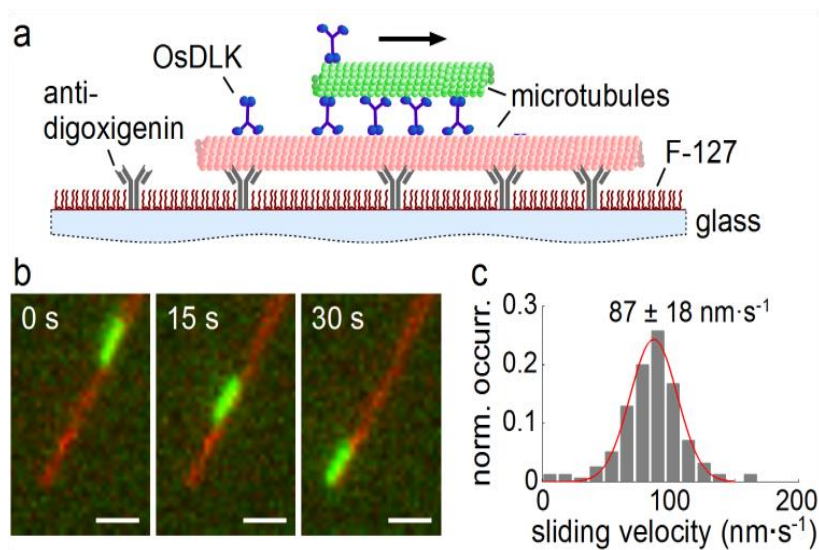


Figure 30 OsDLK is a microtubule minus-end-directed motor along microtubules. (a) Schematic representation of the microtubule sliding assay using recombinant OsDLK (see Methods for details). (b) Fluorescence micrographs of a cargo microtubule (green) being transported by OsDLK along a surface-bound template microtubule (red) at different points in time. Scale bar = 1 μm . (c) Histogram of the point-to-point sliding velocities. A Gaussian fit of the histogram delivers the sliding velocity $v = 87 \pm 18 \text{ nm s}^{-1}$ (mean \pm SD, $N = 155$).

3.6 Exposure for potential role of OsDLK in nucleus

In the previous work, we have displayed that, OsDLK has two subpopulations, in both cell cortex and nucleus. The phenomenon is very rare in plant kinesins, especially for

Kin-14 members. Therefore it is very worth digging the potential role of OsDLK inside nucleus apart from its conventional involvement in cell division and expansion. Interestingly, OsDLK-GFP was found to be imported into the nucleus of overexpressors of both rice and BY-2 cells reversibly. And the cycling between these two cellular subpopulations was further consolidated by treatment with Leptomycin B, which is a nuclear export inhibitor. Furthermore, the expression levels of candidates from cold response genes were detected over time of cold treatment. The results suggested an interaction of OsDLK with a defense response gene *Avr9/Cf9* in tobacco. In addition, OsDLK fused with His-tag was purified from *E. coli* to investigate the possibility of OsDLK in DNA-binding.

3.6.1 OsDLK-GFP accumulates in cell nucleus in response to cold stress

3.6.1.1 OsDLK-GFP accumulates in nuclei of chilling BY-2 cells

To determine whether the two interphase population of OsDLK-GFP (at cMTs and inside the nucleus) can be interconverted, the OsDLK-GFP cells were followed during their response to cold stress, since cold treatment can induce a nuclear import of tobacco tubulin (Schwarzerová et al., 2006). With progressive time of cold treatment in ice-water bath, the GFP signal indicative of OsDLK disintegrated into punctate residual signals in the cell cortex, while at the same time the signal accumulated inside of the nucleus, as well in punctate form (Fig. 31a). This response was rapid and already clearly manifest after 1 h of cold treatment. With progressive cold treatment, the intranuclear signal organised in rods and filaments, evident from 7 hours after the onset of the treatment. After 24 hours, the cortical signal had vanished completely, whereas the filamentous organisation of the intranuclear signal was fully developed. To get insight into the nature of these filaments, immunostaining of microtubules was carried out in the background of OsDLK-GFP cells following cold treatment for 7 hours (Fig. 31b, more see suppl. Fig. S4). Tubulin was seen in and around the nucleus in form of punctate or sometimes rod-shaped structures, whereas the cortical microtubules were

not detectable. The OsDLK-GFP was exclusively observed inside of the nucleus. Here, the filamentous or rod-shaped structures visualised by OsDLK-GFP tightly overlapped with the tubulin signal and also with the chromatin (Fig. 31b, insets, white frame), whereas in the cytoplasm around the nucleus (delineated by the absence of DNA), the tubulin signal was not accompanied by OsDLK-GFP signal.

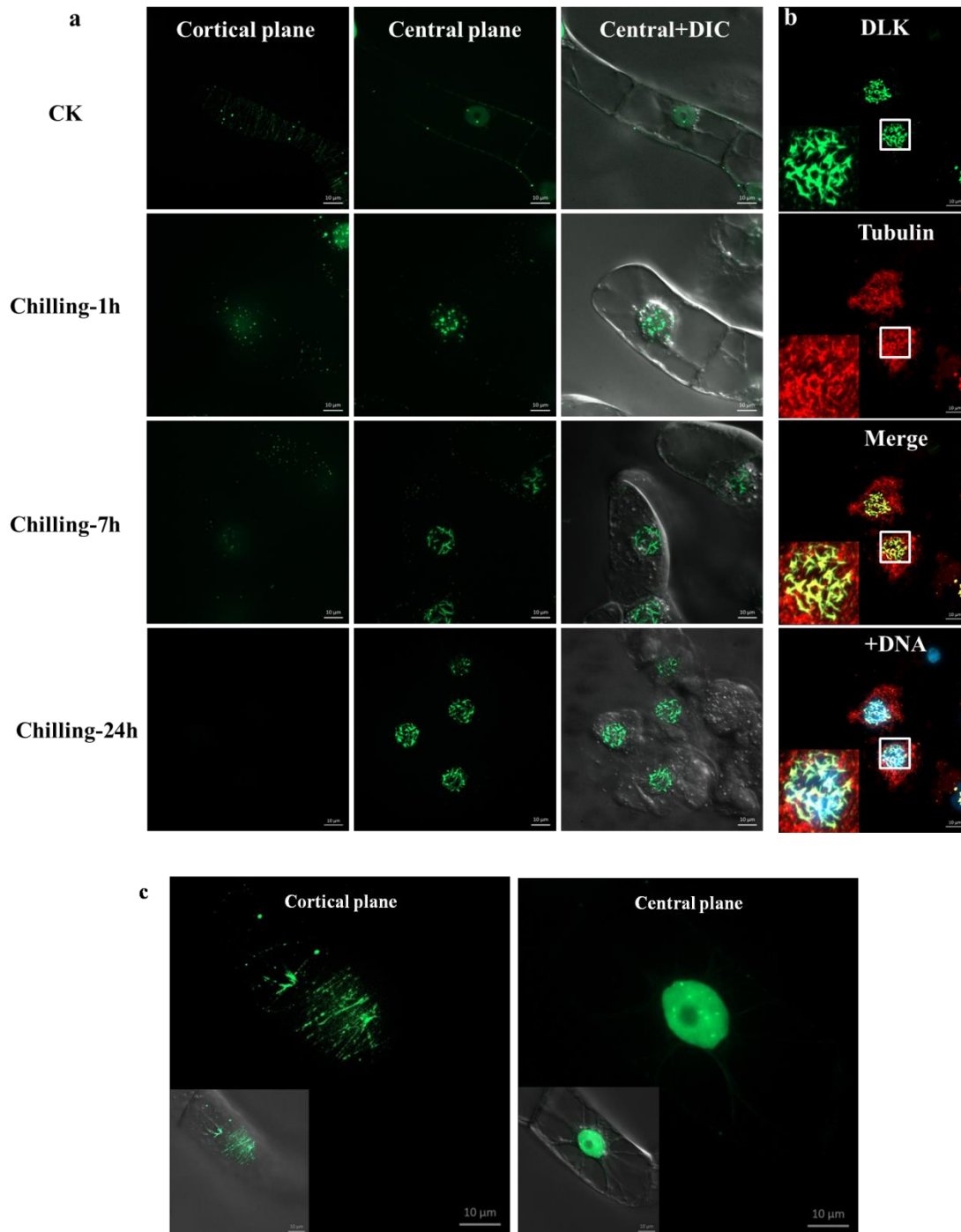


Figure 31 OsDLK-GFP enters the nucleus in response to cold stress. (a) Progressive nuclear import of OsDLK-GFP with increasing time of cold treatment. Confocal sections collected from the cortical and

nuclear planes are shown either for the GFP signal alone or merged with the differential interference contrast image to show the topology. CK represent cells cultivated at 25 °C serving as negative control. (b) Representative cells challenged by cold for 7 hours and triple stained for microtubules (immunofluorescence using a TRITC conjugated antibody), OsDLK-GFP, a merge of both signals, and DNA visualised by Höchst 33258. The white square has been magnified to show details of colocalisation (arrow). (c) OsDLK-GFP is exported from nucleus during recovery from cold treatment. Confocal sections in the cortical and the nuclear plane of OsDLK-GFP expressing cells that had been subjected to cold stress for 7 hours, and were then allowed to recover at 25 °C for 6 hours. Frames in the left corner showed the GFP merge with DIC signals. Scale bars: 10 µm.

To test, whether the nuclear import of OsDLK-GFP was reversible, we conducted a recovery experiment, where cells were subjected to cold treatment for 7 h to induce complete dismantling of the cortical signal. Then, the cells were returned to 25 °C for recovery. During recovery, the rod-like structures in the nucleus dissolved, such that the signal was spread more or less evenly over the entire karyoplasm (although some punctate foci were still detectable) (Fig. 31c). At the same time, punctate signals appeared in the cytoplasm around the nucleus were aligned in transverse orientation like beads on a string. Thus, the nuclear import and the intranuclear filamentous organisation of OsDLK-GFP were reversible.

3.6.1.2 OsDLK-GFP repartitions in chilling rice cells

In order to get more confidence of our result, OsDLK-GFP was transferred into leaf blade of rice. The signals in chilling cells were followed during 24 hours. As shown in Fig. 32, GFP signal appeared in both cytoplasm and nucleus with high intensity in non-treated cells. Under cold stress, signals on cortex reduced gradually with the increment of time for cell exposed to cold, which is consistent with the result from chilling BY-2 overexpressors. The increment of GFP signal inside the nucleus is not distinct, which might be due to the defective photograph angle.

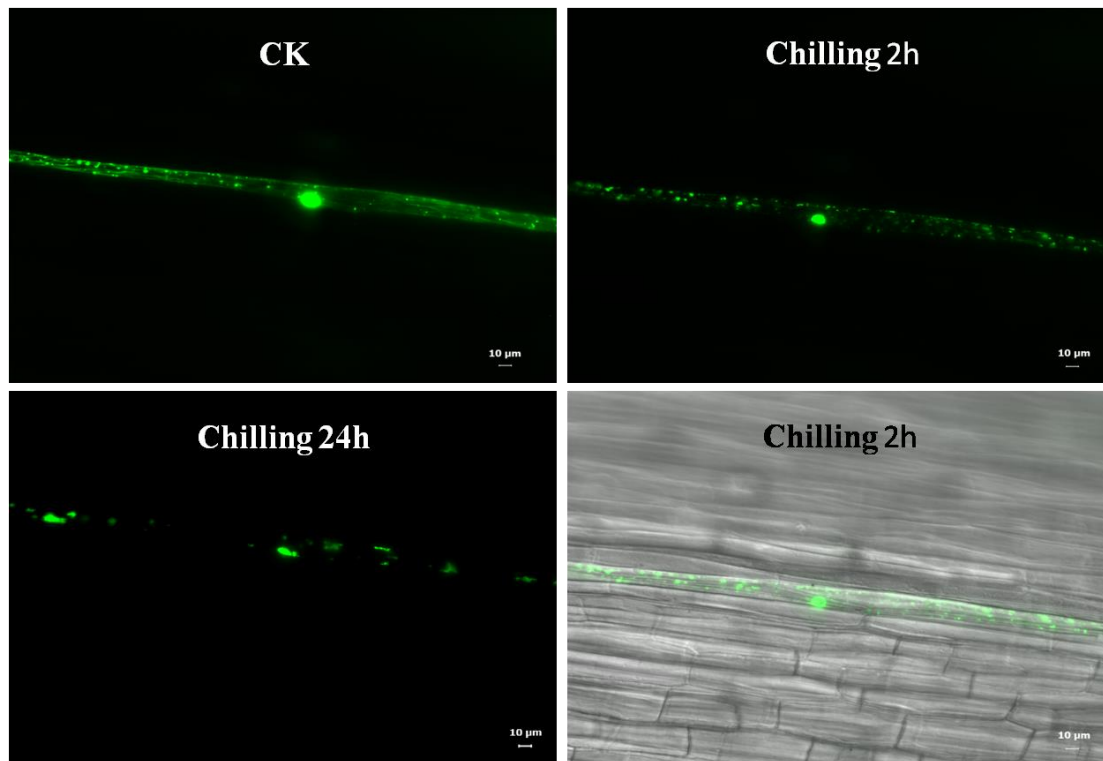


Figure 32 Localisation of OsDLK-GFP in rice cells in response to cold stress. OsDLK-GFP was transformed transiently into blade of rice via gold particle bombardment. After recovery in dark at normal temperature for 24 h, samples were transferred in ice bath for incubation. The signal was caught with a microscope equipped with a spinning-disc device. Representative images of GFP signal at specific time point (0 h, 2 h, 24 h) and DIC signal at 2 h are shown here. Scale bars: 10 µm.

3.6.1.3 Cold response gene expression in chilling cells

To test whether OsDLK has potential role in gene expression regulation, we tried to test the gene expression pattern of BY-2 overexpressors in comparison to wild type cells. Since OsDLK accumulated in nuclei in response to cold stress, cold response genes are the best candidates for us. 3-day-old BY-2 cells were incubated in ice bath and the gene expression levels were checked by real-time PCR analysis. However, most of the transcript changes of selected genes according to Hu et al. (2016) were not different from the WT (Suppl. Fig. S5a). Unexpectedly, a defense response gene, *Avr9/Cf9*, was suppressed clearly in OsDLK-GFP overexpressors during the cold treatment (Fig. 33). In addition, the *Avr9/Cf9* in tobacco was found to be homologous to CBF4 of *Vitis vinifera* (Suppl. Fig. S5b). By the way, VvCBF4 is a CRT-binding transcription factors involved in cold response pathway.

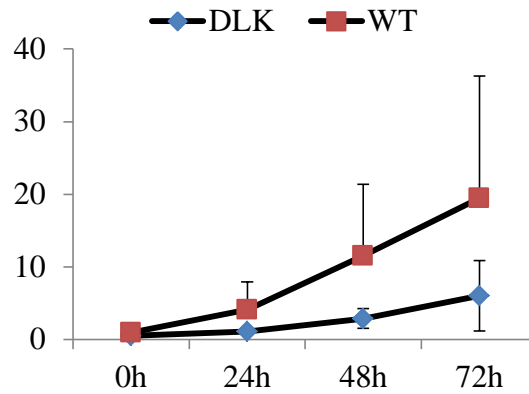


Figure 33 *Avr9/Cf9* transcripts level in chilling cells over time. Transgenic (black bars) and wild type BY-2 (white bars) cells were treated in cold for 72 hours. The transcripts level was addressed over time. Error bars represent the standard deviation of duplicate measurements.

3.6.2 Leptomycin B causes accumulation of OsDLK-GFP in the nucleus

To get insight into the mechanism responsible for the cold-induced accumulation of OsDLK-GFP in the nucleus, we treated OsDLK-GFP cells with Leptomycin B, but in the absence of cold stress, i.e., at 25 °C, starting from day 3 after subcultivation. This specific inhibitor targets CRM1, a receptor for nuclear export signals (Kudo et al., 1998). As a consequence, Leptomycin B inhibits nuclear export very efficiently. We quantified the proportion of GFP signal located inside the nucleus and followed this parameter over time of Leptomycin B treatment compared to the solvent control (Fig. 34a). We observed that the proportion of intranuclear GFP increased from an initial value of around 50% to 75% over 24 hours after onset of the treatment and then dropped back to an intermediate level during the following day. The solvent control did not show this sharp increase, although it should be noted that values increased as well, however only to 62% at 24 h and then levelled off at below 60% for longer incubation. This increase of the intranuclear signal was linked with the loss of the cortical OsDLK-GFP signal (Fig. 34b, c). These results indicate that the intranuclear OsDLK-GFP signal results from a dynamic equilibrium established by import and export. This cycling takes place also at normal temperature (25 °C). On the assumption of around 50% of the

signal being located in the nucleus under steady-state conditions (Fig. 34a), and the increase of the intranuclear signal to 75% within 24 h of Leptomycin B treatment, it can be estimated that, at 25 °C, around half of the intranuclear population is turned over within one day.

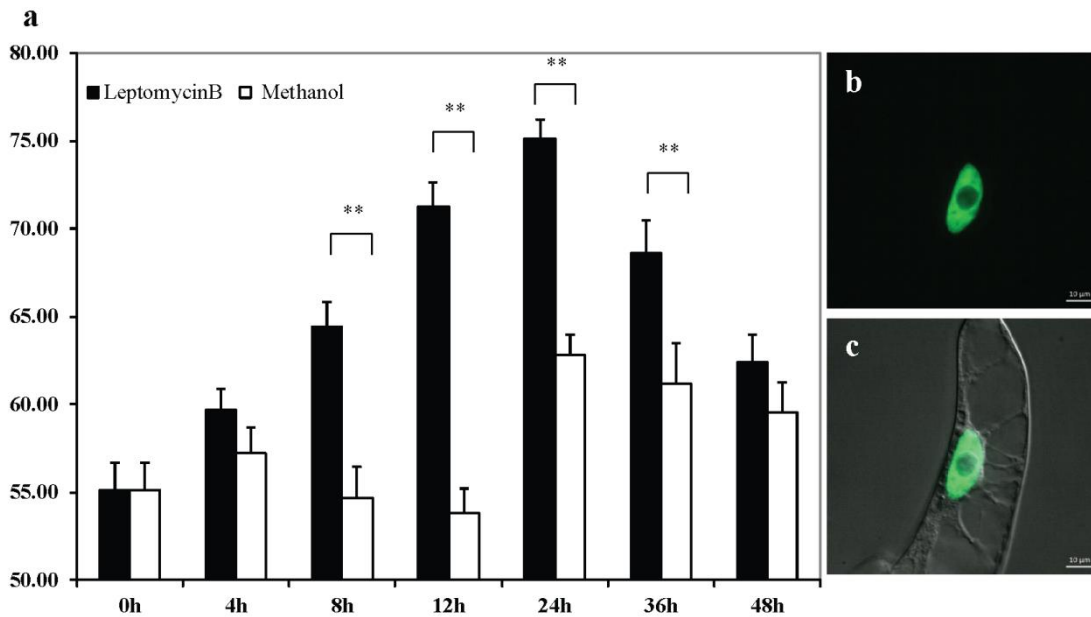


Figure 34 Effect of Leptomycin B, a specific inhibitor of nuclear export on localisation of OsDLK-GFP. (a) Time course of intranuclear localisation in response to 200 nM Leptomycin B compared to the solvent control (the same volume of 70% methanol, corresponding to a final concentration of 1.37% MeOH in the assay as control). At least a total of 20 cells per time point and sample were collected in each experimental series. The results were tested for significance using Student's t-test at 95% and 99% confidence level, labelled with asterisks. Error bars represent the standard error of triplicate measurements. (b, c) Representative image of a OsDLK-GFP cell after 3 days of treatment with 200 nM Leptomycin B. GFP signal shown in (b), overlay with differential interference contrast shown in (c). Scale bars: 10 µm.

3.6.3 OsDLK shows affinity to DNA binding motifs

OsDLK has been to show localisation in nucleus in non-dividing cells and it has a potential role in defense gene regulation (Fig. 33). A putative Leucine Zipper motif contributing to nucleotide binding was found in sequence analysis of OsDLK. Thus, the His-tag labelled OsDLK was purified for library screening of DNA binding motifs.

For the recombinant vectors, full length of *dlk* (1-2295 bp) and tail domain part (1-1209 bp) were inserted into pDEST42 containing His-tag (Fig. 35), and expressed in *E. coli*.

The proteins were monitored on SDS-PAGE gel (Fig. 35a). The expression was finally confirmed by western blotting with primary antibody (Anti-penta His) and the secondary antibody (Anti-mouse IgG, alkaline phosphatase-conjugated). Specific bands were detected in western blotting (Fig. 35b).

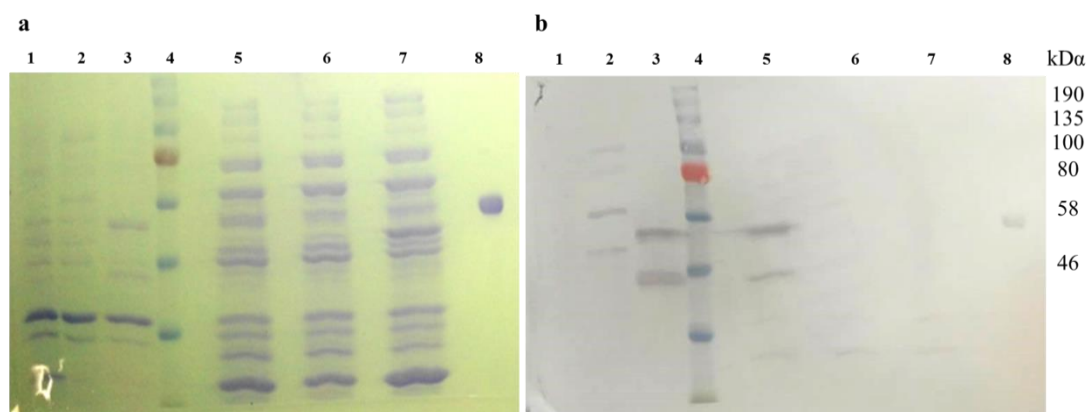


Figure 35 His-tag labelled OsDLK and OsDLKT were isolated from *E. coli*. (a) Insoluble and soluble extracts were separated on SDS-PAGE gels stained with Coomassie Brilliant Blue of a series of full length OsDLK (85.5 kDa) and N-terminal part containing tail domain OsDLKT (47.3 kDa). 1, Insoluble extracts from *E. coli* expressing empty vector as negative control; 2, Insoluble extracts from *E. coli* expressing pDEST42-DLK; 3, Insoluble extracts from *E. coli* expressing pDEST42-DLKT; 4, Protein ladder as markers; 5, 6, 7 Soluble extracts from *E. coli* expressing pDEST42-DLKT, pDEST42-DLK and empty vector; 8, His-tag known labelled proteins as positive control. (b) Western blotting for confirming of his-tag fusions expression.

DNA-binding motives were screened with the crude extracts, through DNA-protein-interaction (DPI)-ELISA reported by Brand et al. 2013. Based on double-stranded DNA (dsDNA) probe library, DPI-ELISA screen allows the high-throughput identification of hexanucleotide DNA-binding motifs (< 6 oligos). 6 oligos positively scored for protein OsDLKT, indicating the DNA binding ability of the tail part of kinesin OsDLK (Table 20). However, a consensus motif was not possible to identify.

The putative cis-elements with of the binding motives were predicted with online software Plant Care. As shown in Table 20, five of the six candidates show cis-elements sites, which normally involve in cis-acting regulatory functions.

Nr.	Binding Motif Sequence	Site name	Organism	Cis-element	Function
50	TGGTCGATCC GCATGCAGTT	NF	NF	NF	NF
182	GTCTGCGTCCT ACCCCATTC	TCA- element	<i>Brassica oleracea</i>	GAGAAG AATA	Involved in salicylic acid responsiveness
272	GTTCGGGGCT TGGTTTGGAA	ARE	<i>Zea mays</i>	TGGTTT	Essential for the anaerobic induction
294	CGTGCGCGTG CATGTCATCG	O2-site	<i>Zea mays</i>	GATGACA TGG	Involved in zein metabolism regulation
	CGTGCGCGTG CATGTCATCG	Skn- 1_motif	<i>Oryza sativa</i>	GTCAT	Required for endosperm expression
299	CTAGGTATCG GTAGGCGCCG	I-box	<i>Flaveria trinervia</i>	CCATATC CAAT	Essential for the anaerobic induction
302	CGCTCCGTTTT TGCAATGCG	CAAT- box	<i>Hordeum vulgare</i>	CAAT	Involved in zein metabolism regulation

Table 20 Sequences of DNA-binding motif screened for OsDLK in DPI-ELISA assay. NF: not found for cis-element. The active sites are colored.

The putative promoter sequence of Av9/Cf9 (included in the 3000 bp nucleotides before the gene of Av9/Cf9, Suppl. Fig. S8) was first aligned with the 6 candidates of binding motif sequences and the overlapped sequences were shown in Suppl. Fig. S9. Binding motif Nr. 294 showed the most continuously overlap region (9 bp).

Then the putative promoter sequence was also put into Plant Care to search the cis-elements. Interestingly, some of the cis-elements found in the putative promoter were overlapped with those found in the binding motif sequence of Nr. 182, 294, 299. Hence,

sequence of the Nr. 294 seemed to be the most potential binding motif for truncated protein OsDLKT, involved in zein metabolism regulation and endosperm expression. By the way, zein is a class of prolamine protein found in maize the major seed storage proteins.

Nevertheless, a consensus motif was not identified for the DNA-Protein interaction of kinesin OsDLK. These results may give us some explanations about the non-survival homozygous mutants to some degree.

3.7 Summary of results

Kinesin-14 members have been mostly expanded in the land plants. They have the minus-end directionality which is in contrast with the conventional kinesins. Many studies have revealed Kinesin-14 motors involved in a lot of functions, such as the microtubule organization at the spindle apparatus during meiosis and mitosis, trichome morphogenesis and interaction between actin filaments and microtubules.

In our study, we reported a rice kinesin from subfamily-14, named as OsDLK, representing a dual localisation kinesin. The *in silico* analysis showed that OsDLK is a highly conserved minus-end directed C-terminally located motor. The core domains are visible in the sequence. Interestingly, a putative Leucine Zipper motif localises in the tail part. Moreover, a nuclear localisation sequence is present in the middle of the protein.

To get insight into the role of kinesin OsDLK in cell growth and cell division, a tobacco BY-2 cell line overexpressing OsDLK in fusion with fluorescent proteins under the control of promoter CaMV 35S promoter (P35S) was established. The phenotypes of the overexpressor showed that OsDLK was dynamically repartitioned during mitosis, decorating spindle apparatus and phragmoplast. Surprisingly, it has two subcellular subpopulations: One located in the cell cortex and the other one located in the nucleus. These results were consistent with that in rice cells overexpressing OsDLK. Moreover, overexpressor can stimulate the cell proliferation while prolonged the transition into metaphase in mitosis. It was also sensitive to oryzalin. OsDLK showed high dynamics in *in vivo* and *in vitro* assay.

However, the rice *dlk* mutants were arrested in early development and could not be studied further. The transcripts level of the intact young seedlings showed that DLK have a relatively higher expression in the first days during germination, which indicated that OsDLK has an important role in seedling development. In coleoptiles *OsDLK* was induced 12 h after a red light pulse applied to etiolated seedlings, indicating a possible function in light induced growth arrest.

Under the cold stress, OsDLK-GFP could progressively enter the nuclei in chilling cells, when cortex signal vanished gradually while intranuclear signal accumulated, organising from punctates to rod and filaments. And this change was reversible when cell recover from cold. Immunostaining showed that tubulin was seen in and around the nucleus, whereas the cortical microtubules were not detectable. OsDLK signal was only visualized inside the nucleus, and mostly overlapped with tubulin and chromatin.

By blocking the nuclear export, the signal of OsDLK was accumulated reversibly inside the nuclei of BY-2 overexpressor, indicating that there is a cycling of the two subpopulations of OsDLK. This result was consistent with the cold-induced accumulated signals in the nucleus.

4. Discussion

The current work deals with the functional characterisation of a class-XIV kinesin from rice, which is homologous to the *Arabidopsis* kinesins ATK1 and ATK5. While this rice homologue shares several molecular and cellular features with its *Arabidopsis* counterparts, such as movement towards the minus end of microtubules in a dynamic fashion, and a similar dynamic repartition during mitosis, it shows a specific difference during interphase: A population of this rice kinesin decorates cortical microtubules, while the other population is found in the nucleus. In response to cold treatment (eliminating cortical microtubules), the intranuclear population increased and formed rod-shaped and reticulate structures. Likewise, inhibition of nuclear export by Leptomycin B increased the abundance of intranuclear kinesin, such that the name Dual Localisation Kinesin (DLK) was coined for this protein.

4.1 OsDLK is a dynamic minus-end directed class

XIV-kinesin

4.1.1 OsDLK is a C-terminal motor of Kinesin-14 members

Based on sequence homologies in their motor domains, kinesins are classified into 14 sub-families (Richardson et al., 2006). In land plants, the class-XIV kinesins have strongly expanded, and many of them differ greatly in structure and function from their animal counterparts. For instance, the rice reference genome constructed for the *japonica* cultivar *Nipponbare* has been predicted to harbour at least 52 kinesins with around one quarter of them falling into class XIV (Guo et al., 2009). However, despite this abundance, rice kinesins are far from being as adequately characterized (Sazuka et al., 2005).

In this study, we investigated a rice kinesin designated as OsDLK (for Dual Localisation Kinesin). Classical member of Kinesin-14 subfamily in animals has a C-terminal motor domain while plant Kinesin-14 protein may harbour motors located either in the N-terminus, C-terminus or in the middle of the protein (Reddy & Day,

2001). For instance, *Arabidopsis* members KatA, KatB and KatC have C-terminal motors (Chen et al., 2002; Marcus et al., 2002, 2003), and kinesin-like calmodulin-binding proteins (KCBPs) also have a motor at the C-terminus of the protein in addition to their unique myosin-tail homology domain (MyTH4) and a talin-like region (ERM) (Reddy & Day, 2001), while calponin-homology domain (KCH) motors normally localise in the center of the protein with a calponin-homology (CH) domain N-terminally positioned (Frey et al., 2010). The rice motor OsDLK was shown to be homologous to two similar *Arabidopsis* class-XIV kinesins, ATK1 and ATK5 (Liu et al., 1996; Ambrose et al., 2005) with overlapping, but not identical function (Fig. 11). It exhibits typical structural features of class-XIV kinesins, such as a highly conserved a motor domain at the C-terminus with an ATP binding motif, a long stalk region in the middle, and a tail at the N-terminus (Mazumdar & Misteli, 2005).

4.1.2 OsDLK is a minus-end directed motor with high

mobility

The “neck”, a region lying between motor domain and the coiled-coil stalk for the connection, has been found in several aspects of motor function (Endow, 1999), such as the determination of motor directionality. Sequence alignments of the neck residues of plus- and minus-end-directed kinesin motors in crystal structure have been shown by Endow, (1999). Based on the amino-acid signature in the OsDLK neck region (Suppl. Fig. S3), it can be predicted that it is moving towards microtubule minus-ends. This has been confirmed by sliding assays *in vitro*: OsDLK has the ability to bind to microtubules and minus-end driven mobility.

The motor velocity *in vitro* is comparable to other class-XIV kinesins (around 5 $\mu\text{m}\cdot\text{min}^{-1}$, Fig. 30d), while the motility along cortical MTs *in-vivo* is considerable higher (16 $\mu\text{m}\cdot\text{min}^{-1}$, Fig. 29), excelling the velocity of its *Arabidopsis* counterpart ATK5 almost threefold (Ambrose et al., 2005). Whether this high velocity *in vivo* is caused by motor clusters, or by cotransport with growing or shrinking MT ends, remains to be elucidated, for instance by means of single-molecule tracking *in vitro*. However, except this elevated velocity (which is not unusual if compared with other kinesins), the

molecular features of OsDLK are that of a mostly non-conspicuous member of the class-XIV kinesin family.

The result also suggests that OsDLK is a non-processive motor, similar to its *Arabidopsis* homolog AtKatA. It is noteworthy: the truncated OsDLKM designed in a shortened version for better expression was not active in the sliding assay.

4.2 OsDLK has an important role in seedling development

4.2.1 Homozygous rice mutant is not viable

The cereal crop rice, one of the most important crops in the world was the first crop plant for which the complete genome was sequenced. It was chosen as a model crop amongst others because of its small genome size compared to other major cereal crops and low redundancy in its genome. In addition, certain molecular and genetic tools were available for rice early such as ESTs, markers, genetic and physical maps. With the completion of genome sequencing, rice is an excellent model cereal crop for genomic research (Gale & Devos, 1998).

Insertional mutagenesis is an important approach to investigate the function of a novel gene. Transfer DNA (T-DNA) insertion via *Agrobacterium tumefaciens* has been used to knockout a gene to alter or eliminate its function. T-DNA insertion is a random event, and the inserted genes are stable through multiple generations (Azpiroz-Leehan & Feldmann, 1997). In rice mutagenesis with an endogenous transposon, Tos-17, is available as well (<https://www.ncbi.nlm.nih.gov/pubmed/12897251>). It is present in 2-5 copies in the rice genome, depending on the cultivar, and is usually not active. However during tissue culture it starts to propagate in the copy-and-paste modus and integrates into random sites of the genome. Integration does not occur entirely random, as certain genomic areas are preferred over others. When plants are regenerated from tissue culture Tos17 becomes inactive again, and the insertion is inherited stably.

In order to get insight into the cellular function of the rice kinesin OsDLK, T-DNA and Tos17 insertion lines were used at the beginning of the project. In the offspring, seeds or seedlings were genotyped by PCR detection with genome specific and insertion site specific primers. Most of them were genotyped to be wild type or heterozygous mutant. Only few of the seeds were genotyped to be homozygous mutants (Fig. 12c). However, they would show delayed germination or die in the early stage of the seedling development (Fig. 12d). None of the grown-up homozygous mutant was gained within several generations.

In fact, homozygous lethal mutations have been identified in many studies. For instance, the seeds of low phytic acid (LPA) rice mutant lines generated by Liu et al. (2007) cannot germinate naturally, and the seedlings were either produced from immature embryos or the embryo of half mature seeds strengthened with MS media (Xu et al., 2009b). This phenomenon may occur due to lethal alleles which may cause the death of the organism that carries them. Depending on the gene, it can be recessive, dominant, or conditional. They are usually caused by the mutations in genes essential in plant growth and development (Gluecksohn-Waelsch, 1963). Thus, they can commonly cause damage becoming manifest early in development. Our results showed that the rice homozygous mutants were not viable.

Actually, we have checked the transcript levels of OsDLK in wild type rice, the results showed a relatively high transcription level in the first 4 days during cultivation (Fig. 14), which may implicate that OsDLK may have an active function during the early stage of seed germination and seedling development.

Since OsDLKs containing a putative Leucine Zipper motif in the tail domain of the protein could occur in the cortex and nucleus in the interphase cells of transgenic tobacco and rice coleoptiles, they were predicted to be involved in the regulation of the expression of certain genes. Hence, the proteins extracted from *E. coli* have been subjected to the detection of DNA-binding motives *in vitro*. Interestingly, six candidates of nucleotide hexamers appeared to interact with the tail domain of protein OsDLK, which is very rare for kinesins, especially the plant Kin-14 members. Furthermore the analysis of these nucleotide hexamers showed that some of them are required for endosperm expression and some are involved in the metabolism regulation of the protein zein, which is the major seed storage protein of plants, such as the grass tribe

Andropogonea (Garratt et al., 1993). Based on these results we hypothesize that the seed germination may be disturbed in the homozygous mutant because of partially impaired gene expression in the endosperm caused by the lack of the protein OsDLK.

4.2.2 Rice mutant is delayed in the coleoptile elongation

Although the homozygous mutants are not available, heterozygous mutants have shown a clear delay in coleoptile elongation in both T-DNA and Tos 17 insertion lines compared to the wild type seedlings. Rice coleoptiles have been physiologically characterized in great detail (Holweg et al., 2004). They grow rapidly and homogeneously, representing a highly suitable organ for physiological investigation. The growth of coleoptile depends on cell elongation exclusively. Because the cells are formed during late embryogenesis, thus there will be no further divisions during the seed germination and development. Hence, rice coleoptiles can record small differences in cell growth rates very sensitively. The kinesin mutants show delayed elongation in many cases. For instance, the coleoptiles of rice Tos 17 insertion mutants of another Kinesin-14 member OsKCH were clearly shorter with respect to the segregating wild-type coleoptiles (Frey et al., 2010), while the heterozygotes almost showed no difference in comparison with wild type plants (Frey et al., 2010). Effects on the elongation of other tissues in rice kinesin mutants have also been reported. For instance, when the *gibberellin-deficient dwarf1* (*gdd1*), encoding a Kinesin-4 motor was knocked out in rice, the length of the root, stems, spikes, and seeds were greatly reduced (Zhang et al., 2010; Li et al., 2011). The rice mutant *short grain length* (*sgl*) is impaired in the function of a gene encoding a kinesin-like protein named as Short Grain Length (SGL) exhibited reduced plant height (about 72% of WT) and short grain length (about 80% of WT) because of problems in cell elongation (Wu et al., 2014).

It is known that cortical microtubules (cMTs) (Shibaoka, 1994) are a cortical array present in the interphase in plant cells, which are highly dynamic during cell morphogenesis (Lloyd, 1994). Microtubule-based motors, such as kinesins, participate in the (re)organization and (de)polymerization of microtubules. Mutation of these kinesin genes sometimes results in disorganized cortical microtubules and abnormal cell shape.

GA can influence the direction of cell growth by controlling the orientation of cellulose microfibrils. In the internodes of deep-water rice, GA₃ prevents the transverse to longitudinal reorientation of cMTs, regulating the direction of cell expansion (Sauter et al., 1993). Transverse MTs predominate under the conditions favourable for cell elongation, e.g. in the presence of auxins or GAs, while there are unfavourable factors, such as irradiation with visible light, growth inhibitors, which promote a predominant longitudinal orientation of MTs in the cell (Shibaoka, 1991; Iwata & Hogetsu, 1989; Sakoda et al., 1992).

Both auxins and GAs can induce the elongation of cells in stems, coleoptiles and roots by loosening and relaxation of cell walls, resulting in increased extensibility of cMTs in the cell wall (Shibaoka, 1994). However, GAs cause a predominance of transverse MTs of cells not in excised segments, but intact plants in which endogenous auxins are supplied, indicating that auxin is required for GA-induced cMT reorientation (Mita & Shibaoka, 1984). The cells, in which auxin causes cMT reorientation, seem to have synthesized a factor identical or equivalent to the mRNA synthesis in response to the endogenous GAs (Kancta et al., 1993).

Interestingly, both of these two kinesin like proteins, BC12/GDD1 and SGL, containing DNA-binding ability, have been demonstrated to have an impact on transcriptional activity on genes related to the gibberellic acid (GA₃) pathway of rice. As mentioned above, OsDLK also contains Leucine Zipper and has the ability to bind DNA. However, whether OsDLK is also involved in GA pathway or not is not addressed in our study.

4.3 OsDLK potentially interacts with other plant hormones

4.3.1 OsDLK is expressed tissue specifically

The gene expression of OsDLK was quantified in different tissues of young wild type rice seedlings, raised up in continuous white light, by real-time PCR. The transcripts were present in the primary leaf, crown root and seminal root, which are tissues with meristematic activity, indicating a potential role of OsDLK in cell division. In addition,

the highest abundance of transcripts was found in the second leaf sheath and the third leaf. The leaf sheath cells play both sink and source functions in the early stage of germination, such as the storing and uploading of carbohydrate from the degradation of reserve starch in the endosperm for plant growth and metabolism (Matsukura et al., 1998). Matsukura et al. (1998) also has demonstrated that the growth of the second leaf sheath was due to the increment of wall extensibility enhanced by GA₃, which is a major effective hormone for growth of rice leaf sheaths.

Other studies have also reported the gene expression of certain kinesins in different tissues at different stage of plant development. For instance, SGL was expressed in various organs at the booting stage and in roots at the seedling stage, but significantly higher in the culms and young panicles (Wu et al., 2014). Quantitative PCR revealed that BC12 is universally expressed mainly in organs undergoing cell division and secondary wall thickening (Zhang et al., 2010); The transcripts of OsKCH1 is highest abundant in young and developing tissues with meristematic activity, pointing towards a possible involvement in cell division and development (Frey et al., 2010).

4.3.2 Gene expression of OsDLK in rice is regulated by red light

Plant hormones are able to induce structural changes in the cytoskeleton, which has been studied very exhaustively (Shibaoka, 1994; Nick, 1998). Light, as a modulator of hormonal pathways, is one of the key signals in early plant development. During growth of rice seedlings, the coleoptiles can protect leaves from mechanical damage under the soil. As soon as they perceive light that change their developmental program from skoto- to photomorphogenesis leading to completely different appearances of the seedling. As this is an important signal leading to massive changes in the development of the young seedling, coleoptiles are extremely sensitive to light and can detect even minute amounts. Coleoptile growth in darkness is promoted, resulting in seedlings with long coleoptiles, while it stops to elongate and start to open upon irradiation with light.

The plant hormone jasmonic acids are important component in the signal-transduction for photoreceptors to their final physiological response (reviewed by Svyatyna & Riemann, 2012). They are pivotal regulators of phytochromic signalling and have a large impact on plant growth development (Riemann et al., 2008). It was first reported that in the JA-deficient mutant *hebiba*, a long coleoptile was developed in red light, while a long mesocotyl and short coleoptile was developed in darkness (Riemann et al., 2003). The results provided evidence for regulation of JA biosynthesis by light and indicated an important role for JA in cell elongation.

Recent findings on jasmonate perception and signalling also give evidence that JAs can crosstalk with auxin to affect growth of plants (Hoffmann et al., 2011). Auxin response factors ARF6 and ARF8 could promote jasmonic acid production in *Arabidopsis thaliana* (Nagpal et al., 2005). There is also evidence that JA has an antagonistic function to auxin. For instance, the auxin-induced stem elongation in oat coleoptiles was inhibited by JA (Ueda et al., 1994); In the gravitropism of rice coleoptiles, a gradient of jasmonate was detected opposing the auxin gradient (Gutjahr et al., 2005); Light can rescue the synchrony of cell division of a tobacco cell line and the synchrony is under the control of polar auxin flux crosstalking with neighbouring cells (Nick, 2006; Qiao et al., 2009). The application of exogenous auxin inhibits the induction of a receptor-like kinase of jasmonate-mediated wound in maize (He et al. 2005). The mechanism of the interaction between auxin and JA pathways is manifold and complex. They share common components in hormone sensing and response, which depend on the 26S proteasome pathway (Santner & Estelle, 2009); The *Arabidopsis coronatine-insensitive1 (coi1)*, a mutant of a jasmonate receptor, encodes an F-box protein which is closely related to an auxin receptor called TIR1 (Xie et al., 1998); The RUB-activating enzyme, AXR1, required for the ubiquitin-proteasome pathway is a link between auxin and JA signalling (Tiryaki & Staswick, 2002). The co-suppressor TOPLESS, a regulator of early response genes, is also shared in both signalling pathways (Pauwels et al., 2010).

Our result showed that the transcript level of JAZ11, one of the JAZ proteins (jasmonate ZIM-domain) which are transcriptional repressors of JA signalling, was extremely high in the first day of WT rice seed germination. In companion, transcripts of OsDLK in young seedlings were more abundant during the 4 days after sowing. In the short term

treatment, transcriptional level of JAZ11 in coleoptiles raised up immediately after being exposed to red light for 3 min, followed closely by an increment of OsDLK expression in coleoptiles. Since OsDLK is a motor based on microtubules, and microtubules are also closely linked with auxin in cell division and expansion, we assume that in rice, OsDLK may play a pivotal role during seed germination and development resulting from an interaction of JA and auxin signalling pathways.

4.4 OsDLK affects the progression through the cell cycle

4.4.1 DLK stimulates cell proliferation

Cell division is a very fundamental process of during plant growth and development, which is reflected in a high number of kinesins involved in mitosis. During cell division, it is required that the spindle apparatus and its associated proteins act precisely in the proper segregation of genetic material into daughter cells. Diverse kinesin motor proteins are involved in the assembly and functioning of spindles. In *Arabidopsis*, more than one third of kinesins have been found to participate in cell division (Vanstraelen et al., 2006). Kinesins involved in cell division also distributes in different subfamilies (Table 3). For instance, NACK1 determines the localisation of a mitogen-activated protein kinase cascade to the phragmoplast midzone, and plays a critical role in MT turnover (Nishihama et al., 2002); The absence of both AtKinesin-12A and AtKinesin-12B causes the lack of the bipolar organization pattern of phragmoplast in developing pollen grains (Pan et al., 2004). In a synchronized cell culture of *Arabidopsis*, 7 class XIV- kinesins were found to be upregulated during re-entry into the cell cycle (Menges et al., 2003), suggesting a core role in mitosis.

Consistent with this, transgenic BY-2 cells overexpressing OsDLK showed characteristic alterations of mitosis with a significant higher mitotic index (Fig. 24). In order to investigate whether it is caused by the promoted proliferation ability or just a prolonged cell cycle, we have monitored the doubling number of cells after subcultivation. The results showed the length of cell cycle of the overexpressor is

comparable with the wild type BY-2 cells, therefore higher mitotic index reflects an increased frequency of cells entering mitosis in the overexpressors (Fig. 24b). Another Kinesin-14 member OsKCH showed a delayed mitosis in BY-2 overexpressors.

The synchronizing assay was also carried out to get insight into the progression of the mitotic phases of cell cycle. Actually, BY-2 suspension is the best cell culture for cell cycle synchronization and cell cycle studies in plants. Since BY-2 cell has a regular cell shape and size, and much lower autofluorescence in comparison with *Arabidopsis* cells. Besides, the arrest of cycling inhibitor is reversible (Humphrey & Brooks, 2005). We achieved a high efficiency of synchronization (Fig. 26a). 60-70% of the cells were progressing into mitosis synchronously after application of propyzamide (a microtubule inhibitor which arrests mitosis) in OsDLK and non-transgenic BY-2 cell lines. The degree of synchronization ranged between 42-81% in an optimized synchronization of tobacco BY-2 cells conducted by Samuels et al. (1998).

The results showed that the progression before metaphase was shifted half an hour later than wild type, in contrast the later progression was shifted half an hour earlier (Fig. 26b). It means that the OsDLK overexpression cell line required more time to pass metaphase, while telophase came earlier. Consistent with the more rapid completion of the later mitotic stages, the OsDLK cells passed more rapidly from proliferation to expansion, as indicated by accelerated nuclear migration from the cell center towards the periphery after proliferation (Fig. 27). Modulations of nuclear positioning had also been observed upon overexpression of another class-XIV kinesin, OsKCH, but here premitotic nuclear positioning in the cell center was delayed (Frey et al., 2010), indicative of specific cellular functions for different members of this kinesin class.

4.4.2 OsDLK overexpression affects cell expansion in

tobacco

We have shown that OsDLK were weakly delayed in the coleoptile elongation of heterozygous mutants. However, whether this phenotype resulted either from a diminished or delayed elongation growth with shorter cells or from a reduced number of cells was not determined. Because the homozygous mutant were not viable, it was

impossible for us to count the coleoptile cells of mutants. Thus, we turned our direction to the gain-of-function method that we overexpressed the OsDLK fusion with GFP in suspension cells of tobacco BY-2 cells.

Directional cell expansion seems to be one of the important targets for kinesin activity in plants. For the stationary plants modulation of cell shape is a central mechanism for the adaption to their environment. Signal-dependent reorganisation of microtubules which is also driven by molecular motors is central for this signal-dependent cellular morphogenesis (reviewed in Nick, 1999). During cell elongation, cortical MTs determine the axis of cell expansion by guiding cellulose synthesising complexes in the plasma membrane. The cell-expansion phenotype of the OsDLK overexpressor indicates that also this kinesin is involved here: While cell elongation was reduced compared to the non-transformed wild type (probably as consequence of the elevated mitotic activity), during the first three days after subcultivation, this was subsequently compensated by an accelerated elongation of the OsDLK overexpressor during the expansion phase. Interestingly, the above-mentioned class-XIV kinesin OsKCH showed the exactly opposite phenomenon, where the overexpressors show stimulated cell elongation but delayed mitosis during the first 3 days after subcultivation (Frey et al., 2010). Again, different members of this kinesin class seem to convey different and specific functions.

4.5 OsDLK is dynamically repartitioned during mitosis

The spindle consists of microtubules oriented with the minus-ends at the poles and the plus-ends at the midzone. Members from Kinesin-5 subfamily are important for spindle formation by aligning antiparallel microtubules in the midzone and generation of outward forces. Mutation of the plus-end-directed kinesin AtKRP125c will lead to the abnormal monopolar or fragmented spindles (Bannigan et al., 2007). In yeast and human cells, class-XIV kinesins (antagonised by class-V kinesins) can regulate microtubule nucleation through the γ -TuRC complex and are conserved elements during formation and function of the spindle apparatus (Vale, 2003). They can cross-link antiparallel microtubules to gather them together and generate inward forces at the

spindle midzone to balance the outward forces generated by Kinesin-5 family, thus contributing to the straightening of the spindle axis and the shortening of the spindle length. ATK5 is targeted to spindle midzone mediated by plus-end tracking to cross-link the antiparallel neighbouring microtubules (Ambrose et al., 2005).

When we followed the dynamic redistribution of OsDLK, a homolog of ATK5 in rice, we observed a pattern that is known from other class-XIV kinesins. OsDLK accumulated in the metaphase plate and then redistributed into clear fibers distal to the metaphase (Fig. 15i-t).

The second feature of class-XIV kinesins is the bundling of parallel minus-ends of microtubules to focus the spindle pole. Conversely, OsDLK accumulated at the minus ends of parallel MTs at the spindle pole during anaphase (Fig. 15a-h), as shown for DmNCD from fruit fly (Fink et al., 2009).

Overall, the localisation pattern of OsDLK resembles that of its *Arabidopsis* homologues, ATK1 and ATK5, both of which are observed at spindle pole and midzone (Liu et al., 1996; Ambrose et al., 2005). This indicates that ATK1/ATK5 and OsDLK may have similar functions in mitosis. Interestingly, another class-XIV kinesin, KCBP, might precede the activity of the ATK1/ATK5/OsDLK type kinesins. Microinjection of antibodies causing constitutive activation of KCBP into stamen hairs of *Tradescantia virginiana* promoted progression into prometaphase but later arrested the cell in metaphase (Vos et al., 2000) indicating that KCBP can accelerate the formation of a bipolar spindle, but then needs to be inactivated to allow entry into anaphase. Whether OsDLK contributes to microtubule bundling during organisation of the PPB, as had been shown for KCBP (Marcus et al., 2003; Bowser & Reddy, 1997), remains to be elucidated. The fact that binding of OsDLK to the PPB was not observed during this study along with the fact that overexpression of OsDLK in BY-2 cells did not lead to abnormal spindles, would be more consistent with a function of OsDLK that differs from that of KCBP.

4.6 OsDLK cycles between two locations during interphase

4.6.1 OsDLK has an unexpected dual localisations in interphase

While the mitotic localisation of OsDLK was meeting the expectations from the findings in its *Arabidopsis* homologues ATK1 and ATK5, its subcellular localisation during interphase was unexpected. We found that, during interphase, OsDLK was found in two populations, one associated with cortical microtubules, the other inside the nucleus.

The association of OsDLK with cortical microtubules (Fig. 19) is not unexpected for a plant kinesin. Plant cMTs bundle extensively in an overlapping manner. Some kinesins moving cargoes linked with cellulose synthesis (Cai & Cresti, 2012), and also others that are not known to interact with cellulose synthases, nevertheless decorate cMTs. These include not only the class-XIV kinesin KCH (Klotz & Nick, 2012), but the *Arabidopsis* homologue of OsDLK, ATK5, as well (Ambrose et al., 2005). During interphase, NtKCH mainly decorates cMTs and is also associated with perinuclear actin cables, acting as a cross-linker of cytoskeletal elements. ATK5 localizes to cMTs and is enriched at microtubule plus-ends. However, kinesin colocalising with cMTs may not play an essential role in cMT organization. The *atk5* mutant has normal cMT organization (Ambrose et al., 2005). The specificity of the colocalisation between OsDLK and cMTs was confirmed by transient transformation with both *Agrobacterium*-mediated cotransformation and immunostaining.

While this binding to microtubules must involve the microtubule binding site located in the motor, the tail domain as well seems to contribute to microtubule binding: OsDLKM, while harbouring the motor domain, does not show this association with cMTs, although it lacks only a part of the tail domain (Fig. 17, 18).

It is important to know that the decoration of a kinesin to cMTs does not necessarily mean that it is active there (Zhu & Dixit, 2012). OsDLK moves along cMTs at high speed highly dynamic (Fig. 29) which might be linked with a function in cell growth. In addition, cMTs are dynamic at both ends and it is important for array organization (Shaw et al., 2003). Kinesins may contribute to the organization of cMT by regulating cMT assembly dynamics. For instance, the overexpression of Kinesin-13A in *Arabidopsis* resulted in partial fragmentation of cMTs (Mucha et al., 2010). In our study, BY-2 cells overexpressing OsDLK were more sensitive to the tubulin assembly inhibitor oryzalin (Fig. 28), indicating an increased dynamic activity of MTs.

Unexpected for a kinesin, OsDLK not only decorates cMTs, but simultaneously appears in the nucleus (Fig. 18), although interphase microtubules are strictly excluded from the karyoplasm by the interphasic nuclear envelope (Hasezawa & Kumagai, 2002; Schwarzerová et al., 2006). However, this strict exclusion from the nucleus is progressively challenged by observations that kinesins can be found in the nucleus. For instance, certain animal KIF4s containing a NLS are in fact found in the nucleus (Wang & Adler, 1995). Interestingly, OsBC12, a rice homologue of the exclusively cytoplasmic kinesin AtFRA1 (Zhong et al., 2002) has been shown to localize in both cytoplasm and nucleus. The nuclear localisation was found to be linked with a function as transcriptional regulator for a specific step in gibberellic acid (GA) biosynthesis (Zhang et al., 2010; Li et al., 2011). Another kinesin like protein SGL (Short Grain Length) fusion with GFP was found to target mainly to the nucleus and was also distributed in other locations in the cells of rice (Wu et al., 2014). Interestingly, both OsBC12 and OsSGL are found to have transcriptional activity in GA pathway and both of them are from Kinesin-4 subfamily.

A putative NLS (Nuclear Localization Signal) motif exists in the amino acid sequence of OsDLK. Moreover, the one in the middle of the protein is predicted to function in both cytoplasm and nuclear localisation, which supports the nuclear of localisation of OsDLK. Actually, most members of Kinesin-4 subfamily in animals contain such signals and function in mitosis. However, the phylogenetic relationship of OsDLK is far from Kinesin-4 members (Fig. 11).

The dual localisations of OsDLK were also confirmed in rice coleoptiles in a transient transformation approach via particle bombardment. The intensity of the fluorescent

signal was high in both cortex and nucleus (Fig. 18g), which is consistent with the result in BY-2 cells.

4.6.2 OsDLK has two cycling subpopulations

We have shown the two localisations of OsDLK in BY-2 overexpressors. However, it is not clear whether there is any cycling between these two subpopulations. Since people have reported that MT can enter nucleus under cold stress (Schwarzerová et al., 2006), we also check the OsDLK overexpressor response to cold. We found that the localisation of OsDLK was dynamic and regulated - in response to cold, this kinesin was repartitioned from the cortical cytoplasm into the nucleus, and even in the absence of cold, the intranuclear population of DLK was constantly cycled between cytoplasm and nucleoplasm but inhibition of export leads to a nuclear accumulation.

When we probed this intranuclear population of OsDLK in more detail, we observed in overexpression tobacco BY-2 cells that cold-induced disassembly of cMTs was followed by a progressive accumulation of OsDLK that was organised in a reticular structure closely associated with chromatin and also tubulin (Fig. 31b). This result was also confirmed in rice coleoptiles that overexpressed OsDLK-GFP transiently (Fig. 32b). The signal condensed and disappeared around the nucleus progressively with the increment of cold treatment time.

This nuclear transport was reversible since cortical OsDLK recovered after cells were returned to room temperature. This behaviour parallels the cold-induced accumulation of tubulin in the nucleus observed in those cells (Schwarzerová et al., 2006).

When OsDLK-RFP was cotransformed with microtubule marker TuB6-GFP, the OsDLK signal seemed to accumulate in the nucleus earlier in some special pattern while MTs accumulate in a diffuse manner under cold stress (Suppl. Fig. S4). However, whether OsDLK enters the nucleus in a complex with tubulin or independently, remains to be elucidated more precisely.

Even under normal temperature, there seems to be considerable recycling between the intranuclear and the cortical population of OsDLK, since treatment with the specific nuclear-export inhibitor leptomycin B (Kudo et al., 1998) caused a progressive

accumulation of the fluorescent signal in the nuclei of transgenic BY-2 cells (Fig. 34a), while the cortical signal was depleted (Fig. 34b-c). Leptomycin B can specially block the function of CRM1, an essential receptor for the leucine-rich nuclear export of proteins. Thus, our result may also reveal the mechanism of accumulation in the nucleus that OsDLK can enter the nucleus through some special nuclear transporter in nuclear pore.

5. Conclusion and Perspectives

A rice member of the class-XIV kinesin family, OsDLK, has been found to cycle during interphase between the cortical MTs and the nucleus, and accumulates in the nucleus in response to cold. The same protein also conveys some functions during mitosis. These functions seem to overlap with those of the previously published homologues in *Arabidopsis* (ATK1 and ATK5). The fact that nuclear transport of OsDLK occurs also at room temperature, but is promoted by cold stress in both transgenic BY-2 cells and rice coleoptile cells, indicating that this kinesin plays a specific function in the nucleus under cold stress. This function, at the current stage, is completely enigmatic. Preliminary data from rice insertion mutants indicate that OsDLK is essential for early development which hampered functional analysis of this gene in rice. This importance for early development is supported by the observation that the steady-state levels of OsDLK transcripts are upregulated during coleoptile elongation.

We are currently investigating, whether OsDLK can bind to DNA in a specific manner, and six candidate DNA-binding motives have been identified in the DPI-ELISA assay. Moreover, the motives were predicted to possess cis-element functions involved in seed germination. This may explain to us that the homozygous rice mutant could not survive in the early stage of seedling development. However, whether it can exert transcriptional regulation which is similar to the above mentioned rice fra1 homologue or not has to be studied in future. Irrespective of the outcome, it is clear already now that this class-XIV kinesin is able to convey novel, specific functions that had not been inferred from its *Arabidopsis* homologues. In other words: there is still a lot to be discovered, even for homologues of well-studied members of the kinesin superfamily.

6. Reference

Akhmanova, A. & Steinmetz, M.O. (2008). Tracking the ends: a dynamic protein network controls the fate of microtubule tips. *Nature reviews Molecular cell biology* **9**, 309-322.

Ambrose, J.C. & Cyr, R. (2007). The kinesin ATK5 functions in early spindle assembly in *Arabidopsis*. *The Plant Cell* **19**, 226-236.

Ambrose, J.C., Li, W., Marcus, A., Ma, H. (2005). A minus-end-directed kinesin with plus-end tracking protein activity is involved in spindle morphogenesis. *Molecular biology of the cell* **16**, 1584-1592.

Ambrose, C. & Wasteney, G.O. (2014). Microtubule initiation from the nuclear surface controls cortical microtubule growth polarity and orientation in *Arabidopsis thaliana*. *Plant and cell physiology*, pcu094.

Amos, L.A. & Hirose, K. (1997). The structure of microtubule-motor complexes. *Current opinion in cell biology* **9**, 4-11.

Asbury, C.L., Fehr, A.N., Block, S.M. (2003). Kinesin moves by an asymmetric hand-over-hand mechanism. *Science* **302**, 2130-2134.

Azpiroz-Leehan, R. & Feldmann, K.A. (1997). T-DNA insertion mutagenesis in *Arabidopsis*: going back and forth. *Trends in Genetics* **13**, 152-156.

Bannigan, A., Scheible, W-R., Lukowitz, W. (2007). A conserved role for kinesin-5 in plant mitosis. *Journal of Cell Science* **120**, 2819-2827.

Bowser, J. & Reddy, A.S.N. (1997). Localization of a kinesin-like calmodulin-binding protein in dividing cells of *Arabidopsis* and tobacco. *The Plant Journal* **12**, 1429-1437.

Brand, L.H., Henneges, C., Schüssler, A., Kolukisaoglu, H.Ü., Koch, G., Wallmeroth, N., Hecker, A., Thurow, K., Zell, A., Harter, K. (2013). Screening for protein-DNA interactions by automatable DNA-protein interaction ELISA. *PloS one* **8**,

e75177.

Brand, L.H., Kirchler, T., Hummel, S., Chaban, C., Wanke, D. (2010). DPI-ELISA: a fast and versatile method to specify the binding of plant transcription factors to DNA in vitro. *Plant Methods* **6**, 25.

Bryksin, A. & Matsumura, I. (2013). Overlap extension PCR cloning. *Synthetic Biology*, 31-42.

Buschmann, H., Green, P., Sambade, A. (2011). Cytoskeletal dynamics in interphase, mitosis and cytokinesis analysed through *Agrobacterium*-mediated transient transformation of tobacco BY-2 cells. *New Phytologist* **190**, 258-267.

Buschmann, H. & Zachgo, S. (2016). The evolution of cell division: from streptophyte algae to land plants. *Trends in plant science* **21**, 872-883

Cai, D., Verhey, K.J., Meyhöfer, E. (2007). Tracking single kinesin molecules in the cytoplasm of mammalian cells. *Biophysical journal* **92**, 4137-4144.

Cai, G. & Cresti, M. (2012). Are kinesins required for organelle trafficking in plant cells? *Frontiers in plant science* **3**, 170.

Chandra, R., Salmon, E.D., Erickson, H.P., Lockhart, A., Endow, S.A. (1993). Structural and functional domains of the *Drosophila* ncd microtubule motor protein. *Journal of Biological Chemistry* **268**, 9005-9013.

Chen, C.B., Marcus, A., Li, W.B., Hu, Y., Calzada, J-P.V., Grossniklaus, U., Cyr, R.J., Ma, H. (2002). The *Arabidopsis* ATK1 gene is required for spindle morphogenesis in male meiosis. *Development* **129**, 2401-2409.

Coy, D.L., Wagenbach, M., Howard, J. (1999). Kinesin takes one 8-nm step for each ATP that it hydrolyzes. *Journal of Biological Chemistry* **274**, 3667-3671.

Day, I.S., Miller, C., Golovkin, M., Reddy, A.S.N. (2000). Interaction of a kinesin-like calmodulin-binding protein with a protein kinase. *Journal of Biological Chemistry*

275, 13737-13745.

Desai, A. & Mitchison, T.J. (1997). Microtubule polymerization dynamics. Annual review of cell and developmental biology **13**, 83-117.

Eichinger, L., Pachebat, J.A., Glöckner, G., Rajandream, M-A., Sucgang, R., Berriman, M., Song, J., Olsen, R., Szafranski, K., Xu, Q. (2005). The genome of the social amoeba *Dictyostelium discoideum*. Nature **435**, 43-57.

Endow, S.A. (1999). Determinants of molecular motor directionality. Nature Cell Biology **1**, E163-E167.

Endow, S.A. & Barker, D.S. (2003). Processive and nonprocessive models of kinesin movement. Annual review of physiology **65**, 161-175.

Endow, S.A., Kang, S.J., Satterwhite., L.L., Rose., M.D., Skeen, V.P., Salmon, E.D. (1994). Yeast Kar3 is a minus-end microtubule motor protein that destabilizes microtubules preferentially at the minus ends. The EMBO Journal **13**, 2708.

Endow, S.A. & Waligora, K.W. (1998). Determinants of kinesin motor polarity." Science **281**, 1200-1202.

Euteneuer, U. & Mcintosh, J.R. (1981). Structural polarity of kinetochore microtubules in PtK1 cells. The Journal of cell biology **89**, 338-345.

Fink, G., Hajdo, L., Skowronek, K.J., Reuther, C., Kasprzak, A.A., Diez, S. (2009). The mitotic kinesin-14 Ncd drives directional microtubule–microtubule sliding. Nature Cell Biology **11**, 717-723.

Foth, B.J., Goedecke, M.C., Soldati, D. (2006). New insights into myosin evolution and classification. Proc. Natl. Acad. Sci. USA **103**, 3681-3686.

Frey, N., Klotz, J., Nick, P. (2009). Dynamic bridges-a calponin-domain kinesin from rice links actin filaments and microtubules in both cycling and non-cycling cells. Plant and cell physiology **50**, 1493-1506.

- Frey, N., Klotz, J., Nick, P. (2010).** A kinesin with calponin-homology domain is involved in premitotic nuclear migration. *Journal of experimental botany* **61**, 3423-3437.
- Fujii, K. (1899).** On the morphology of the spermatozoid of *Ginkgo biloba*. *Bot. Mag., Tokyo* **13**, 260-266.
- Gale, M.D. & Devos, K.M. (1998).** Comparative genetics in the grasses. *Proceedings of the National Academy of Sciences* **95**, 1971-1974.
- Garratt, R., Oliva, G., Caracelli, L., Leite A., Arruda P. (1993).** Studies of the zein-like α -prolamins based on an analysis of amino acid sequences: Implications for their evolution and three-dimensional structure. *Proteins: Structure, Function, and Bioinformatics* **15**, 88-99.
- Gluecksohn-Waelsch, S. (1963).** Lethal genes and analysis of differentiation. *Science* **142**, 1269-1276.
- Goodwin, S.S. & Vale, R.D. (2010).** Patronin regulates the microtubule network by protecting microtubule minus ends. *Cell* **143**, 263-274.
- Green, P.B. (1962).** Mechanism for plant cellular morphogenesis. *Science* **138**, 1404-1405.
- Guo, L., Ho, C-M.K., Kong, Z.S., Lee, Y-R.J., Qian, Q., Liu, B. (2009).** Evaluating the microtubule cytoskeleton and its interacting proteins in monocots by mining the rice genome. *Annals of botany* **103**, 387-402.
- Gutjahr, C., Riemann, M., Müller, A., Düchting, P., Weiler, E.W., Nick, P. (2005).** Cholodny-Went revisited: a role for jasmonate in gravitropism of rice coleoptiles. *Planta* **222**, 575-585.
- Hancock, W.O. & Howard, J. (1998).** Processivity of the motor protein kinesin requires two heads. *The Journal of cell biology* **140**, 1395-1405.
- Hasezawa, S. & Kumagai, F. (2002).** Dynamic changes and the role of the

cytoskeleton during the cell cycle in higher plant cells. *International Review of Cytology* **214**, 161-191.

He, G., Tarui, Y., Lino, M. (2005). A novel receptor kinase involved in jasmonate-mediated wound and phytochrome signaling in maize coleoptiles. *Plant and cell physiology* **46**, 870-883.

Hirokawa, N., Noda, Y., Tanaka, Y., Niwa, S. (2009). Kinesin superfamily motor proteins and intracellular transport. *Nature reviews Molecular cell biology* **10**, 682-696.

Hoffmann, M., Hentrich, M., Pollmann, S. (2011). Auxin–Oxylipin Crosstalk: Relationship of AntagonistsF. *Journal of integrative plant biology* **53**, 429-445.

Holweg, C., Süßlin, C., Nick, P. (2004). Capturing in vivo dynamics of the actin cytoskeleton stimulated by auxin or light. *Plant and cell physiology* **45**, 855-863.

Howard, J. (2001). *Mechanics of motor proteins and the cytoskeleton.* Sinauer Associates, Sunderland.

Howard, J., Hudspeth, A.J., Vale, R.D. (1989). Movement of microtubules by single kinesin molecules. *Nature* **342**, 154-158.

Hoyt, M.A. & Geiser, J.R. (1996). Genetic analysis of the mitotic spindle. *Annual review of genetics* **30**, 7-33.

Hu, R., Zhu, X.X., Xiang, S.P., Zhan, Y.G., Zhu, M.D., Yin, H.Q., Zhou, Q.M., Zhu, L.S., Zhang, X.W., Liu, Z. (2016). Comparative transcriptome analysis revealed the genotype specific cold response mechanism in tobacco. *Biochemical and biophysical research communications* **469**, 535-541.

Hua, W., Young, E.C., Fleming, M.L. (1997). Coupling of kinesin steps to ATP hydrolysis. *Nature* **388**, 390-393.

Humphrey, T.C. & Brooks, G. (2005). *Cell cycle control: mechanisms and protocols.* Vol. 296, Humana Press, New York.

Hyman, A.A. & Mitchison, T.J. (1991). Two different microtubule-based motor activities with opposite polarities in kinetochores. *Nature* **351**, 206.

Iwata, K. & Hogetsu, T. (1989). The Effects of Light Irradiation on the orientation of microtubules in seedlings of *Avena sativa* L. and *Pisum sativum* L. *Plant and cell physiology* **30**, 1011-1016.

Jovanović, A.M., Durst, S., Nick, P. (2010). Plant cell division is specifically affected by nitrotyrosine. *Journal of experimental botany* **61**, 901-909.

Karimi, M., Inz é D., Depicker, A. (2002). GATEWAY™ vectors for Agrobacterium-mediated plant transformation. *Trends in plant science* **7**, 193-195.

Kim, J-Y. (2005). Regulation of short-distance transport of RNA and protein. *Current opinion in plant biology* **8**, 45-52.

Klotz, J. & Nick, P. (2012). A novel actin–microtubule cross–linking kinesin, NtKCH, functions in cell expansion and division. *New Phytologist* **193**, 576-589.

Kong, L-J. & Hanley-Bowdoin, L. (2002). A geminivirus replication protein interacts with a protein kinase and a motor protein that display different expression patterns during plant development and infection. *The Plant Cell* **14**, 1817-1832.

Koonce, M. & Samsó, M. (1996). Overexpression of cytoplasmic dynein's globular head causes a collapse of the interphase microtubule network in *Dictyostelium*. *Molecular biology of the cell* **7**, 935-948.

Kozielski, F., Sack, S., Marx, A., Thormählen, M., Schönbrunn, E., Biou, V., Thompson, A., Mandelkow, E-M., Mandelkow E. (1997). The crystal structure of dimeric kinesin and implications for microtubule-dependent motility. *Cell* **91**, 985-994.

Kudo, N., Wolff, B., Sekimoto, T., Schreiner, E.P., Yoneda, Y., Yanagida, M., Horinouchi, S., Yoshida, M. (1998). Leptomycin B inhibition of signal-mediated nuclear export by direct binding to CRM1. *Experimental cell research* **242**, 540-547.

- Kuthanova, A., Fischer, L., Nick, P., Opatrny, Z. (2008).** Cell cycle phase-specific death response of tobacco BY-2 cell line to cadmium treatment. *Plant, cell & environment* **31**, 1634-1643.
- Laemmli, U.K. (1970).** Cleavage of structural proteins during the assembly of the head of bacteriophage T4. *Nature* **227**, 680-685.
- Lawrence, C.J., Dawe, R.K., Christie, K.R., Cleveland, D.W., Dawson, S.C., Endow, S.A., Goldstein, L.S.B., Goodson, H.V., Hirokawa, N., Howard, J. (2004).** A standardized kinesin nomenclature. *The Journal of cell biology* **167**, 19-22.
- Lawrence, C.J., Morris, N.R., Meagher, R.B., Dawe, R.K. (2001).** Dyneins have run their course in plant lineage. *Traffic* **2**, 362-363.
- Lee, Y-R.J. & Liu, B. (2004).** Cytoskeletal motors in Arabidopsis. Sixty-one kinesins and seventeen myosins. *Plant physiology* **136**, 3877-3883.
- Lloyd, C. & Chan, J. (2008).** The parallel lives of microtubules and cellulose microfibrils. *Current opinion in plant biology* **11**, 641-646.
- Li, J., Jiang, J.F., Qian, Q., Xu, Y.Y., Zhang, C., Xiao, J., Du, C., Luo, W., Zou, G.X., Chen, M.L. (2011).** Mutation of rice BC12/GDD1, which encodes a kinesin-like protein that binds to a GA biosynthesis gene promoter, leads to dwarfism with impaired cell elongation. *The Plant Cell* **23**, 628-640.
- Liu, B., Cyr, R.J., Palevitz, B.A. (1996).** A kinesin-like protein, KatAp, in the cells of arabidopsis and other plants. *The Plant Cell* **8**, 119-132.
- Liu, Q.L., Xu, X.H., Ren, X.L., Fu, D.X., Shu, Q.Y. (2007).** Generation and characterization of low phytic acid germplasm in rice (*Oryza sativa* L.). *Theoretical and applied genetics* **114**, 803-814.
- Lupas, A., Van Dyke., Stock, J. (1991).** Predicting coiled coils from protein sequences. *Science* **252**, 1162-1164.
- Mandelkow, E. & Mandelkow, E. (1990).** Microtubular structure and tubulin

polymerization. *Current opinion in cell biology* **2**, 3-9.

Marcus, A.I., Ambrose, J.C., Blickley, L., Hancock, W.O., Cyr, R.J. (2002). *Arabidopsis thaliana* protein, ATK1, is a minus-end directed kinesin that exhibits non-processive movement. *Cell motility and the cytoskeleton* **52**, 144-150.

Marcus, A.I., Li, W., Ma, H., Cyr, R.J. (2003). A kinesin mutant with an atypical bipolar spindle undergoes normal mitosis. *Molecular biology of the cell* **14**, 1717-1726.

Matsukura, C., Itoh, S-i., Nemoto, K., Tanimoto, E., Yamaguchi, J. (1998). Promotion of leaf sheath growth by gibberellic acid in a dwarf mutant of rice. *Planta* **205**, 145-152.

Mazumdar, M. & Misteli, T. (2005). Chromokinesins: multitasking players in mitosis. *Trends in cell biology* **15**, 349-355.

McDonald, H.B., Stewart, R.J., Goldstein, L.S.B. (1990). The kinesin-like *ncd* protein of *Drosophila* is a minus end-directed microtubule motor. *Cell* **63**, 1159-1165.

Menges, M., Hennig, L., Gruissem, W., Murray, J.A.H. (2003). Genome-wide gene expression in an *Arabidopsis* cell suspension. *Plant molecular biology* **53**, 423-442.

Miki, H., Okada, Y., Hirokawa, N. (2005). Analysis of the kinesin superfamily: insights into structure and function. *Trends in cell biology* **15**, 467-476.

Mita, T. & Shibaoka, H. (1984). Gibberellin stabilizes microtubules in onion leaf sheath cells. *Protoplasma* **119**, 100-109.

Misumi, O., Yoshida, Y., Nishida, K., Fujiwara, T., Sakajiri, T., Hirooka, S., Nishimura, Y., Kuroiwa, T. (2008). Genome analysis and its significance in four unicellular algae, *Cyanidioshyzon merolae*, *Ostreococcus tauri*, *Chlamydomonas reinhardtii*, and *Thalassiosira pseudonana*. *Journal of plant research* **121**, 3-17.

Mitsui, H., Nakatani, K., Yamaguchi-Shinozaki, K., Shinozaki, K., Nishikawa, K., Takahashi, H. (1994). Sequencing and characterization of the kinesin-related genes

- katB and katC of *Arabidopsis thaliana*. *Plant molecular biology* **25**, 865-876.
- Mitsui, H., Yamaguchi-Shinozaki, K., Shinozaki, K., Nishikawa, K., Takahashi, H. (1993).** Identification of a gene family (kat) encoding kinesin-like proteins in *Arabidopsis thaliana* and the characterization of secondary structure of KatA. *Molecular and General Genetics MGG* **238**, 362-368.
- Mostowy, S. & Cossart, P. (2012).** Septins: the fourth component of the cytoskeleton. *Nat Rev Mol Cell Biol* **13**, 183-194.
- Mucha, E., Hoefle, C., Hückelhoven, R., Berken, A. (2010).** RIP3 and AtKinesin-13A—a novel interaction linking Rho proteins of plants to microtubules. *European journal of cell biology* **89**, 906-916.
- Nagata, T., Nemoto, Y., Hasezawa, S. (1992).** Tobacco BY-2 cell line as the “HeLa” cell in the cell biology of higher plants. *International Review of Cytology* **132**, 1-30.
- Nagpal, P., Ellis, C.M., Weber, H., Ploense, S.E., Barkawi, L.S., Guilfoyle, T.J., Hagen, G., Alonso, J.M., Cohen, J.D., Farmer, E.E (2005).** Auxin response factors ARF6 and ARF8 promote jasmonic acid production and flower maturation. *Development* **132**, 4107-4118.
- Nakamura, M., Naoi, K., Shoji, T., Hashimoto, T. (2004).** Low concentrations of propyzamide and oryzalin alter microtubule dynamics in *Arabidopsis* epidermal cells. *Plant and cell physiology* **45**, 1330-1334.
- Ni, C.Z., Wang, H.Q., Tao, X., Zhe, Q.U., Liu, G.Q. (2005).** AtKP1, a kinesin-like protein, mainly localizes to mitochondria in *Arabidopsis thaliana*. *Cell research* **15**, 725-733.
- Nick, P. (1998).** Signaling to the microtubular cytoskeleton in plants. *International Review of Cytology* **184**, 33-80.
- Nick, P. (1999).** Signals, motors, morphogenesis-the cytoskeleton in plant development.

Plant Biology **1**, 169-179.

Nick, P. (2000). Control of Plant Shape. In: Plant microtubules-potential for biotechnology. Nick P (ed), Springer, Berlin Heidelberg, New York, pp 24-46.

Nick, P. (2006). Noise yields order-auxin, actin, and polar patterning. Plant Biology **8**, 360-370.

Nick, P. (2008). Control of cell axis. In: Plant Microtubules. Nick P (ed), Plant Cell Monogr, **143**, 3-46.

Nick, P. (2014). Why to spent tax money on plant microtubules? Plant Cell Monogr **22**, 39-67.

Nick, P., Yatou, O., Furuya, M., Lambert, A-M. (1994). Auxin-dependent microtubule responses and seedling development are affected in a rice mutant resistant to EPC. The Plant Journal **6**, 651-663.

Nishihama, R., Soyano, T., Ishikawa M., Araki, S., Tanaka, H., Asada, T., Irie, K., Ito, M., Terada, M., Banno, H. (2002). Expansion of the cell plate in plant cytokinesis requires a kinesin-like protein/MAPKKK complex. Cell **109**, 87-99.

Oppenheimer, D.G., Pollock, M.A., Vacik, J., Szymanski, D.B., Ericson, B., Feldmann, K., Marks, M.D. (1997). Essential role of a kinesin-like protein in *Arabidopsis* trichome morphogenesis. Proceedings of the National Academy of Sciences **94**, 6261-6266.

Pan, R., Lee, Y-R.J., Liu, B. (2004). Localization of two homologous *Arabidopsis* kinesin-related proteins in the phragmoplast. Planta **220**, 156-164.

Pauwels, L., Barbero, G.F., Geerinck, J., Tilleman, S., Grunewald, W., Pérez, A.C., Chico, J.M., Bossche, R.V., Sewell, J., Gil, E. (2010). NINJA connects the co-repressor TOPLESS to jasmonate signalling. Nature **464**, 788.

Preuss, M.L., Kovar, D.R., Lee, Y-R.J., Staiger, C.J., Delmer, D.P., Liu, B. (2004). A plant-specific kinesin binds to actin microfilaments and interacts with cortical

microtubules in cotton fibers. *Plant physiology* **136**, 3945-3955.

Qiao, F., Petrášek, J., Nick, P. (2010). Light can rescue auxin-dependent synchrony of cell division in a tobacco cell line." *Journal of experimental botany* **61**, 503-510.

Reddy, A.S.N & Day, I.S. (2001). Kinesins in the *Arabidopsis* genome: a comparative analysis among eukaryotes. *BMC genomics* **2**, 2.

Reddy, A.S.N., Narasimhulu, S.B., Safadi, F., Golovkin, M. (1996). A plant kinesin heavy chain-like protein is a calmodulin-binding protein. *The Plant Journal* **10**, 9-21.

Reddy, A.S.N. (2001). Molecular motors and their functions in plants. *Int Rev Cytol & Cell Bio* **204**, 97-178.

Reddy, A.S.N. (2003). Molecular motors in plant cells. In *Molecular Motors*. Schliwa M (ed), Weinheim: Wiley-VCH; 433-469.

Richardson, D.N., Simmons, M.P., Reddy, A.S.N. (2006). Comprehensive comparative analysis of kinesins in photosynthetic eukaryotes. *BMC genomics* **7**, 18.

Richards, T.A. & Cavalier-Smith, T. (2005). Myosin domain evolution and the primary divergence of eukaryotes. *Nature* **436**, 1113-1118.

Riemann, M., Müller, A., Korte, A., Furuya, M., Weiler, E.W., Nick, P. (2003). The rice mutant *hebiba* lacks jasmonate induction. *Plant Physiol* **133**, 1820-1830.

Riemann, M., Riemann, M., Takano, M. (2008). Rice JASMONATE RESISTANT 1 is involved in phytochrome and jasmonate signalling. *Plant, cell & environment* **31**, 783-792.

Rogers, K.R., Weiss, S., Crevel, I., Brophy, P.J., Geeves, M., Cross, R. (2001). KIF1D is a fast non-processive kinesin that demonstrates novel K-loop-dependent mechanochemistry. *The EMBO Journal* **20**, 5101-5113.

Rosenbaum, J.L. & Witman, G.B. (2002). Intraflagellar transport. *Nature reviews Molecular cell biology* **3**, 813-825.

Ruhnow, F., Zwicker, D., Diez, S. (2011). Tracking single particles and elongated filaments with nanometer precision. *Biophysical journal* **100**, 2820-2828.

Sack, S., Kull, F.J., Mandelkow, E. (1999). Motor proteins of the kinesin family. *European journal of biochemistry* **262**, 1-11.

Sakoda, M., Hasegawa, K., Ishizuka, K. (1992). Mode of action of natural growth inhibitors in radish hypocotyl elongation—influence of raphanusanin on auxin-mediated microtubule orientation. *Physiologia Plantarum* **84**, 509-513.

Sambrook, J. & Russell, D.W. (2001). *Molecular cloning: a laboratory manual* / Joseph Sambrook, David W. Russell. (Cold Spring Harbor, N.Y.: Cold Spring Harbor Laboratory Press).

Samuels, A., Meehl, J., Lipe, M., Staehelin, L.A. (1998). Optimizing conditions for tobacco BY-2 cell cycle synchronization. *Protoplasma* **202**, 232-236.

Santner, A. & Estelle, M. (2009). Recent advances and emerging trends in plant hormone signalling. *Nature* **459**, 1071-1078.

Sauter, M., Seagull, R.W., Kende, H. (1993). Internodal elongation and orientation of cellulose microfibrils and microtubules in deepwater rice. *Planta* **190**, 354-362.

Sazuka, T., Aichi, I., Kawai, T., Matsuo, N., Kitano, H., Matsuoka, M. (2005). The rice mutant dwarf bamboo shoot 1: a leaky mutant of the NACK-type kinesin-like gene can initiate organ primordia but not organ development. *Plant and cell physiology* **46**, 1934-1943.

Schneider, N. (2015). *The enigma of tubulin deetyrosination-functional evidence from plants*, Karlsruhe, Karlsruher Institut für Technologie (KIT), Diss., 2015.

Schnitzer, M.J. & Block, S.M. (1997). Kinesin hydrolyses one ATP per 8-nm step. *Nature* **388**, 386-390.

Schwarzerová, K., Petrášek, J., Panigrahi, K.C.S., Zelenková, S., Opatrný, Z., Nick,

- P. (2006).** Intranuclear accumulation of plant tubulin in response to low temperature. *Protoplasma* **227**, 185-196.
- Sharp, D.J., Rogers, G.C., Scholey, J.M. (2000).** Cytoplasmic dynein is required for poleward chromosome movement during mitosis in *Drosophila* embryos. *Nature Cell Biology* **2**, 922-930.
- Shaw, S.L., Kamyar, R., Ehrhardt, D.W. (2003).** Sustained microtubule treadmilling in *Arabidopsis* cortical arrays. *Science* **300**, 1715-1718.
- Shibaoka, H. (1991).** Microtubules and the regulation of cell morphogenesis by plant hormone. In *The Cytoskeletal Basis of Plant Growth and Form* (ed. C. W. Lloyd), London: Academic Press, pp,159-168.
- Shibaoka, H. (1994).** Plant hormone-induced changes in the orientation of cortical microtubules: alterations in the cross-linking between microtubules and the plasma membrane." *Annual review of plant biology* **45**, 527-544.
- Soldati, T. & Schliwa, M. (2006).** Powering membrane traffic in endocytosis and recycling. *Nature reviews Molecular cell biology* **7**, 897-908.
- Song, H., Golovkin, M., Reddy, A.S.N., Endow, S.A. (1997).** In vitro motility of AtKCBP, a calmodulin-binding kinesin protein of *Arabidopsis*. *Proceedings of the National Academy of Sciences* **94**, 322-327.
- Suetsugu, N., Yamada, N., Kagawa, T., Yonekura, H., Uyeda, T.Q.P., Kadota, A., Wada, M. (2010).** Two kinesin-like proteins mediate actin-based chloroplast movement in *Arabidopsis thaliana*. *Proceedings of the National Academy of Sciences* **107**, 8860-8865.
- Svyatyna, K. & Riemann, M. (2012).** Light-dependent regulation of the jasmonate pathway. *Protoplasma* **249**, 137-145.
- Tamura, K., Nakatani, K., Mitsui, H., Ohashi, Y., Takahashi, H. (1999).**

Characterization of *katD*, a kinesin-like protein gene specifically expressed in floral tissues of *Arabidopsis thaliana*. *Gene* **230**, 23-32.

Tamura, K., Peterson, D., Peterson, N., Stecher, G., Nei, M., Kumar, S. (2011). MEGA5: molecular evolutionary genetics analysis using maximum likelihood, evolutionary distance, and maximum parsimony methods. *Molecular biology and evolution* **28**, 2731-2739.

Tiryaki, I. & Staswick, P.E. (2002). An *Arabidopsis* mutant defective in jasmonate response is allelic to the auxin-signaling mutant *axr1*. *Plant physiology* **130**, 887-894.

Toprak, E., Yildiz, A., Hoffman, M.T., Rosenfeld, S.S., Selvin, P.R. (2009). Why kinesin is so processive. *Proceedings of the National Academy of Sciences* **106**, 12717-12722.

Ueda, J., Miyamoto, K., Aoki, M. (1994). Jasmonic acid inhibits the IAA-induced elongation of oat coleoptile segments: a possible mechanism involving the metabolism of cell wall polysaccharides. *Plant and cell physiology* **35**, 1065-1070.

Vale, R.D. (2003). The molecular motor toolbox for intracellular transport. *Cell* **112**, 467-480.

Vale, R.D., Schnapp, B.J., Mitchison, T., Steuer, E., Reese, T.S., Sheetz, M.P. (1985). Different axoplasmic proteins generate movement in opposite directions along microtubules in vitro. *Cell* **43**, 623-632.

Vanstraelen, M., Acosta, J.A.T., De Veylder, L., Inzé D., Geelen, D. (2004). A plant-specific subclass of C-terminal kinesins contains a conserved a-type cyclin-dependent kinase site implicated in folding and dimerization. *Plant physiology* **135**, 1417-1429.

Vanstraelen, M., Inzé D., Geelen, D. (2006). Mitosis-specific kinesins in *Arabidopsis*. *Trends in plant science* **11**, 167-175.

- Vöchting, H. (1878).** Über Organbildung im Pflanzenreich: Physiologische Untersuchungen über Wachstumsursachen und Lebenseinheiten, Bonn, FR Cohen.
- von Delius, M. & Leigh, D.A. (2011).** Walking molecules. *Chemical Society Reviews* **40**, 3656-3676.
- Vos, J.W., Safadi, F., Reddy, A.S.N., Hepler, P.K. (2000).** The kinesin-like calmodulin binding protein is differentially involved in cell division. *The Plant Cell* **12**, 979-990.
- Walter, W.J., Beránek, V., Fischermeier, E., Diez, S. (2012).** Tubulin acetylation alone does not affect kinesin-1 velocity and run length in vitro. *PloS one* **7**, e42218.
- Walter, W.J., Machens, I., Rafieian, F., Diez, S. (2015).** The non-processive rice kinesin-14 OsKCH1 transports actin filaments along microtubules with two distinct velocities. *Nature plants* **1**, 15111.
- Wang, S.Z. & Adler, R. (1995).** Chromokinesin: a DNA-binding, kinesin-like nuclear protein. *Journal of Cell Biology* **128**, 761-768.
- Wang, W., Takezawa, D., Narasimhulu, S.B., Reddy, A.S.N., Poovaiah, B.W. (1996).** A novel kinesin-like protein with a calmodulin-binding domain. *Plant molecular biology* **31**, 87-100.
- Wickstead, B. & Gull, K. (2007).** Dyneins across eukaryotes: a comparative genomic analysis. *Traffic* **8**, 1708-1721.
- Winkler, R.G., & Feldmann, K.A. (1998).** PCR-based identification of T-DNA insertion mutants. *Methods Mol Biol* **82**, 129-136.
- Wu, T., Shen, Y.Y., Zheng, M., Yang, C.Y., Chen, Y.L., Feng, Z.M., Liu, X., Liu, S.J., Chen, Z.J., Lei, C.L. (2014).** Gene SGL, encoding a kinesin-like protein with transactivation activity, is involved in grain length and plant height in rice. *Plant cell reports* **33**, 235-244.

- Xie, D.X., Feys, B.F., James, S., Nieto-Rostro, M., Turner, J.G. (1998).** COI1: an *Arabidopsis* gene required for jasmonate-regulated defense and fertility. *Science* **280**, 1091-1094.
- Xu, T., Qu, Z., Yang, X.Y., Qin, X.H., Xiong, J.Y., Wang, W.Q., Ren, D.T., Liu, G.Q. (2009).** A cotton kinesin GhKCH2 interacts with both microtubules and microfilaments. *Biochemical Journal* **421**, 171-180.
- Xu, X.H., Zhao, H.J., Liu, Q.L., Frank, T., Engel, K-H., An, G., Shu, Q.Y. (2009).** Mutations of the multi-drug resistance-associated protein ABC transporter gene 5 result in reduction of phytic acid in rice seeds. *Theoretical and applied genetics* **119**, 75-83.
- Yang, C.Y., Spielman, M., Coles, J.P., Li, Y., Ghelani, S., Bourdon, V., Brown, R.C., Lemmon, B.E., Scott, R.J., Dickinson, H.G. (2003).** TETRASPORE encodes a kinesin required for male meiotic cytokinesis in *Arabidopsis*. *The Plant Journal* **34**, 229-240.
- Yang, J.T., Laymon, R.A., Goldstein, L.S.B. (1989).** A three-domain structure of kinesin heavy chain revealed by DNA sequence and microtubule binding analyses. *Cell* **56**, 879-889.
- Yildiz, A., Tomishige, M., Vale, R.D., Selvin, P.R. (2004).** Kinesin walks hand-over-hand. *Science* **303**, 676-678.
- Zhang, M., Zhang, B., Qian, Q., Yu, Y.C., Li, R., Zhang, J.W., Liu, X.L., Zeng, D.L., Li, J.Y., Zhou, Y.H. (2010).** Brittle Culm 12, a dual-targeting kinesin-4 protein, controls cell-cycle progression and wall properties in rice. *The Plant Journal* **63**, 312-328.
- Zhong, R.Q., Burk, D.H., Morrison, W.H., Ye, Z.H. (2002).** A kinesin-like protein is essential for oriented deposition of cellulose microfibrils and cell wall strength. *The Plant Cell* **14**, 3101-3117.

Zhu, C. & Dixit, R. (2012). Functions of the *Arabidopsis* kinesin superfamily of microtubule-based motor proteins. *Protoplasma* **249**, 887-899.

7. Appendix

>pGA2715 vector T-DNA sequence (from RB to LB)

Border: [Border sequence](#)

Primers used for iPCR: [Primer sequence](#)

```

1  GTTTACCCGC CAATATATCC TGTCAAACAC GGATCCGAGG TACCAGGTAC
51  CAGGTGAGTT CCATTCTTAC TACCACGGTG CTATTTTTTTT TGCTATGTGG
101 CTAATTACAT GACTAACTTG GGGTGCTAAA TCTTACAGGT TATATGCAGG
151 TTATATGCAG GTCCCGGGTA GGTCAGTCCC TTATGTTACG TCCTGTAGAA
201 ACCCCAACCC GTGAAATCAA AAAACTCGAC GGCCTGTGGG CATTACAGTCT
251 GGATCGCGAA AACTGTGGAA TTGATCAGCG TTGGTGGGAA AGCGCGTTAC
301 AAGAAAGCCG GGCAATTGCT GTGCCAGGCA GTTTTAACGA TCAGTTCGCC
351 GATGCAGATA TTCGTAATTA TGCGGGCAAC GTCTGGTATC AGCGCGAAGT
401 CTTTATACCG AAAGGTTGGG CAGGCCAGCG TATCGTGCTG CGTTTCGATG
451 CGGTCACTCA TTACGGCAA GTGTGGGTCA ATAATCAGGA AGTGATGGAG
501 CATCAGGGCG GCTATACGCC ATTTGAAGCC GATGTCACGC CGTATGTTAT
551 TGCCGGGAAA AGTGTACGTA TCACCGTTTG TGTGAACAAC GAACTGAACT
601 GGCAGACTAT CCCGCCGGGA ATGGTGATTA CCGACGAAAA CGGCAAGAAA
651 AAGCAGTCTT ACTTCCATGA TTTCTTTAAC TATGCCGGAA TCCATCGCAG
701 CGTAATGCTC TACACCACGC CGAACACCTG GGTGGACGAT ATCACCGTGG
751 TGACGCATGT CGCGCAAGAC TGTAACCACG CGTCTGTTGA CTGGCAGGTG
801 GTGGCCAATG GTGATGTCAG CGTTGAACTG CGTGATGCGG ATCAACAGGT
851 GGTTGCAACT GGACAAGGCA CTAGCGGGAC TTTGCAAGTG GTGAATCCGC
901 ACCTCTGGCA ACCGGGTGAA GGTTATCTCT ATGAACTGTG CGTCACAGCC
951 AAAAGCCAGA CAGAGTGTGA TATCTACCCG CTTTCGCTCG GCATCCGGTC
1001 AGTGGCAGTG AAGGGCCAAC AGTTCCTGAT TAACCACAAA CCGTTCCTACT
1051 TTACTGGCTT TGGTCGTCAT GAAGATGCGG ACTTACGTGG CAAAGGATTC
1101 GATAACGTGC TGATGGTGCA CGACCACGCA TTAATGGACT GGATTGGGGC
1151 CAACTCCTAC CGTACCTCGC ATTACCCTTA CGCTGAAGAG ATGCTCGACT
1201 GGGCAGATGA ACATGGCATC GTGGTGATTG ATGAAACTGC TGCTGTCGGC
1251 TTTAACCTCT CTTTAGGCAT TGGTTTCGAA GCGGGCAACA AGCCGAAAGA
1301 ACTGTACAGC GAAGAGGCAG TCAACGGGGA AACTCAGCAA GCGCACTTAC
1351 AGGCGATTAA AGAGCTGATA GCGCGTGACA AAAACCACCC AAGCGTGGTG
1401 ATGTGGAGTA TTGCCAACGA ACCGGATACC CGTCCGCAAG TGCACGGGAA
1451 TATTTGCGCA CTGGCGGAAG CAACCGGTAA ACTCGACCCG ACGCGTCCGA
1501 TCACCTGCGT CAATGTAATG TTCTGCGACG CTCACACCGA TACCATCAGC
1551 GATCTCTTTG ATGTGCTGTG CCTGAACCGT TATTACGGAT GGTATGTCCA

```

1601 AAGCGGCGAT TTGGAAACGG CAGAGAAGGT ACTGGAAAAA GAACTTCTGG
1651 CCTGGCAGGA GAAACTGCAT CAGCCGATTA TCATCACCGA ATACGGCGTG
1701 GATACGTTAG CCGGGCTGCA CTCAATGTAC ACCGACATGT GGAGTGAAGA
1751 GTATCAGTGT GCATGGCTGG ATATGTATCA CCGCGTCTTT GATCGCGTCA
1801 GCGCCGTCGT CGGTGAACAG GTATGGAATT TCGCCGATTT TCGGACCTCG
1851 CAAGGCATAT TGCGCGTTGG CGGTAACAAG AAAGGGATCT TCACTCGCGA
1901 CCGCAAACCG AAGTCGGCGG CTTTTCTGCT GCAAAAACGC TGGACTGGCA
1951 TGAACTTCGG TGAAAAACCG CAGCAGGGAG GCAAAACAATG AATCAACAAC
2001 TCTCCTGGCG CACCATCGTC GGCTACAGCC TCGGGAATTG CTACCGAGCT
2051 CGAATTTCCC CGATCGTTCA AACATTTGGC AATAAAGTTT CTTAAGATTG
2101 AATCCTGTTG CCGGTCTTGC GATGATTATC ATATAATTTT TGTTGAATTA
2151 CGTTAAGCAT GTAATAATTA ACATGTAATG CATGACGTTA TTTATGAGAT
2201 GGGTTTTTAT GATTAGAGTC CCGCAATTAT ACATTTAATA CGCGATAGAA
2251 AACAAAATAT AGCGCGCAAA CTAGGATAAA TTATCGCGCG CGGTGTCAATC
2301 TATGTTACTA GATCGGGAAT TAATTCATCG ATAGGCTAGT CATGGTGACT
2351 GTACGTTGTA AGTGCAGCAA ACTGCCGACG CGATGCAAAAC TGTACACGTT
2401 AACATGCCAC TCACCTGGAA CGCACAATGG CCACTAGGTG CGGCCGTAGT
2451 GTGGATTTCA AAGAGAGAGA GAGAGAGAGA GAGCTAATCA CGTAAACGTA
2501 AACACAGCAG ATAGCAGAGA TGTTGATTAG GCAAAACAGT ATAAAAGCCA
2551 ATCCAATAAA CTACATTTAG CGAAGTGCTA TACTAATGCA CTAATAACGA
2601 ACTGTTCTTT TCTTAAGATC GGAGCCAGTA ATGGGTTGTC AGCAGGAGAA
2651 GCACGTAAAC CTTGAAACAT ACTAAGTTCC ACAGTCGAGA GTAAACCGTA
2701 ATCAACACAA GAAACAAACA TAAAATTGAA CAAACGCGCA TATTATAAGT
2751 GACGAAGCGG TCTCACATAA AACAGGGCAC ACAGGTTACA ACAACGAGGG
2801 TTGTAAGCCC ATTAAGCCCC AAACATCAGA TCACCACAAG CAAATGTCTC
2851 GAAGACACAC GCACACGGCA ACAGGATAAC TCCACACTGG CAGATCATGG
2901 GATAGCAGCA GTTATCAATC AGGCCTTGAC ACACAGAACA TCAAGCCCCC
2951 AGACGACGAC GACTCCTCTA GATCCCGGTC GGCATCTACT CTATTCCTTT
3001 GCCCTCGGAC GAGTGCTGGG GCGTCGGTTT CCACTATCGG CGAGTACTTC
3051 TACACAGCCA TCGGTCCAGA CGGCCGCGCT TCTGCGGGCG ATTTGTGTAC
3101 GCCCGACAGT CCCGGCTCCG GATCGGACGA TTGCGTCGCA TCGACCCTGC
3151 GCCCAAGCTG CATCATCGAA ATTGCCGTCA ACCAAGCTCT GATAGAGTTG
3201 GTCAAGACCA ATGCGGAGCA TATACGCCCG GAGCCGCGGC GATCCTGCAA
3251 GCTCCGGATG CCTCCGCTCG AAGTAGCGCG TCTGCTGCTC CATAACAAGC
3301 AACCACGGCC TCCAGAAGAA GATGTTGGCG ACCTCGTATT GGGAAATCCCC
3351 GAACATCGCC TCGCTCCAGT CAATGACCGC TGTTATGCGG CCATTGTCCG
3401 TCAGGACATT GTTGGAGCCG AAATCCCGGT GCACGAGGTG CCGGACTTCG
3451 GGGCAGTCCT CGGCCCAAAG CATCAGCTCA TCGAGAGCCT GCGCGACGGA

3501 CGCACTGACG GTGTCGTCCA TCACAGTTTG CCAGTGATAC ACATGGGGAT
3551 CAGCAATCGC GCATATGAAA TCACGCCATG TAGTGTATTG ACCGATTCTT
3601 TGCGGTCCGA ATGGGCCGAA CCCGCTCGTC TGGCTAAGAT CGGCCGCAGC
3651 GATCGCATCC ATGGCCTCCG CGACCGGCTG CAGAACAGCG GGCAGTTCGG
3701 TTTTCAGGCAG GTCTTGCAAC GTGACACCCT GTGCACGGCG GGAGATGCAA
3751 TAGGTCAGGC TCTCGCTGAA TTCCCAATG TCAAGCACTT CCGGAATCGG
3801 GAGCGCGGCC GATGCAAAGT GCCGATAAAC ATAACGATCT TTGTAGAAAAC
3851 CATCGGCGCA GCTATTTACC CGCAGGACAT ATCCACGCCC TCCTACATCG
3901 AAGCTGAAAAG CACGAGATTC TTCGCCCTCC GAGAGCTGCA TCAGGTTCGGA
3951 GACGCTGTCTG AACTTTTTCGA TCAGAAACTT CTCGACAGAC GTCGCGGTGA
4001 GTTCAGGCTT TTTCATATCT CATTGCCCCC CGGGATCCGT CGAGTCAGCC
4051 TGAAAGGACA AAATACATGT TAGCGCCTTA GTGGTACATT ATTATTTTTCAG
4101 TACAGCAAGA TAACACAATT CAAAAGACTG ACCCATAATA AATAACTAGT
4151 CCTCAATTTA AAATTTGAGT TCCTAAATAG ACATCTATGA ATATGCTGTA
4201 CATCGGCACT ACAGAAAATA CGATTCCCAA TAATTGAACA ATTGTACTTT
4251 ATTTAGTTGT TACTACAACA ATGGAAGATA CAAGATCGTT TCAAAACTAC
4301 CATACTGCA TGGAGTATTT GTTCCACAGA TCTGGAAAAA ACAGATCTGA
4351 CGGGCAGTGT CACCAAACAC TAGACATATG TATTTGTATT AGGTGGATGA
4401 CGTGTACAAA CATGACTACC AGATCTAGAA TTAGAACGCG GCGTGCTTTG
4451 GAAATGTTAA GTAGATCCAA ATACATCGGT AACAAATGAA CATATTCATA
4501 TGACATAGCT GTAAAACATC ATGATCTATC ATATCAACTA GAGGGGATCT
4551 CGGCATGTAT CATTCTATTG CATCTAGAAC CATAGCATTT CCATGTGACA
4601 AACAAATTTG AACATACAT TGCTCAGATC TACCATAAGA ACACCATGTT
4651 CATGACAGCA TCGACCATGA TTTCCACATT TAACAGCATC CCGAGGTCAG
4701 ATCCAGTGT TAGAACTATC ATTTTCAGCAA AATTCACAAA ATAAATCCTC
4751 CAATTCGCCT ACATATATCC ATTCCACGCA TCCTAGGACC AGATCCACCA
4801 TACCAGTATA CACGAACACT AAACATTTCA TCAGATCCGC TAACTACGAC
4851 AGAGAAAACG CAGATCCAGA CAACCAGATC CACCGACAAA TAAACACAGC
4901 CCCCCACATC CAACAACCGC GAATCCACCC AGATCTGACC CAGAAGCAGG
4951 CACGAAGAAC ACGGGGGGTG AGGGAGATGG GACGCGGATC CAAGCTTGGC
5001 GGCGGATTGG GTTGATGCTG CGACGGCGGC GGAGAAGGGA GAGAGGGGAG
5051 AGGAGGAAAA GCGCGGAGGC GCGGAGAGAG GCGAGTACGA AGACGCCTTT
5101 CTCTGCGTTG TCTCGGCTTA GGGTTTGCGA TCCCCGCACT CCGCCCGTTT
5151 TATAGGGCCA GACAGCCTGG ACCTCTCAGG AGCGGAAGCG AAGGGATGGG
5201 GGAGTTTTTC GTTTTACCCC CTTTGACGTC TTCAAAATTC ACTCGCATCT
5251 CACATCGTGC CTGCAAAGGT CGGGTGGTTG GATCATATCG AGAATATTTA
5301 ATAAGTTAGG GAGCTTTCTG ATAATATCCA CCGCAAGGAG GCCATTTCTG
5351 TTGCACTCGG TTGAAGTCCA TACCCGCCTC TCGTTAGTTT CACTGACAGG

5401 TGGGTCCAGA GGCTTCCTTC GTGTGCGGTT AGCGAGTGCA CGCGTCGCTC
5451 CAAGAAAAAG CAGTAGGTGA CCTGGCCACC TCGTTGTAGG TGCGACCGAT
5501 GCAGACGTCC CGCTTGCCGG TGGGCCACG TTACAGCTGG GTCCACATA
5551 TCGGTGGGTG CGATGAGTTG TTCGGTGCCT AGGAGTAGAT TGGATCCCAA
5601 CGGGTGGTTG CGTCGTCCGC GGCCCTGCCG ATTTTATTTT CGATTTTGA
5651 AATGCGAGAG CGGGAGAACG GCACCGTTGG CTTGGCTGTG GATGCCGTTA
5701 GCCGCACCGG ACTATTCCGC CCAGTTCCAT TTTGGCCCAA CTTGAAACAG
5751 CGCGGAGCAC AAGACGGGGG AGCCCATTTA GGCCCGTAAT CTCAGCCCTG
5801 TAGAAAGTCC GTGTGCTTGC GATGGACCAG AAAGCCATA AACCTTGAG
5851 GCGTTCTCTG CTGGGAATAA AATAAGTTCA CACTCTGTCC CTCAACTTTA
5901 CGTCGAGTTT GTTTGACATC GCTAATGCC AGTACCAGAA ATCTTGATA
5951 CAAATAAGGT TTGATATAAA GTGGCACGTG GTGAATGGCA TCGTTTGAAA
6001 AATCTTCAGA TCGAGCGGGC TTCACAAGCC GTAAGTGCAA GTGCCAAAAT
6051 TTGTGAAGAA AATTACTTCC TTCATTTTAC AATGTAAGTT ATTTTAGCAT
6101 TTTCCACATT CATATTGATA TCAATAAATT TAGATAGATA TATATGTCTG
6151 AATTCGTACC GTTAACGAGC TCTAGAAGCT TCAGTACTAC GCGTCTCGAG
6201 GCCTATTATT GAAGCATTTA TCAGGGTTAT TGTCTCATGA GCGGATACAT
6251 ATTTGAATGT ATTTAGAAAA ATAAACAAAT AGGGGTCCG CGCACATTTT
6301 CCCGAAAAGT GCCACCTGAC GTCTAAGAAA CCATTATTAT CATGACATTA
6351 ACCTATAAAA ATAGGCGTAT CACGAGGCC TTTTCGTCTCG CGCGTTTCGG
6401 TGATGACGGT GAAAACCTCT GACACATGCA GCTCCCGGAG ACGGTCACAG
6451 CTTGTCTGTA AGCGGATGCC GGGAGCAGAC AAGCCCGTCA GGGCGCGTCA
6501 GCGGGTGTG GCGGGTGTG GGGCTGGCTT AACTATGCGG CATCAGAGCA
6551 GATTGTACTG AGAGTGCACC ATATGCGGTG TGAAATACCG CACAGATGCG
6601 TAAGGAGAAA ATACCGCATC AGGCGCCATT CGCCATTCAG GCTGCGCAAC
6651 TGTTGGGAAG GCGGATCGGT GCGGGCCTCT TCGCTATTAC GCCAGCTGGC
6701 GAAAGGGGGA TGTGCTGCAA GCGGATTAAG TTGGGTAACG CCAGGGTTTT
6751 CCCAGTCACG ACGTTGTAAA ACGACGGCCA GTGAATTCAC TAGTGATTGC
6801 TCTAGACACT GATAGTTTCG GATCTAGATA TCACATCAAT CCACTTGCTT
6851 TGAAGACGTG GTTGGAACGT CTTCTTTTTT CACGATGTTT CTCGTGGGTG
6901 GGGGTCCATC TTTGGGACCA CTGTCCGTAG AGGCATCTTG AACGATAGCC
6951 TTTCTTTTAT CGCAATGATG GCATTTGTAG AAGCCATCTT CCTTTTCTAC
7001 TGTCTTTTCG ATGAAGTGAC AGATAGCTGG GCAATGGAAT CCGAGGAGGT
7051 TTCCCGATAT TACCCTTTGT TGAAAAGTCT CAATAGCCCT CTGGTCTTCT
7101 GAGACTGTAT CTTTGATATT CTTGGAGTAG ACGAGAGTGT CGTGCTCCAC
7151 CATGTTGGGG ATCTAGATAT CACATCAATC CACTTGCTTT GAAGACGTGG
7201 TTGGAACGTC TTCTTTTTCC ACGATGTTCC TCGTGGGTGG GGGTCCATCT
7251 TTGGGACCAC TGTCGGTAGA GGCATCTTGA ACGATAGCCT TTCCTTTATC

7301 GCAATGATGG CATTGTAGAG AGCCATCTTC CTTTTCTACT GTCCTTTCGA
7351 TGAAGTGACA GATAGCTGGG CAATGGAATC CGAGGAGGTT TCCCGATATT
7401 ACCCTTTGTT GAAAAGTCTC AATAGCCCTC TGGTCTTCTG AGACTGTATC
7451 TTTGATATTC TTGGAGTAGA CGAGAGTGTC GTGCTCCACC ATGTTGGGGA
7501 TCTAGATATC ACATCAATCC ACTTGCTTTG AAGACGTGGT TGGAACGTCT
7551 TCTTTTTCCA CGATGTTCCCT CGTGGGTGGG GGTCCATCTT TGGGACCACT
7601 GTCGGTAGAG GCATCTTGAA CGATAGCCTT TCCTTTATCG CAATGATGGC
7651 ATTTGTAGAA GCCATCTTCC TTTTCTACTG TCCTTTGAT GAAGTGACAG
7701 ATAGCTGGGC AATGGAATCC GAGGAGGTTT CCCGATATTA CCCTTTGTTG
7751 AAAAGTCTCA ATAGCCCTCT GGTCTTCTGA GACTGTATCT TTGATATTCT
7801 TGGAGTAGAC GAGAGTGTG TGCTCCACCA TGTTGGGGAT CTAGATATCA
7851 CATCAATCCA CTTGCTTTGA AGACGTGGTT GGAACGTCTT CTTTTTCCAC
7901 GATGTTCCCT GTGGGTGGGG GTCCATCTTT GGGACCACTG TCGGTAGAGG
7951 CATCTTGAAC GATAGCCTTT CCTTTATCGC AATGATGGCA TTTGTAGAAG
8001 CCATCTTCC TTTCTACTGT CCTTTGATG AAGTGACAGA TAGCTGGGCA
8051 ATGGAATCCG AGGAGGTTTC CCGATATTAC CCTTTGTTGA AAAGTCTCAA
8101 TAGCCCTCTG GTCTTCTGAG ACTGTATCTT TGATATTCTT GGAGTAGACG
8151 AGAGTGTCGT GCTCCACCAT GTTGGGGATC CTCTAGAGTC GAGAATTCAG
8201 TACATTA AAA ACGTCCGCAA TGTGTTATTA AGTTGTCTAA GCGTCAATTT
8251 GTTTACACCA CAATATATCC TGCCA

>pGA2717 vector T-DNA sequence (from RB to LB)

Border: [Border sequence](#)

Primers used for iPCR: [Primer sequence](#)

```

1  GTTTACCCGC CAATATATCC TGTCAAACAC GGATCCGAGG TACCAGGTAC
51  CAGGTGAGTT CCATTCTTAC TACCACGGTG CTATTTTTTTT TGCTATGTGG
101 CTAATTACAT GACTAACTTG GGGTGCTAAA TCTTACAGGT TATATGCAGG
151 TTATATGCAG GTCCCGGGTA GGTGAGTCCC TTATGTTACG TCCTGTAGAA
201 ACCCCAACCC GTGAAATCAA AAAACTCGAC GGCCTGTGGG CATTGAGTCT
251 GGATCGCGAA AACTGTGGAA TTGATCAGCG TTGGTGGGAA AGCGCGTTAC
301 AAGAAAGCCG GGCAATTGCT GTGCCAGGCA GTTTTAACGA TCAGTTCGCC
351 GATGCAGATA TTCGTAATTA TGCGGGCAAC GTCTGGTATC AGCGCGAAGT
401 CTTTATACCG AAAGGTTGGG CAGGCCAGCG TATCGTGCTG CGTTTCGATG
451 CGGTCACTCA TTACGGCAAA GTGTGGGTCA ATAATCAGGA AGTGATGGAG
501 CATCAGGGCG GCTATACGCC ATTTGAAGCC GATGTCACGC CGTATGTTAT
551 TGCCGGGAAA AGTGTACGTA TCACCGTTTG TGTGAACAAC GAACTGAACT
601 GGCAGACTAT CCCGCCGGGA ATGGTGATTA CCGACGAAAA CGGCAAGAAA
651 AAGCAGTCTT ACTTCCATGA TTTCTTTAAC TATGCCGGAA TCCATCGCAG
701 CGTAATGCTC TACACCACGC CGAACACCTG GGTGGACGAT ATCACCGTGG
751 TGACGCATGT CGCGCAAGAC TGTAACCACG CGTCTGTTGA CTGGCAGGTG
801 GTGGCCAATG GTGATGTCAG CGTTGAACTG CGTGATGCGG ATCAACAGGT
851 GGTTGCAACT GGACAAGGCA CTAGCGGGAC TTTGCAAGTG GTGAATCCGC
901 ACCTCTGGCA ACCGGGTGAA GGTTATCTCT ATGAACTGTG CGTCACAGCC
951 AAAAGCCAGA CAGAGTGTGA TATCTACCCG CTTGCGGTCG GCATCCGGTC
1001 AGTGGCAGTG AAGGGCCAAC AGTTCCTGAT TAACCACAAA CCGTTCTACT
1051 TTAAGTGGCTT TGGTCGTCAT GAAGATGCGG ACTTACGTGG CAAAGGATTC
1101 GATAACGTGC TGATGGTGCA CGACCACGCA TTAATGGACT GGATTGGGGC
1151 CAACTCCTAC CGTACCTCGC ATTACCCTTA CGCTGAAGAG ATGCTCGACT
1201 GGGCAGATGA ACATGGCATC GTGGTGATTG ATGAAACTGC TGCTGTCCGC
1251 TTAAACCTCT CTTTAGGCAT TGGTTTCGAA GCGGGCAACA AGCCGAAAGA
1301 ACTGTACAGC GAAGAGGCAG TCAACGGGGA AACTCAGCAA GCGCACTTAC
1351 AGGCGATTAA AGAGCTGATA GCGCGTGACA AAAACCACCC AAGCGTGGTG
1401 ATGTGGAGTA TTGCCAACGA ACCGGATAAC CGTCCGCAAG TGCACGGGAA
1451 TATTTGCGCA CTGGCGGAAG CAACCGGTAA ACTCGACCCG ACGCGTCCGA
1501 TCACCTGCGT CAATGTAATG TTCTGCGACG CTCACACCGA TACCATCAGC
1551 GATCTCTTTG ATGTGCTGTG CCTGAACCGT TATTACGGAT GGTATGTCCA
1601 AAGCGGCGAT TTGGAAACGG CAGAGAAGGT ACTGGAAAAA GAACTTCTGG
1651 CCTGGCAGGA GAAACTGCAT CAGCCGATTA TCATCACCGA ATACGGCGTG
1701 GATACGTTAG CCGGGCTGCA CTCAATGTAC ACCGACATGT GGAGTGAAGA
1751 GTATCAGTGT GCATGGCTGG ATATGTATCA CCGCGTCTTT GATCGCGTCA
1801 GCGCCGTCGT CGGTGAACAG GTATGGAATT TCGCCGATTT TGCGACCTCG
1851 CAAGGCATAT TGCGCGTTGG CGGTAACAAG AAAGGGATCT TCACTCGCGA

```

1901 CCGCAAACCG AAGTCGGCGG CTTTTCTGCT GCAAAAACGC TGGACTGGCA
1951 TGAACTTCGG TGAAAAACCG CAGCAGGGAG GCAAACAATG AATCAACAAC
2001 TCTCCTGGCG CACCATCGTC GGCTACAGCC TCGGGAATTG CTACCGAGCT
2051 CGAATTTCCC CGATCGTTCA AACATTTGGC AATAAAGTTT CTTAAGATTG
2101 AATCCTGTTG CCGGTCTTGC GATGATTATC ATATAATTTT TGTTGAATTA
2151 CGTTAAGCAT GTAATAATTA ACATGTAATG CATGACGTTA TTTATGAGAT
2201 GGGTTTTTAT GATTAGAGTC CCGCAATTAT ACATTTAATA CGCGATAGAA
2251 AACAAAATAT AGCGCGCAA CTAGGATAAA TTATCGCGCG CGGTGTTCATC
2301 TATGTTACTA GATCGGGAAT TAATTCATCG ATAGGCTAGT CATGGTGACT
2351 GTACGTTGTA AGTGCAGCAA ACTGCCGACG CGATGCAAAC TGTACACGTT
2401 AACATGCCAC TCACCTGGAA CGCACAATGG CCACTAGGTG CGGCCGTAGT
2451 GTGGATTTCA AAGAGAGAGA GAGAGAGAGA GAGCTAATCA CGTAAACGTA
2501 AACACAGCAG ATAGCAGAGA TGTTGATTAG GCAAAACAGT ATAAAAGCCA
2551 ATCCAATAAA CTACATTTAG CGAAGTGCTA TACTAATGCA CTAATAACGA
2601 ACTGTTCTTT TCTTAAGATC GGAGCCAGTA ATGGGTTGTC AGCAGGAGAA
2651 GCACGTAAAC CTTGAAACAT ACTAAGTTCC ACAGTCGAGA GTAAACCGTA
2701 ATCAACACAA GAAACAAACA TAAAATTGAA CAAACGCGCA TATTATAAGT
2751 GACGAAGCGG TCTCACATAA AACAGGGCAC ACAGGTTACA ACAACGAGGG
2801 TTGTAAGCCC ATTAAGCCCC AAACATCAGA TCACCACAAG CAAATGTCTC
2851 GAAGACACAC GCACACGGCA ACAGGATAAC TCCACACTGG CAGATCATGG
2901 GATAGCAGCA GTTATCAATC AGGCCTTGAC ACACAGAACA TCAAGCCCCC
2951 AGACGACGAC GACTCCTCTA GATCCCGGTC GGCATCTACT CTATTCCTTT
3001 GCCCTCGGAC GAGTGCTGGG GCGTCGGTTT CCACTATCGG CGAGTACTTC
3051 TACACAGCCA TCGGTCCAGA CGGCCGCGCT TCTGCGGGCG ATTTGTGTAC
3101 GCCCGACAGT CCCGGCTCCG GATCGGACGA TTGCGTCGCA TCGACCCTGC
3151 GCCCAAGCTG CATCATCGAA ATTGCCGTCA ACCAAGCTCT GATAGAGTTG
3201 GTCAAGACCA ATGCGGAGCA TATACGCCC GAGCCGCGGC GATCCTGCAA
3251 GCTCCGGATG CCTCCGCTCG AAGTAGCGCG TCTGCTGCTC CATAACAAGC
3301 AACCACGGCC TCCAGAAGAA GATGTTGGCG ACCTCGTATT GGGAAATCCCC
3351 GAACATCGCC TCGCTCCAGT CAATGACCGC TGTTATGCGG CCATTGTCCG
3401 TCAGGACATT GTTGGAGCCG AAATCCGCGT GCACGAGGTG CCGGACTTCG
3451 GGGCAGTCCT CGGCCCAAAG CATCAGCTCA TCGAGAGCCT GCGCGACGGA
3501 CGCACTGACG GTGTCGTCCA TCACAGTTTG CCAGTGATAC ACATGGGGAT
3551 CAGCAATCGC GCATATGAAA TCACGCCATG TAGTGTATTG ACCGATTCTT
3601 TGCGGTCCGA ATGGGCCGAA CCCGCTCGTC TGGCTAAGAT CGGCCGACG
3651 GATCGCATCC ATGGCCTCCG CGACCGGCTG CAGAACAGCG GGCAGTTCGG
3701 TTTCAGGCAG GTCTTGCAAC GTGACACCCT GTGCACGGCG GGAGATGCAA
3751 TAGGTCAGGC TCTCGCTGAA TTCCCAATG TCAAGCACTT CCGGAATCGG
3801 GAGCGCGGCC GATGCAAAGT GCCGATAAAC ATAACGATCT TTGTAGAAAC
3851 CATCGGCGCA GCTATTTACC CGCAGGACAT ATCCACGCCC TCCTACATCG
3901 AAGCTGAAAG CACGAGATTC TTCGCCCTCC GAGAGCTGCA TCAGGTCCGA

3951 GACGCTGTCTG AACTTTTTTCGA TCAGAAACTT CTCGACAGAC GTCGCGGTGA
4001 GTTCAGGCTT TTTTCATATCT CATTGCCCCC CGGGATCCGT CGAGTCAGCC
4051 TGAAAGGACA AAATACATGT TAGCGCCTTA GTGGTACATT ATTATTTTCAG
4101 TACAGCAAGA TAACACAATT CAAAAGACTG ACCCATAATA AATAACTAGT
4151 CCTCAATTTA AAATTTGAGT TCCTAAATAG ACATCTATGA ATATGCTGTA
4201 CATCGGCACT ACAGAAAATA CGATTCCCAA TAATTGAACA ATTGTACTTT
4251 ATTTAGTTGT TACTACAACA ATGGAAGATA CAAGATCGTT TCAAAACTAC
4301 CATACTGCA TGGAGTATTT GTTCCACAGA TCTGGAAAAA ACAGATCTGA
4351 CGGGCAGTGT CACCAAACAC TAGACATATG TATTTGTATT AGGTGGATGA
4401 CGTGTACAAA CATGACTACC AGATCTAGAA TTAGAACGCG GCGTGCTTTG
4451 GAAATGTTAA GTAGATCCAA ATACATCGGT AACAAATGAA CATATTCATA
4501 TGACATAGCT GTAAAACATC ATGATCTATC ATATCAACTA GAGGGGATCT
4551 CGGCATGTAT CATTCTATTG CATCTAGAAC CATAGCATTT CCATGTGACA
4601 AACAAATTTG AAACATACAT TGCTCAGATC TACCATAAGA ACACCATGTT
4651 CATGACAGCA TCGACCATGA TTTCCACATT TAACAGCATC CCGAGGTCAG
4701 ATCCAGTGTT TAGAACTATC ATTTTCAGCAA AATTCACAAA ATAAATCCTC
4751 CAATTCGCCT ACATATATCC ATTCCACGCA TCCTAGGACC AGATCCACCA
4801 TACCAGTATA CACGAACACT AAACATTTCA TCAGATCCGC TAACTACGAC
4851 AGAGAAAACG CAGATCCAGA CAACCAGATC CACCGACAAA TAAACACAGC
4901 CCCCCACATC CAACAACCGC GAATCCACCC AGATCTGACC CAGAAGCAGG
4951 CACGAAGAAC ACGGGGGGTG AGGGAGATGG GACGCGGATC CAAGCTTTGGC
5001 GCGGATTGG GTTGATGCTG CGACGGCGGC GGAGAAGGGA GAGAGGGGAG
5051 AGGAGGAAAA GCGCGGAGGC GCGGAGAGAG GCGAGTACGA AGACGCCTTT
5101 CTCTGCGTTG TCTCGGCTTA GGGTTTGCGA TCCCCGCACT CCGCCGTTT
5151 TATAGGGCCA GACAGCCTGG ACCTCTCAGG AGCGGAAGCG AAGGGATGGG
5201 GGAGTTTTTC GTTTTACCCC CTTTGACGTC TTCAAAATTC ACTCGCATCT
5251 CACATCGTGC CTGCAAAGGT CGGGTGGTTG GATCATATCG AGAATATTTA
5301 ATAAGTTAGG GAGCTTTCTG ATAATATCCA CCGCAAGGAG GCCATTTCTG
5351 TTGCACTCGG TTGAAGTCCA TACCCGCTC TCGTTAGTTT CACTGACAGG
5401 TGGGTCCAGA GGCTTCCTTC GTGTGCGGTT AGCGAGTGCA CGCGTCGCTC
5451 CAAGAAAAAG CAGTAGGTGA CCTGGCCACC TCGTTGTAGG TGCGACCGAT
5501 GCAGACGTCC CGCTTGCCGG TGGGCCACG TTACAGCTGG GTCCACATA
5551 TCGGTGGGTG CGATGAGTTG TTCGGTGCCT AGGAGTAGAT TGGATCCCAA
5601 CGGGTGGTTG CGTCGTCGGC GGCCCTGCCG ATTTTATTTT CGATTTTTGA
5651 AATGCGAGAG CGGGAGAACG GCACCGTTGG CTTGGCTGTG GATGCCGTTA
5701 GCCGCACCGG ACTATTCGGC CCAGTTCCAT TTTGGCCCAA CTGAAACAG
5751 CGCGGAGCAC AAGACGGGGG AGCCCATTTA GGCCCGTAAT CTCAGCCCTG
5801 TAGAAAGTCC GTGTGCTTGC GATGGACCAG AAAGCCATA AACCTTGAG
5851 GCGTTCTCTG CTGGGAATAA AATAAGTTCA CACTCTGTCC CTCAACTTTA
5901 CGTCGAGTTT GTTTGACATC GCTAATGCC AGTACCAGAA ATCTTGATA
5951 CAAATAAGGT TTGATATAAA GTGGCACGTG GTGAATGGCA TCGTTTGAAA

6001 AATCTTCAGA TCGAGCGGGC TTCACAAGCC GTAAGTGCAA GTGCCAAAAT
6051 TTGTGAAGAA AATTACTTCC TTCATTTTAC AATGTAAGTT ATTTTAGCAT
6101 TTTCCACATT CATATTGATA TCAATAAATT TAGATAGATA TATATGTCTG
6151 AATTCGTACC GTTAACGAGC TCTAGAAGCT TCAGTACTAC GCGTCTCGAG
6201 GAGCTCCACC GCGGTGGCGG CCGCTCTAGA ACTAGTGGAT CCCCCGGGCT
6251 GCAGGAATTC CTCATGTTTG ACAGCTTATC ATCGGATCTA GTAACATAGA
6301 TGACACCGCG CGCGATAATT TATCCTAGTT TGC GCGCTAT ATTTTGT TTT
6351 CTATCGCGTA TTAAATGTAT AATTGCGGGA CTCTAATCAT AAAAACCCAT
6401 CTCATAAATA ACGTCATGCA TTACATGTTA ATTATTACAT GCTTAACGTA
6451 ATTCAACAGA AATTATATGA TAATCATCGC AAGAACCGGC AACAGGGATT
6501 TCAATCCTTA AGAAAAC TTT TATTGGCCAA ATGTTTTGAA CGAATCTGCA
6551 GCCCCGGGCGG CCGCTTTACT TGTACAGCTC GTCCATGCCG TGAGTGATCC
6601 CGGCGGCGGT CACGAACTCC AGCAGGACCA TGTGATCGCG CTTCTCGTTG
6651 GGGTCTTTGC TCAGGGCGGA CTGGGTGCTC AGGTAGTGGT TGTCGGGCAG
6701 CAGCACGGGG CCGTCGCCGA TGGGGGTGTT CTGCTGGTAG TGGTCGGCGA
6751 GCTGCACGCT GCCGTCCTCG ATGTTGTGGC GGATCTTGAA GTTCACCTTG
6801 ATGCCGTTCT TCTGCTTGTC GGCCATGATA TAGACGTTGT GGCTGTTGTA
6851 GTTGTACTCC AGCTTGTGCC CCAGGATGTT GCCGTCCTCC TTGAAGTCGA
6901 TGCCCTTCAG CTCGATGCGG TTCACCAGGG TGTCGCCCTC GAACTTCACC
6951 TCGGCGCGGG TCTTGTAGTT GCCGTCGTCC TTGGAGAAGA TGGTGCGCTC
7001 CTGGACGTAG CCTTCGGGCA TGGCGGACTT GAAGAAGTCG TGCTGCTTCA
7051 TGTGGTCGGG GTAGCGGCTG AAGCACTGCA CGCCGTAGGT GAAGGTGGTC
7101 ACGAGGGTGG GCCAGGGCAC GGGCAGCTTG CCGGTGGTGC AGATGAACTT
7151 CAGGGTCAGC TTGCCGTAGG TGGCATCGCC CTCGCCCTCG CCGGACACGC
7201 TGAAC TTGTG GCCGTTACG CCGCCGTCCA GCTCGACCGG GATGGGCACC
7251 ACCCCGGTGA ACAGCTCCTC GCCCTTGCTC ACCATGGATC AAGCTTATCG
7301 ATGAATTCGA GCTCGGTACC ACCTGCATAT AACCTGCATA TAACCTGCGA
7351 CATTAGCAAT AAACAAGTTG GTTAGAGAAC AGCACAAACA AGAAATGGCA
7401 GTGAATTAAC ATAGCAGAGA ATTTGAGATC ATTGCAAGGA TACAAGTCTG
7451 TACCTTG TAC CTTGTACCTC GTCGAGAATT CAGTACATTA AAAACGTCCG
7501 CAATGTGTTA TTAAGTTGTC TAAGCGTCAA TTT**GTTTACA CCACAATATA**
7551 **TCCTGCCA**

>PFG_3A-07110.R A17813 Vector: 2715 Variety: Dongjin

Vector sequence (T-DNA right border)

Partial sequence of Cultivar *Dongjin* genome

**AAGNNGACTACCGGGACTGCATATAACCTGCATATAACCTGTAAGATTTAGCACCCCAAGTNAGTCA
TGTAATTAGCCACATAGCAAAAAAATAGCACCGTGGTAGTAAGAATGGAACCTCACCTGGTACCTGGT
ACCTCGGATCCGTGTTTCAGNTCGTTGACTGCCTCTTCGCTGAAACTTCATTGATACTCGATAACATCGA
CAATTGTGAGATCTGATACATGGGTATTACCATTGGCATCATGCTTGATACTGTACTTTGAAGCGCCA
CCATCTTGAACAGTTGTGCGATTAGTGGCTAGCAGATCACGTATGGCTTCATTGTAGATTTCCAGCAT
AGATGCCTAGATGTTCAATGTAAACATGACAGTTACAACATAGAAAGCCTGCACCTTTGTTAGCTCA
AACAACTGACCAATTGAAGTGGGTAAGAACTCACCTGCATCTTATATTTCCATCCCTGTGAAATAAG
AGCCTGGCTTGTGGAAAATTTGTTCAAGTGATCTCGGAATTAATCCTTTCTGGTCATGCAATTCTG
GATTTCCCATCATTTGTGTATGTTTTACCCGAGCCAGTTTGGCCATATGCAAATATGCACACCTGAGTT
GTTTTACATTAGTTAGCACGAATTATAAATACTAACTTTTTATGGACAACTTTTTTCCCTCTCCTAT
AGCGAGGTTGTGCTCTTGCACTTCTCAAAACACAGCAACAAGTAAATGTTACCTTGTAGCCATCANGG
GCGCTTTGGATGAGTGGGAAATCTCAATGAACACTCTTCTGGNGAGCCGACTGCTCAATACTTTGCNA
ATGGAAAGANACATTNGACCTGNGAGAAAATGAGATTACTGGATGNAATCTCCAGGNGCGACTGANG
TAAANNANAGTCNGTAGTNTTCATNGGCACCAGCNGCTAGTTCCTTGA...**

>PFG_1B-09105.L C05283 Vector: 2717 Variaty: *Dongjin*

Vector sequence (T-DNA left border)

Partial sequence of Cultivar *Dongjin* genome

**CGCANGTGNCTCNTTTGCCTATCTCCGGTGGCACCGCTCTTTGTTAAGCCGCTCACTGCCGGCAANAT
CGATTAGATTGAGCACTCCTTGCACCTGCTGGTCTGTTCCCTGTAGAGAAAACAATCCAAATGATGAA
TACAAAAAATTACCAGGCATTAGCAAGACCTACATTAGAAGATATCGCATACCTCATTGACACCAAAA
ATTCTGAAGCGTGAACACACAATGACTTCTAGATGATTCCTCGTTTCATCTGTGTTCTTCCAACAGATCT
GCAGCCGGGCGGCCGCTTTACTTGTACAGCTCGTCCATGCCGTGAGTGATCCCGGCGGCGGTACAGAA
CTCCAGCAGGACCATGTGATCAGCTTCTNNGTTGGGTCTTTGCTCAGGGCGGGACTGGGGTNCCTAG
GTTGNGGTTTTTCGGNNAATGGCAGGGGAATTNAACAAANNCNAAAATTTTTNTTTTCTTTTGCNGGG
AAAGNAANNNTGGTTCNTNNAAGGGGNGGGGNNNNNGGGAANTNCATTTNNNTTNAAAAANNNC
CCNCNAGGNNNTTCTTTTGGNANNANCCNNGGGGGGGNNNNCTTTTTTTTAAANCCCCCCCCCCC
CCCNNAANAAAAAANNNNGNGNCCCCCNCCCCCGGGGTNTTTNTTTTGNNGNAAAAA
ANTTTTTGNNGGNNAAAAAATNNTNCNNNTTTNGGGGGGCNCNNTTAAANANNNTNNTTTTTTTTTTT
NNAAAAAATTTGGNNGGNNCCAAAAANTTTNGGGNNTNNGTGNCCNNNNNTNNNNAANAAGAGGG
GGGGGNTTTTTTTTCCNCNNNNGNGNNAANNGGGGNNAAANTANNNNNNNNNANNATNNNGGN
NTTNNNNNGNNTNNTTTTTTNNNNANANAAAAAAGGNNNGNNGGGGNGNG**

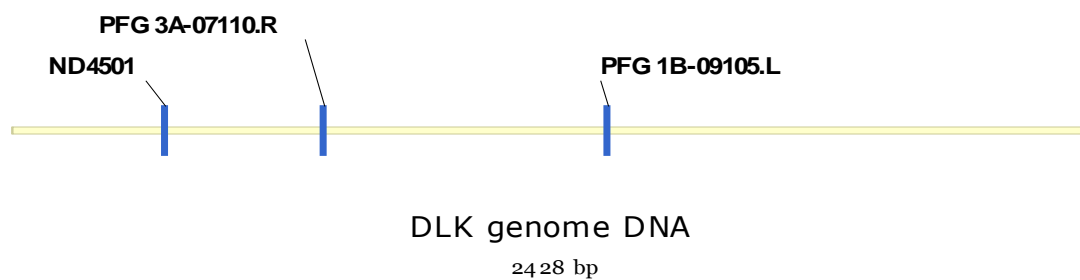
>ND4501_0_508_1A

Sequence of Tos 17 fragment

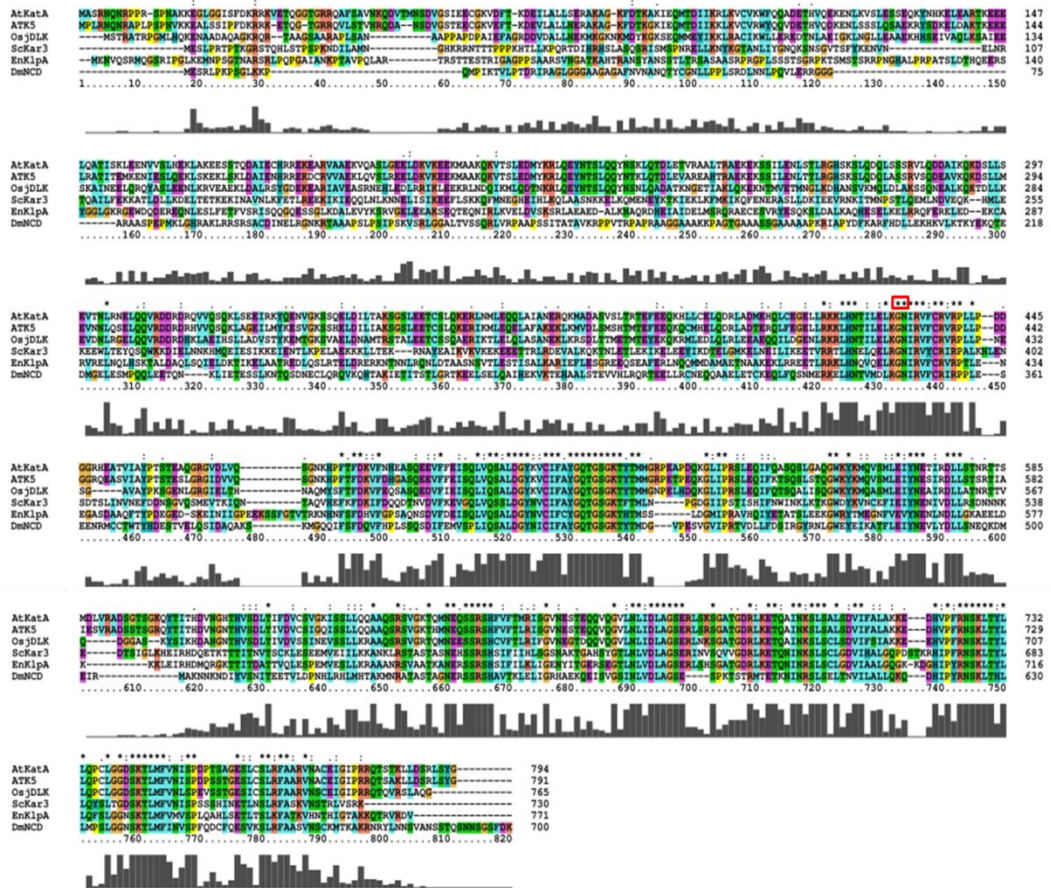
GACGACACCTCTGGAGACAGATTCACAAACATAAGTGTCTTCGAGTCTCCTCCAAGGCATGGCTGTG
 TCCAAGGGGAACAAAATCATTACACATTATAGCCACGGAAACTAGAACAAGTTTGCAGATATTCTT
 AGCTGAGTGCTTAGAATTTACCTGTAGCAAGTACGTTAATTTTGGAGTTCTCTGAACGGAACGTGCTCC
 TCTTTCTTTGCAATGGAGAAGATTACATCGCTCAAGCATGAGAGGCTCTTATTAATAGCCTAAATAG
 CAAATTTATATCATAACATTAGACTTCGACA

Supplementary Figure 1 Information about the sequence of OsDLK genomic DNA and insertion fragments. T-DNA fragments were inserted into *Oryza sativa* ssp. *japonica* cv. *Dongjin*, while Tos-17 was inserted into *Oryza sativa* ssp. *japonica* cv. *Nipponbare*.

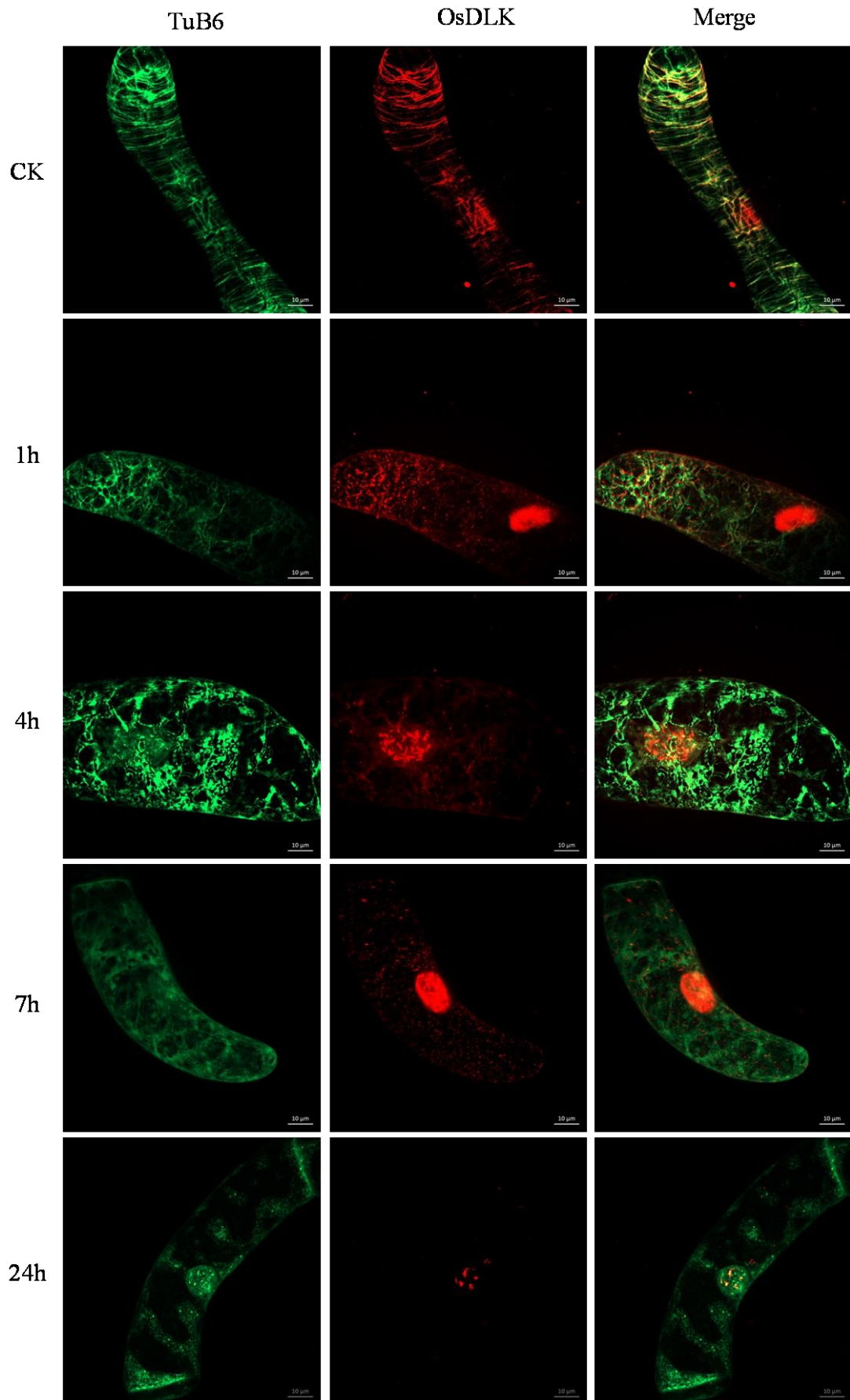
Gene	Clone	Chr	Locn	Hit	Position	Type
Os07g01490	ND4501_0_508_1A	7	C/306384-308576	Exon	306490-306775	RTIM Tos17
Os07g01490	PFG_1B-09105.L	7	C/306384-308576	Exon	306859-307118	PFG T-DNA
Os07g01490	PFG_3A-07110.R	7	C/306384-308576	Exon	307487-308119	PFG T-DNA



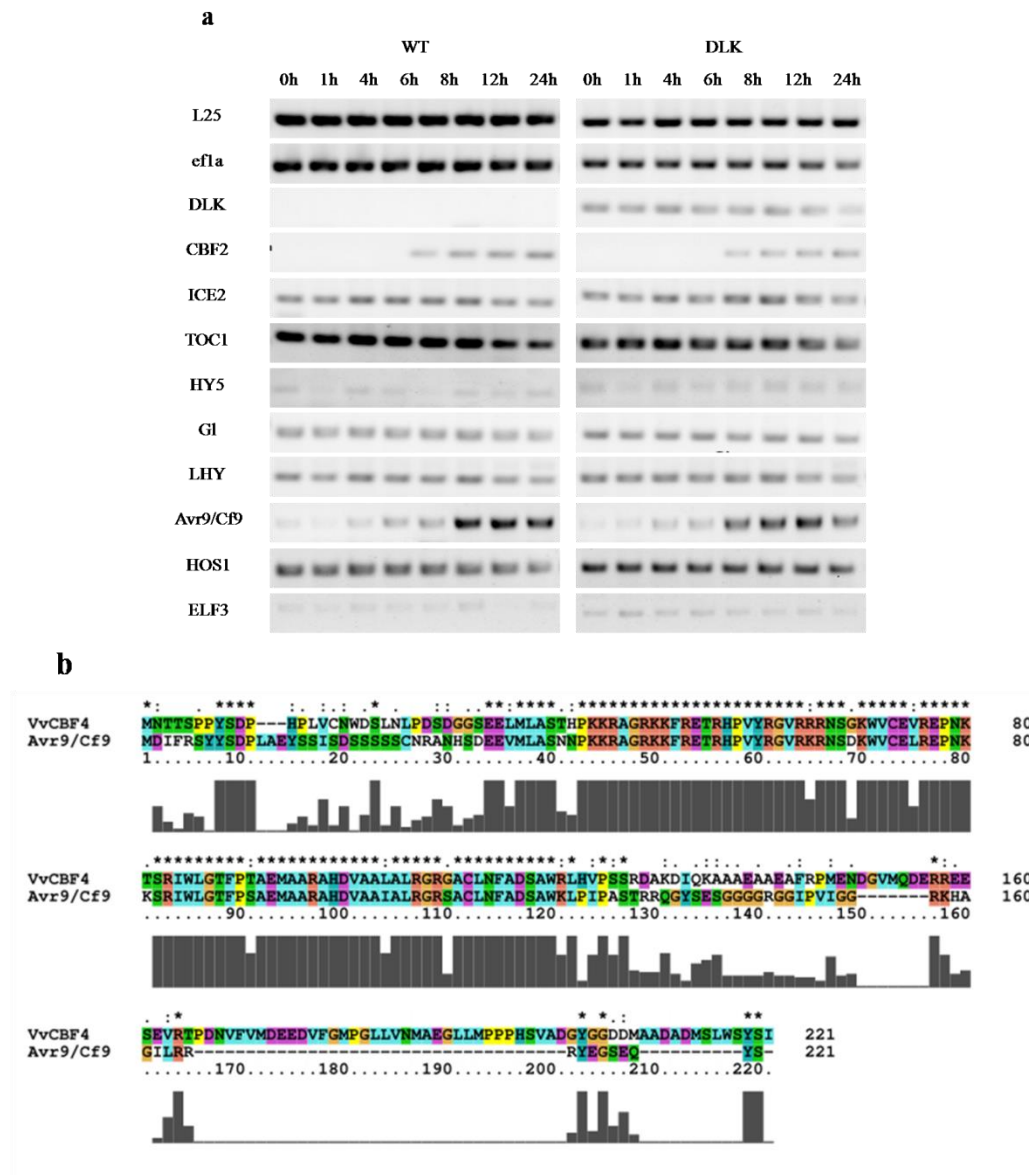
Supplementary Figure 2 Overview of the insertion position for the rice mutants.



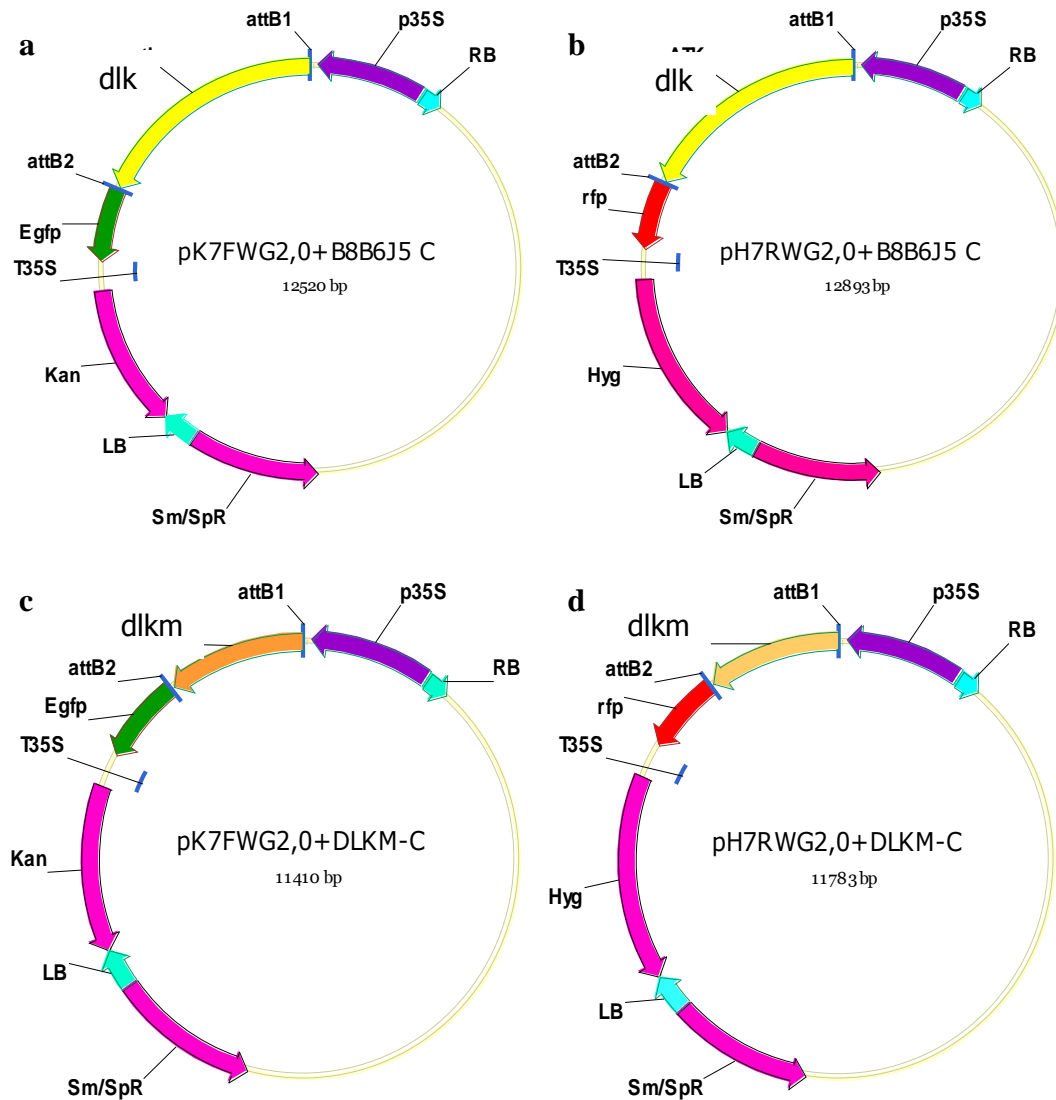
Supplementary Figure 3 Alignment of OsDLK and other members of kinesin AtKatA, ATK5, DmNCD, ScKar3, EnKlpA. An amino-acid sequence alignment of the putative neck linker region of OsDLK and related kinesins shows that the 14-aa stretch (marked by rectangle) associated with minus-end directionality in the kinesin-14 family is partially conserved. Small rectangle indicates the two amino acids known to be mostly connected with kinesin minus-end directed movement.



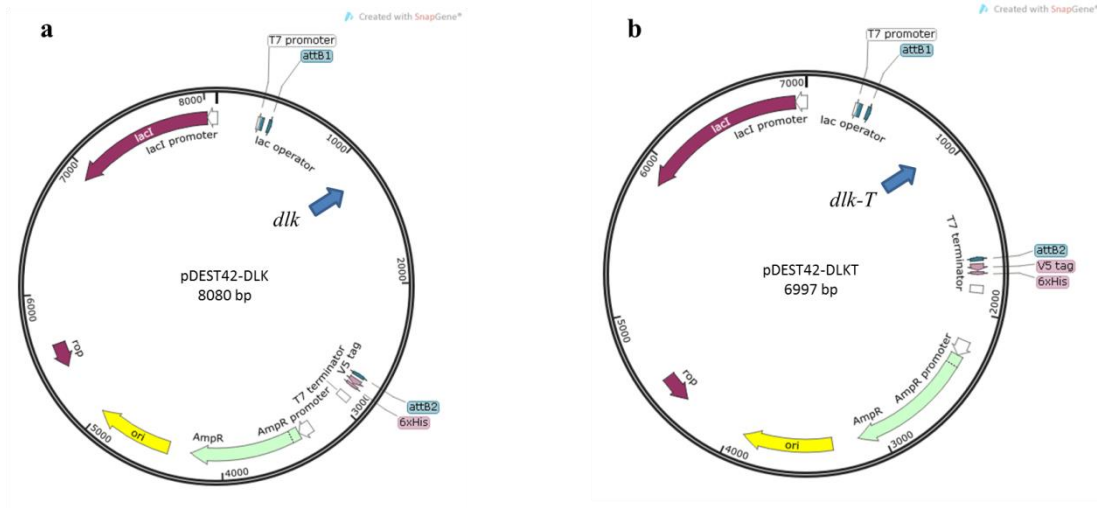
Supplementary Figure 4 Tobacco BY-2 cells co-transformed with OsDLK-RFP and TuB6-GFP in response to cold stress. OsDLK-GFP accumulated progressively inside the nuclei with increasing time of cold treatment. Confocal sections collected from the cortical and nuclear planes are shown either for the GFP signal alone or merged with the differential interference contrast image to show the topology. CK represent cells cultivated at 25 °C serving as negative control.



Supplementary Figure 5 (a) Representative gel electrophoresis results of semi-qPCR for gene expression of candidates from cold responsible genes. (b) Alignment information of cold response gene CBF4 (C-repeat-binding factor 4) from vitis and Avr9/Cf9 (rapidly elicited genes from tobacco).



Supplementary Figure 6 Constructs for fluorescent protein fusions. (a,c) The maps show the fusion of GFP (green arrows) with full length of *dlk* (yellow arrows) and *dlkm* (orange arrows) combined with recombinations sites attBs for Gateway cloning in the binary Gateway plasmid pK7FWG2.0 under control of the 35S-CaMV promoter p35S (purple arrows). The blue arrows show LB/RB representing the left and right boarder for Agrobacterium-mediated transformation. Kanamycin (Kan) and Spectinomycin (Sm/SpR) represent antibiotic selection markers (pink arrows). b, d The maps show the fusion of RFP (red arrows) with full length of *dlk* (yellow arrows) and *dlkm* (orange arrows).



Supplementary Figure 7 His-tag labelled DLK and DLKT were isolated from *E. coli*. (a) Map of recombinant vector of pDEST42-DLK and (b) pDEST42-DLKT.

>NM_001325817.1 *Nicotiana tabacum* dehydration-responsive element-binding protein 1D-like (LOC107808010), mRNA >AF211531.1 *Nicotiana tabacum* Avr9/Cf-9 rapidly elicited protein 111B (ACRE111B) mRNA, complete cds

Atggatatctttagaagctattatttcggaccacttgctgaatattcatcaatttctgacagtagtagc
 agctcctgtaatagagctaaccattctgatgaggaagtgatgtagcttcgaataaccccaagaagcga
 gcagggagaaaagaagtttagagaaaactcgacaccagatatacaggggagtgaggaagaggaattcagac
 aagtgggtttgtgaactcagagaaccaaaacaagaaatcaagaatatggctgggcactttcccttctgca
 gaaatggcggctagagctcatgacgtggcggctattgcattaaggggcccgttctgcttgcttgaaacttt
 gctgactctgcttgggaagttgcctattccagcttcaaccgacgccaaggatattcagaaaagcggcggc
 ggaggccgaggagcattccggtcacgaggccgaaaacatgccggaataactcaggagaagatacgaa
 ggaagtgaacagtactcctgaaaatatgttttatatggatgaggaggcgtattcttcatgcctggatt
 actagtgaatatggcagaaggactaatgttacctccacctcagtggtcacaaattggagatcatatgga
 agctgatgttgacatgcctttgtggagttattctatctaa

>Sequence of the predicted promoter for Avr9/Cf9

Tattcttgggtcagtgattgaaaagtgtattggatggtgtttcagtttgaggttttttcttctggtc
 aatgtgaaaaagtggctactctctctctatatatatagtggaagtaagattatgataagcgaagagcat
 tgaagctaaaaaggtttgatgacgcgaaatataacacacacggagttgaaggggtgataaggagacaggc
 tggatTTTTGAAAAGGGTATTAaaaattgtcctaattaattagtgacagctggcagctgttttatgggaca
 actggaattctagttagtctaattgtgtgtataactcgcgtggattctgcggatgcggcaacttggtact
 ctttctacttttctacttttctacttttctgctctctttcttcttctccttctcctttttggaatatactcctat
 ctatctagagtactgggactacactttggctacgactgaccaatctttgtcatcatttgaaacaatta
 aaataagtatatttaattcatgttgcacatctattttgtaccaccaatttaatttactagtgaatctttgg

ggaaccaccaatattgcccggtagctgtcaaaggtcagcaaccatatatggctactgaatacaactaatct
tcttgctaattaggctacgtaagcatttccgaaggctaatactgtaaataatacttattcttagtgaatc
catttggtagaatctttttcaataatttttatgccaaacttgatcttttagaggatatatactactaatg
cgtattagttaattattgtgtcaattctgattaggctgcttacttttctccctgtatatatgactcatt
ttttatgggagagtgtgtttcttttaaaaaaaaaatatacttcttttagcaaattttcacttttaaagttggt
ttccattccaaaaataattagtgctatcatacaaatgaatattttatcgaagactacttagcaatagtc
taatagatgaaaaaggatgtgtatcatttatgtgacgttattccaatttggagtgtcaaacaagttggt
gtaattttttatatatttttgaaatatttttaataattagttattgtgacttatattacttttttaagtt
atttttaattcgcataatcctatgttcaattagataagaagttttaatctcaaaaagtgaaaagcgtca
taaattatagtagtaatttataggcgatattttttctagcaaattattcagagaagaatggggaaagc
taaagaatgagttgcctttcgagtttctcttgaagaccaagtgcaaactctgtttttgaagggataagt
tagaaaaatgacctttcaacaattgaaagccacttatgtctaactgatactacactcacttgtatcta
acacacacggttttgacagtttaatacccatatccaactgcccgccctttgcaagaaatcaaagaaagct
tttcagttcaccacggtaacgtgtggaccacgtggcacatttccagggtccaggattttcttctggtaga
ttagctaggataggtagactagagcactaacctagaaaactgagtacatagacttttttttaaaaaaaaa
aaagaaaaacttaatttttttactctatcagtttttgaaaaagggaatctgaaagaaaattatctagt
tccaataattggtttgggctgttacgataaatatcatattatgggtggatgtctactcttcttccatgat
cttcatctcaaatgttttaataacatattttgtatgttcaatgacatatttcatgacatattttcttcac
ttttatgtctatataaatgctttgtaatagatagaaaaatacacacaattgaagaagcaaatctcttc
tttctctctatcctattttcttgttcatgttttatttaattgcttttatttcttgttcatgttttactaa
attggttttatttcataacacgttatcagcacgagtctctaaccaattgtatgtacatctacaaaaaat
ttcctacaaccgaaaagattgcaattagcagacatacatatcatctcatgggttagatgtaaagagaaac
tacataggtgaagtaataagaatataagaaggatgattatcttatatttgtcatttctctaattgtctcg
tatgcacacaacttcataccatacctgtattgcataagcacataactaatattacatctttcatatcaca
tgaatggaataaaaattttcgaaattttatatgtgaaaatcatagtagcagtttaattggtgatagaggc
atgtcatggttaaccaaggatattgtatgtaagttgtcttattcatatttgtgtgttaactatcttaaat
atgtcctaccgcttttaataattttcttttacttggatgaatatttttcttttggatttttgcacttg
cttatagtaaaaaaaaggagaataaaaattaaaaaatgtcatactgattagaagcataaatcatcttg
aagaaaataagaataacttcacatctttatctagggttgattaacttcttttgaaatttggaaaacaa
atcagctactgagaaagtatacttcataatttatgggtgtatcatttgaaaacaaacagtgattagtat
gactactagaagaggtatttttgagtatccatgatctacttggatgcttgttaccgacttaccattttca
agtattttatatgaatgatgcataaactacaactggtaagttgttacctataatgtcacttttcaggta
atataaatgctgaatttatgtatttagtactatatagatgttgttacctatataatgtacttttgataaa
tttattcactaattgcttgggtgaattgagtgaggaaagtcagggcgttaaatcaaatccaataggta
gggtataccccaataataataatatttttttagagaggctcaataaatattatgacaatgattttatgat
ccatttaactctaatagaattttagaagaatattttgactacaaatgggttgtatttcatatagatgct
acaataattgataaagctttacgctt

Supplementary Figure 8 Nucleotide sequences for *Avr9/Cf9* gene and its predicted promoter.

	1955	1960	1970	1980	1990	2000	2010	2020	
50s rc	1			AACTGCATG	CGGATCGACA				
r. avr9cf9	1955	TTATCAGCACGAGTCTCTAACCANTTGTATGTACATCTACAAAAAATTCCTACAACCGAAAAGATTGCAAT							
onsensus	1955	AA TG ATG ATC AC A							
	2838	2840	2850	2860	2870	2880	2890	2900	
50s	1			TG GTC	GA TCCG	CATG	CA GTT		
r. avr9cf9	2838	CTAATTGCTTGGTTGAATTGAGTAAAGGAAAGT CATGGC GTTAAATCAAATCCCAATAGGTAGGGTATACCCCAA							
onsensus	2838	TG GA CATG GTT							
	1206	1210	1220	1230	1240	1250	1260	1270	
182s rc	1			GAATGGGG	TAGG	ACGC	AGAC		
r. avr9cf9	1206	TTTTCTAGCAAATTATTTCGAGAA GAATGGGG A G AGA							
onsensus	1206	GAATGGGG A G AGA							
	2115	2120	2130	2140	2150	2160	2170	2180	
102s	1			GTTCGG	GTC	TAC	CC	CA	
r. avr9cf9	2115	TATTTGTCATTTCTCTAATGTCTGTATGACAAACTTCATATACATACCTGTATTGCATAAGCACATACTAATA							
onsensus	2115	GT TGC C AC CAT C							
	1237	1240	1250	1260	1270	1280	1290	1300	
272s rc	1			TTCCA	AACCAAG	CCCG	GAAC		
r. avr9cf9	1237	GAAAGCTAAAGAATGAGTTGCCTTTCGAGTTTCCTCTTGAAGACCAAGTGCAAATCTGTTTTTGAAGGGATAAGTTA							
onsensus	1237	TT A ACCAAG C A C							
	1237	1240	1250	1260	1270	1280	1290	1300	
272s rc	1			TTCCA	AACCAAG	CCCG	GAAC		
r. avr9cf9	1237	GAAAGCTAAAGAATGAGTTGCCTTTCGAGTTTCCTCTTGAAGACCAAGTGCAAATCTGTTTTTGAAGGGATAAGTTA							
onsensus	1237	TT A ACCAAG C A C							
	594	594	594	594	594	594	594	594	
272s	1			GTTCGGGG	CTGG	TTT	GTG	AA	
r. avr9cf9	594	ATATATGGCTACTGAATACAACATAATCTCTTGTCTAATTAAGCTACTTACGATTTCCGAAGGCTAATACTGTAAAT							
onsensus	594	TT TGG T G A							
	2094	2100	2110	2120	2130	2140	2150	2160	
294s rc	1			CGATG	AATG	CAC	GG	CAG	
r. avr9cf9	2094	TAAGAAGGTATGATTATCTTATATTTGTCAATTTCTCTAATGATGCTATGCACTTACACCAACTTCATACCATACCTGTATTGCA							
onsensus	2094	ATG C G A GC CAC							
	2240	2240	2250	2260	2270	2280	2290	2300	
294s	1			CGTGC	CGGTGC	ATG	TCAT	CG	
r. avr9cf9	2240	GTGAAAATCATAGTAGCAGTTAATTGTTGATAGGCATGTCATGTTAACCAAGGATATGTTATGTAAGTTGCTTTATTC							
onsensus	2240	T G G GCATGTCAT G							
	1374	1380	1390	1400	1410	1420	1430	1440	
299s	1			CTAGGT	ATCGG	TAGGC	BCC	G	
r. avr9cf9	1374	GTATCTAACACACACGGTTTTGACAGTTAATCCCTATCCACTTCCCGCCCTTTGCAAGAAATCAAAGAAAGCTTT							
onsensus	1374	TA AT A GCC							
	1368	1370	1380	1390	1400	1410	1420	1430	
299s rc	1			CGCGCC	TACG	GATAC	CTAG		
r. avr9cf9	1368	TCACTTGTATCTAACACACACGGTTTTGACAGTTAATCCCTATCCACTTCCCGCCCTTTGCAAGAAATCAAAGAA							
onsensus	1368	C G TACC ATA C A							
	1401	1400	1410	1420	1430	1440	1450	1460	
302s rc	1			GGATTG	CAAA	CGG	AGCG		
r. avr9cf9	1401	TAATACCCATATCCAACTGCGCGCTTTGACAGTTAATCCCTATCCACTTCCCGCCCTTTGCAAGAAATCAAAGAAAGCTTT							
onsensus	1401	C G TGGT AA A G							
	1592	1600	1610	1620	1630	1640	1650	1660	
302s	1			GCATC	GT	TTTTG	CAA	TGC	
r. avr9cf9	1592	AAAACTTAAATTTTTTACTTATCAATTTTTGAAAAGGAATCTGAAAGAAAATTTCTAGTTCCAATAA							
onsensus	1592	C TC GTTTTIG AA G							

Supplementary Figure 9 The alignment results of the 6 binding sequences with the putative promoter *Avr9/Cf9* gene coding the rapidly elicited protein via program NTI Vector. The yellow showed the overlapped regions.

CURRICULUM VITAE

<i>Family Name / Nachname</i>	Xu
<i>Vorname / Given Name</i>	Xiaolu
<i>Geburtsort / Place of Birth</i>	Yancheng, Jiangsu, P. R. China
<i>Geschlecht / Sex</i>	Weiblich / Female
<i>Staatsangehörigkeit / Nationality</i>	Volksrepublik China / P. R. China
<i>E-Mail</i>	xiaolu.xu@student.kit.edu
<i>Bildung / Education</i>	PhD , supervisor: Prof. Dr. Peter, Nick, Karlsruhe Institute of Technology (10/2013-07/2017) Master of science , supervisor: Prof. Dr. Peilong Yang, Chinese Academy of Agricultural Sciences (09/2010-07/2013)